Sequence Stratigraphy of the Marginal Marine Facies of the Jurassic Sundance Formation, South Dakota and Wyoming: Implications for Controls of Higher-order Cyclicity in a Greenhouse World

Karen Elaine Bossenbroek

A thesis submitted to the faculty of the University of North Carolina at Chapel Hill in partial fulfillment of the requirements for the degree of Master of Science in the Department of Geological Sciences.

Chapel Hill
2011

Approved By:

Dr. Louis R. Bartek III

Dr. Kevin G. Stewart

Dr. Brian W. Horn

ABSTRACT

Karen Elaine Bossenbroek: Sequence Stratigraphy of the Marginal Marine Facies of the Jurassic Sundance Formation, South Dakota and Wyoming: Implications for Controls of Higher-order Cyclicity in a Greenhouse World
(under the direction of Dr. Louis R. Bartek III)

The Sundance Formation was produced by three marine inundations of the Western Interior during the Mesozoic, and the passive margin sediments are exposed in the Black Hills region of Wyoming and South Dakota. This study applies sequence-stratigraphic principles in correlation of geophysical well-log data and measured outcrops to establish a chronostratigraphic framework, in order to identify possible processes that govern stratigraphic architecture. The Sundance is part of a higher-order trend of marine inundations on the Western Interior governed by 3rd order cyclicity. The stratigraphy of the Lower Sundance displays a long-term trend of transgression and regression, punctuated by multiple parasequences. High-frequency variation in stratal architecture observed was likely shaped by cyclic variation in sediment supply governed by climate change. This study supports the current view that eustacy during greenhouse intervals is governed by low-frequency slow variations, and higher-frequency short-order cyclicity in sedimentation may also be superimposed during these long-term intervals.

Acknowledgements:

Many thanks go to my committee Members, Dr. Lou Bartek, Dr. Kevin Stewart, and Dr. Brian Horn for their encouragement, guidance and oversight of this project. I'd also like to thank the UNC Martin Fund for providing the funding for this project.

I would like to thank the South Dakota Department of Environment and Natural Resources Oil and Gas Section for providing well-log data and assistance, along with Mr. Roger Barton of True Oil Company in Casper, WY for providing the cuttings data. Thanks also go out to the land owners in Wyoming and South Dakota who allowed access to their land, especially to Wade Wilkins for his generous accommodation. Thanks to Joe Forrest for his insights and technical support.

I would like to thank my family for their support of me during this project, including my parents, Kathleen and James Bossenbroek, my sisters Kristen Bossenbroek and Kelly Fedoriw, my brother-in-law Yuri Fedoriw, and nephew Adrian James and niece Emily Kathleen. Without the support, encouragement, and love of my family I would not have completed this journey, or be where I am today. Words cannot express how much their encouragement and support has meant to me.

I would like to thank my fellow graduate students Kristin Walker, Tyson Smith, Jesse Davis and Michael Lester for their constructive criticism, technical support, and insights into this project.

Special thanks go to Laura Neser, the best field assistant ever, and Michael Mobilia, the best office-mate ever.

TABLE OF CONTENTS

LIST OF APPENDICES

LIST OF FIGURES

I. INTRODUCTION

Separating relative contributions of eustacy, climate and sediment flux in controlling the deposition of modern and ancient sediments is a long-standing problem in stratigraphy (since Sloss,1962). Multiple workers (Haq et al., 1988; Vail et al., 1977; Posamentier and Vail, 1989) theorize that changes in relative sea level are one of the most dominant agents in shaping stratigraphic architecture. However, during greenhouse climatic intervals, global ice volume is minimal, so the rate and magnitude of relative sea level change is low. Consequently, alternative hypotheses about the nature of the processes that control the evolution of stratigraphic architecture must be considered. Hay and Leslie (1990), and Jacobs and Sahagian (1995) hypothesize that changes in the amount of groundwater stored on continents may help compensate for the absence of dynamic ice sheets, and Jacobs and Sahagian (1995) hypothesize that changes in monsoonal circulation during climatic maximums may cause increased groundwater storage on land and thus sea level fluctuations on Milankovitch-frequency time scales. Yet constraints on controls of deposition during greenhouse climatic intervals are generally lacking or not clearly outlined. The goal of this study is to test hypotheses about the relative roles of eustacy, climatically driven sediment supply, and active tectonics during greenhouse intervals in shaping stratigraphic architecture of marginal marine successions. This study aims to test these hypotheses by examining the linkages between depositional processes and the associated stratigraphy in the Jurassic Sundance Formation, which was deposited during the Mesozoic greenhouse period of Earth's history (Johnson, 1992; Kocurek and Dott, 1983; Brenner, 1983).

The Western Interior of North America experienced many marine inundations in the Mesozoic Era. Specifically, during the Jurassic, the Sundance Formation was deposited during no less than two marine transgressive-regressive cycles (Johnson, 1992). Recent studies of the Sundance Formation have focused on lithostratigraphic correlations of the sedimentary units. In this paper, sequence stratigraphic analysis was used to establish chronostratigraphic correlations among the

lithostratigraphic units. The chronostratigraphy reveals new relationships among facies and a new depositional model of the stratigraphic architecture of the Sundance Formation. Cyclic facies relationships in the Sundance yield insight into the nature of climate dynamics of the western interior of North America during the Jurassic.

The Black Hills area is ideal for examining eustatic and climatic influence on the deposition of units because of the tectonic stability of the eastern coast of the Jurassic Interior Seaway and the excellent exposure of the Sundance Formation (Johnson 1992) (Figure 1). This study focuses on the Lower Sundance Formation, consisting of the Canyon Springs, Stockade Beaver Creek, Hulett, and Lak Members, outcropping near the Black Hills in Wyoming and South Dakota (Figure 1).

1. Previous Investigations

Eustacy is the predominate force cited in many studies as to the controlling factor of sedimentation in marginal marine strata of higher-order cyclicity (Haq et al., 1988; Vail et al., 1977; Posamentier and Vail, 1989). However, higher-order Milankovitch-driven glacioeustacy during greenhouse worlds is unlikely (Plint et al, 1992, Jacobs and Sahagian, 1995). Other hypotheses regarding higher-order influence on greenhouse sediments include continental groundwater storage (Hay and Leslie, 1990). Strasser et al (2000) show the influence of climatically-driven sea level changes on Milankovitch timescales in carbonate-dominated stratigraphy of Oxfordian and Berriasian-Valanginian ages, and suggest thermal expansion and contraction of the uppermost layer of ocean water, thermally induced volume changes in deep-water circulation, or changes in continental freshwater storage as drivers, rather than glacioeustacy. Other studies have shown higher-order cyclicity in deep-ocean sediments and suggested that sedimentary cycles aren't definitively linked to sea level change, as opposed to cyclic changes in sediment supply (Huang et. al., 2010). Higher-order cyclicity is still evident in stratigraphy produced in greenhouse climates, but the driving forces are not well delineated (Plint et al., 1992). This research aims to take a sequence-stratigraphic

approach to the stratigraphy of the Sundance Formation and de-convolve the controls of sedimentation in the U.S. Western interior during the greenhouse Jurassic time period.

Previous investigations of the Sundance focused mainly on descriptive sedimentology and regional correlation of lithostratigraphic units. The larger-scale sea level cycles of the Western interior were described by Pipiringos and O'Sullivan (1978), who identified six regional unconformities that divide the Jurassic sediments into sequences. They labeled these Jurassic unconformities J-0 to J-5, and identified one Cretaceous unconformity that they labeled K-1 (Figure 2). Brenner and Peterson (1994) conducted a large-scale investigation of the sedimentary history of the Western interior. They identified several marine transgressive-regressive cycles and named them the Lower Continental, First Marine, Second Marine, Third Marine, Fourth Marine, and Upper Continental, and compared these marine cycles with the unconformities that Pipiringos and O'Sullivan (1978) identified. The lower Sundance Formation, consisting of the Canyon Springs Sandstone, Stockade Beaver Creek Shale, Hulett Sandstone, and Lak Members, lies within the third marine cycle that Brenner and Peterson (1994) identified. The Redwater Shale Member lies within the fourth marine cycle and unconformably overlies the Lak Member (Figure 2).

Lithostratigraphic correlation of the lower Sundance Formation in the Black Hills area resulted in the interpretation of the lower Members of the Sundance as components of a barrier-island depositional system (Rautman, 1976, 1978). The Stockade Beaver Shale was interpreted to be a product of offshore marine deposition. A gradual vertical transition from offshore marine deposits to shoreface facies suggests the coast prograded over time. The coastal deposits are overlain by a succession of facies that Rautman (1976, 1978) interpreted as a tidal-channel environment and an associated back-barrier island lagoon. Rautman (1976, 1978) interpreted the red shales of the Lak Member as subaerial wind-blown silts.

Johnson (1992) provides a detailed description of the Jurassic rocks in the Powder River Basin area, along with interpretations of the environments of deposition of the facies, and a synthesis of the depositional history of the Jurassic. In particular, he describes the lower Sundance and cites and agrees with Rautman's (1976, 1978) interpretation of the Hulett Sandstone Member as a barrier-island deposit.

While these studies give valuable descriptions of lithologies and higher-order transgressive-regressive cycles, they focus primarily on descriptive sedimentology. They do not provide the high-resolution chronostratigraphic framework that is required to identify lateral and vertical facies transitions and their association with unconformities. These chronostratigraphically determined facies relationships are absolutely required to develop accurate models of stratigraphic architecture and the associated depositional history. This study aims to undertake this in order to test hypotheses regarding relative roles of climate, eustacy, and sediment flux in creating the stratigraphy and stratigraphic architecture of the Sundance Formation.

II. GEOLOGIC SETTING

1. Tectonic Setting/Structural Controls

The western margin of North America went through many dynamic tectonic changes during the Jurassic. The apparent polar wander path derived from Mid- to Late-Jurassic sediments indicates that the North American craton rotated clockwise while moving north from a subtropical position toward temperate latitudes in the northern hemisphere (Kauffman and Caldwell, 1993; Lawton 1994). The Farallon plate subducted along the west coast and the Cordilleran region uplifted, providing a siliciclastic source to the Western interior during the migration (Kauffman and Caldwell, 1993) (Figure 3). The Gulf of Mexico and Atlantic Ocean opened during this time (Kauffman and Caldwell, 1993), and sea level fluctuated in accordance with the tectonically driven ocean-basin volume changes. The northward migration of the North American craton caused the climate to change

conditions from hot and arid to a more humid, temperate climate (Brenner, 1983, Johnson, 1992). The Jurassic stratigraphy of the Western interior records the complex interactions between eustacy, tectonics and climate change during a greenhouse phase of Earth's history.

The Middle Jurassic basin of the Western interior was a retroarc foreland basin that was created by flexural deformation associated with adjacent thrust loading, most likely the Central Nevada Thrust Belt or the Elko Orogenic Belt of the Rocky Mountain Cordillera (Lawton 1994). The basin that the Middle Jurassic marine strata fill has been related to the flattening of the angle of the subducted slab of the Farallon plate beneath the North American plate, accompanied by the development of a broad, uplifted plateau between the continental margin and the basin formed on the craton by dynamic subsidence (Lawton 1994). Middle Jurassic strata were deposited on a regional unconformity known as the J-2 unconformity that formed in response to the eastward migration of the forebulge. (Figure 3) (Lawton, 1994).

The Western interior experienced many marine inundations in the Mesozoic. During the Middle to Late Jurassic, marine inundation created an irregularly shaped Jurassic Western Interior Seaway in which the Sundance Formation was deposited (Figure 4) (Johnson, 1992). The basin has an asymmetrical geometry in which the western region consists of a relatively deep retro-arc basin that ran through western Montana, eastern Idaho, western Wyoming and Northern Utah, named the Idaho or Twin Creek Trough (Figure 3). The eastern side of the Seaway was shallower, and a low-gradient marine shelf existed in eastern Wyoming, along with an intracratonic basin in eastern Montana and western South Dakota (Williston basin) (Johnson, 1992) (Figure 3). The lack of coarse-grained clastic rocks in the eastern portion of the Western interior Basin, along with the great lateral persistence of stratigraphic units, the lack of volcanogenic sedimentary rocks, and the absence of high-angle unconformities, present further west in the basin, indicate that the eastern margin of the Western interior Basin was tectonically stable (Johnson, 1992). The sources of sediment for the eastern side of

the Seaway were the likely from the craton (Johnson 1992). There are no known modern analogs to the Jurassic Western interior Seaway (Johnson, 1992).

The broad, shallow marine portion of the eastern flank of the Wyoming shelf contained areas of positive and negative relief that influenced deposition in this area (Johnson, 1992). Near the Black Hills, the submerged, northeast-trending, Sheridan arch in northern Wyoming, and the emergent Gillette high in northeast Wyoming, along with the Belle Fourche arch likely affected marine circulation and deposition (Figure 3) (Johnson, 1992).

2. Regional Climate

The Mesozoic is thought to be a warm interval in the U.S. Western interior (Kocurek and Dott 1983). Evidence indicating that the Mesozoic climate was globally warm and locally dry include a global lack of glacial deposits, the wide extent of evaporites and eolinites formed during this time, the fossilized flora and fauna, and oxygen isotopes from carbonates (Frakes, 1979). The global mean temperature of the Jurassic is estimated to be as high as 10° C warmer than the present day. There are many studies describing global climate model results for the Jurassic time period, but simulations for the study area are generally lacking. Ziegler et al. (2003) show that through the Jurassic, the study area migrated from an area of high evaporation to a more temperate climate. The modeled air surface temperatures range from 8°-12° Celsius (C) during winter, and 40°-44° C in summer months (Rees et al., 2000). Precipitation is estimated to be 1-2 millimeters per day during winter, and 0.5-1 millimeters per day in the summer (Rees et al., 2000). The temporal transition from abundant Early and Mid-Jurassic carbonates and evaporites to the increase of siliciclastic rocks toward the end of the Jurassic indicates that the climate in the region changed from warm and arid to more temperate and wet (Johnson, 1992) (Brenner, 1983). These transitions in climate conditions are attributed to the northward drift of the North American craton from lower latitudes associated with

the warm and arid conditions of the subtropical high-pressure zone to the higher latitudes of the wetter, more temperate climate belt (Johnson, 1992; Brenner, 1983).

3. Description of Facies

The Jurassic sedimentary rocks of the Western interior consist of marine and continental siliciclastic, evaporite, and carbonate rocks ranging in thickness from approximately 300 m to nearly 1,500 m (Brenner and Peterson, 1994). In the Black Hills uplift area of northeastern Wyoming and western South Dakota, Jurassic sedimentary rocks range in thickness from 190 m to 485 m. These units include the Late Permian/Early Jurassic Spearfish Formation, the Mid-Jurassic Gypsum Springs Formation, and the Middle to Late Jurassic Sundance and Morrison Formations (Robinson et al., 1964). The marine units found in this area were deposited during several transgression-regression cycles of the Jurassic Interior Sea.

The Sundance Formation consists of green shale, yellowish-gray and red very fine-grained sandstone and siltstone, and, in some horizons, thin beds of gray limestone. In most areas, it is between 114 m and 122 m in thickness. It is composed of five Members, from oldest to youngest, are the Canyon Springs Sandstone, Stockade Beaver Shale, Hulett Sandstone, Lak, and Redwater Shale Members. The Canyon Springs Sandstone Member of the Sundance Formation consists of fine-grained friable calcareous sandstone, and varies in color from light yellowish gray, pink, light gray, or greenish-gray (Robinson et al., 1964). The Stockade Beaver Shale Member consists of dark greenish-grey fissile shale with thins beds and laminae of gray sandstone and siltstone. The Hulett Sandstone Member consists mostly of fine-grained calcareous thin-to thick-bedded firmly cemented sandstone. Ripple marks and cross-beds are common. Color ranges from light gray, yellowish gray, pink, or grayish red. The Lak Member consists of yellowish-gray and pink poorly sorted siltstone and very fine-grained sandstone. The Redwater Shale Member consists of grayish-green shale, light-gray sandstone and gray sandy limestone (Robinson et al., 1964).

The Pine Butte Member is thin to non-existent in the study area and not well exposed (Brenner and Peterson, 1994, Imlay, 1980, Johnson, 1992). It is part of the Lower Sundance and is interpreted as an open marine shale. Because of its poor exposure and limited lateral extent, it is not considered in this study.

4. Focus of Study

The focus of this study is to determine the relative roles of climate, tectonic, and eustatic fluctuations on deposition of the Lower Sundance Formation in the Black Hills region by applying sequence stratigraphic concepts to the Sundance stratigraphy and determining stacking patterns. The Lower Sundance Formation records deposition during a transgressive event of the epeiric Sundance Sea.

III. METHODS

Three different types of data were analyzed during this project. Outcrop measurements (Appendix 1, 2), wireline well logs (Appendix 3), and a lithologic description of cuttings from one well (Figure 6) were used to construct three cross sections in the study area.

1. Outcrops

Nine outcrop descriptions were made in the Black Hills area where the Sundance Formation is well exposed (Figure 5). The locations and descriptions of these outcrops are summarized in Appendix 1 and 2. Sandstone composition percentages were estimated visually using hand samples, a hand lens, and comparing to a percentage chart. The fine-grained units of the Sundance are commonly covered in the study area, especially the Lak and Redwater Shale Members. Outcrop data are the highest-resolution data used in this study and facies seen in outcrop were correlated to adjacent well logs.

2. Well logs

Over 70 well logs were gathered and correlated in the study area (Appendix 3). Gamma ray and resistivity logs were most frequently used. The well log data were downloaded from the Wyoming Oil and Gas Conservation Commission's website. The wells were input into the Kingdom Suite Program, where correlations were identified and cross sections were created.

Rock lithologies in wells were interpreted based on the gamma ray logs. High gamma ray values were interpreted to represent shale-rich sediments, and low gamma ray values were interpreted to represent sandier sediments. Facies were interpreted in well log cross sections by comparing facies present in outcrop and interpreted facies in well logs.

3. Cuttings Description

A description of rock cuttings from the Krauss Patented 1 well, located in Crook County, Wyoming, was used to aid in interpretation of well data (Figure 6). The cuttings description notes prolific caving of the Cretaceous units above the study interval, therefore the sample descriptions were matched to the corresponding wireline log to calibrate lithology identification.

4. Stratigraphically Significant Surfaces

This study utilized sequence stratigraphic concepts and associated chronostratigraphy in this investigation to correlate stratigraphic units in outcrops and well logs. Correlation of maximum flooding surfaces and sequence boundaries are the sequence stratigraphic tools used to establish chronostratigraphic equivalence of units in different wells and outcrops. Marine-flooding surfaces were also used to identify parasequences and parasequence sets. Stacking patterns of parasequence sets were used to identify the position of sequence boundaries and to subdivide the Lower Sundance into sequences and systems tracts.

Many different definitions exist of sequence stratigraphically significant surfaces. The following defines and describes significant surfaces and concepts used in this study, and specifies which definition used in this study.

Marine-Flooding Surfaces

A marine-flooding surface is defined as "a surface separating younger from older strata across which there is evidence of an abrupt increase in water depth" (Van Wagoner et al., 1990). In a beach or marginal marine setting marine-flooding surfaces display a transition from rocks deposited in shallow water, such as foreshore sandstones to overlying deeper-water facies, such as marine shales or limestones. In outcrop, abrupt facies shifts, such as from wave-influenced sandstones to marine shales, delineate the position of the marine-flooding surface, while in well logs, these surfaces are generally associated with coarsening-upward successions that are capped by abrupt increases in gamma ray emission.

Parasequences

Parasequences are defined as "a relatively conformable succession of genetically related beds or bedsets bound by marine-flooding surfaces or their correlative conformities" (Van Wagoner et al., 1990). Particularly, in a beach or marginal marine setting, a parasequence is known as a "genetically related succession of strata dominated by wave and current processes" (Van Wagoner et al., 1990). In outcrop, this can be recognized as a shallowing-upward succession of strata with relatively fine grained marine facies, at the base, and overlain bye a coarsening-upward succession of strata (Figure 7). In well logs, parasequences are identified by a decrease in gamma ray emission from bottom to top. This succession is bound at the base and top by an abrupt change in gamma ray emission, indicative of a marine-flooding surface. These coarsening up successions can be correlated down

depositional dip to other coarsening up successions that are finer-grained due to their more distal position.

Sequence Boundaries

Sequence boundaries are recognized by multiple criteria in well log and outcrop cross sections. Evidence of subaerial-erosional truncation and submarine erosion that is laterally correlative and a general basin-ward shift in facies must be present (Van Wagoner et al., 1990). The expression of this subaerial-erosional truncation and submarine erosion consists of an unconformity up-dip and correlative conformity down-dip (Van Wagoner et al., 1990). Evidence of subaerial-erosional truncation includes soil and root horizons and truncation of marginal-marine strata (Van Wagoner et al., 1990). Ravinement surfaces, or transgressive surfaces of marine erosion, are also important bounding discontinuities, and are often associated with sequence boundaries due to wave scouring action that re-works sediments during relative sea level rise (Walker, 1992). This wave scouring frequently reworks the subaerial unconformity that has its maximum extent at lowstand. Sequence boundaries identified in this study were identified based on unconformities present in outcrop and in well logs. Evidence of subaeriel exposure, such as eolian deposits or paleosol development lying unconformably over marine facies, indicates a relative fall of sea level, thus indicating the presence of a sequence boundary. Sequence boundaries are generally created during base-level fall (Van Wagoner et al., 1990).

IV. RESULTS

Outcrops described in the field are categorized into nine facies types described below. Facies were compared with published facies models in order to identify associated depositional environments. Well logs were correlated based on comparison to adjacent outcrops, and interpretation of the well log signature. The lithologic cuttings description was also integrated into interpretation of well logs.

1. Facies

Facies 1: High-Angle Cross-bedded Sandstone Facies

The High-Angle Cross-bedded Sandstone Facies generally consists of fine-grained, very well-sorted sandstone (Figure 8, Appendix 5). Composition of the sand is approximately 97% quartz and 3% lithic fragments. The color ranges from grayish pink, very pale orange to moderate reddish orange (Appendix 4). Structures present are bi-directional high-angle cross-lamination; bed-sets are on the order of 0.5 to 1 meter thick. This facies ranges in thickness from 8 meters to 20 meters and is present at the Alabaugh Canyon and Red Canyon locations. It is only present in the southwestern and southern Black Hills, and is absent in the northern region of the Black Hills, where the Members above it rest directly upon the Spearfish Formation. The contact with the underlying Spearfish Formation is sharp. This facies is mapped as part of the Canyon Springs Sandstone Member. It does not appear that it is possible to correlate the High-Angle Cross-bedded Sandstone Facies along strike or up and down depositional dip, as it is laterally discontinuous, and laterally related facies are not observable in the study area.

Interpretation:

The bi-directional, high-angle cross-stratification observed in this unit is insufficient in and of itself to determine the environment of deposition. Observations made by Ahlbrandt and Fox (1997) suggest an eolian origin for this unit. Observations in the Red Canyon area, Wyoming, (Figure 5) include inversely graded sandstone laminae, a fraction of an inch thick, interpreted as wind ripples, overlying high-angle avalanche or grainflow strata, (tabular, tapering-upwards wedges that exhibit loose packing and typically a two-fold grain-size segregation) and granule ripples (megaripples composed of larger grained (4-30 millimeters) particles), and suggest a subaerial, eolian origin of the unit (Hunter, 1977). These key observations lead to the interpretation that this unit was deposited in an eolian setting. The unit displays a distinctive, box-shaped gamma ray signature in well logs,

indicating that the transitions from the underlying and overlying units are abrupt, and that the sand contains a high percentage of quartz. While this signature is not exclusive to eolian deposits, it suggests the presence of an underlying unconformity (potentially subaerial) and an abrupt transition to the conditions associated with the overlying environment, that sediments are uniform and clay-poor, and is consistent with eolian features described above and observations of outcrops.

The limited lateral continuity of this facies may be a consequence of preservation only in paleovalleys incised into the underlying Triassic Spearfish Formation (Ahlbrandt and Fox, 1997). Ahlbrandt and Fox (1997) mapped these paleovalleys into the subsurface of the Powder River Basin by creating isopach maps and using descriptions of stratigraphy from well logs. They indicate that the paleovalleys dip and increase in relief in a westerly direction toward the basin. The lower and upper unit of sandstone (High-Angle Cross-bedded Sandstone Facies and Flat-Bedded Sandstone Facies in this study) is separated by a "Limestone Marker" and a "Brown Shale" further west in the Powder River Basin (Ahlbrandt and Fox, 1997).

Facies 2: Flat-Bedded Sandstone Facies

This facies generally consists of fine- to medium-grained well-sorted, well-rounded sandstone (Figure 9). Composition of the sand is approximately 92% quartz, 5% lithic fragments, and 3% feldspar. The color ranges from grayish pink to light gray (Appendix 4). Structures present include thick laminations that are parallel with wavy to flat bedding planes, ripple marks and cross-laminations. In some areas, Johnson (1992) describes the presence of ooids in this facies, as well as the presence of algal laminations on the top of this unit. Johnson (1992) indicates that poorly preserved external molds of oysters and bivalves are present, but rare, and bioturbation, tracks and trails, and *Ophiomorpha* and possibly *Terebellina* burrows to be locally present. Small shell fragments (<1 inch) are present in the sandstone, and show evidence of abrasion. This facies ranges in thickness from 0.5 meters to 5 meters. The contact with the underlying and overlying unit is

generally sharp. Locally, this unit cuts through and erodes into the underlying High-Angle Cross-bedded Sandstone Facies. It is not laterally continuous along depositional dip or along strike, and is only present at sites where the High-Angle Cross-bedded Sandstone Facies is present. The Flat-Bedded Sandstone Facies unit is present at the Red Canyon location, and is part of the Canyon Springs Sandstone Member (Figure 9, Appendix 5).

Interpretation:

The lack of eolian features present in the underlying unit, along with the presence of marine to marginal marine attributes indicate that this unit is likely not associated with eolian processes. A shallow marine environment is supported by the presence of ripple marks and cross-beds, ooids, algal mats, and the previously mentioned marine fossils. The unit is generally coarser grained than the underlying sediments, and locally it cuts into underlying units. This, along with abraded shell fragments indicates that the underlying sand was likely reworked from the underlying unit during the transgression of the Sundance Sea. This unit is thus interpreted as a transgressive ravinement surface (Catuneanu, 2006). Although ooids are not diagnostic of a particular environment, carbonate grains may form in systems that are not overwhelmed by clastic material (Reading, 1996). The presence of ooids here suggests that sediment supply may have been cut off during the transgression, and shoaling conditions existed (Reading,1996) The limited lateral continuity of this facies is hypothesized to be a product of preservation occurring only in the paleovalleys that were incised into the underlying Triassic Spearfish Formation (Ahlbrandt and Fox, 1997).

Facies 3: Mudstone and Limestone Facies

The Mudstone and Limestone Facies is part of the Stockade Beaver Creek Member of the lower Sundance Formation. It generally consists of light olive gray to olive gray silt and clay, with rare interbeds of very-fine to fine sand and limestone (Figure 10, Appendix 5). The shales are

fissile. The silt and clay units are the predominant lithology in this facies. Fossils were not found in outcrop during this study, however, Imlay (1947) and Wright (1973, 1974) identified bivalves, oysters, ammonites and crinoids in deposits of this facies. The shale units range in thickness from 9 meters to 23 meters. In general, the Mudstone and Limestone Facies is thicker in down-dip areas (northwest Black Hills) and thinner in up-dip areas (southeast and eastern Black Hills). There is an inverse relationship in the variation of unit thickness with the underlying Canyon Springs Sandstone Member; it is thicker where the Canyon Springs Sandstone Member is absent, and is thinner when it is present. The shale facies is found at every measured location in this study. In the southwestern Black Hills, it is in sharp contact with the underlying Flat-Bedded Sandstone Facies. At all other locations, the basal contact is either not exposed or there is a sharp contact with the underlying Spearfish Formation or Gypsum Springs Formation. It grades upwards into the Bioturbated Facies.

Sand interbeds are rare and range in thickness from 2 millimeters to 1 meter. They are composed of approximately 90-95% quartz and 5-10% lithic fragments, and are rounded and well-sorted. Sedimentary structures are absent or poorly exposed in thinner beds (2 millimeters to 1 centimeter range). In thicker sand beds, structures consist of parallel lamination, and parallel bedding. There does not seem to be an up-section trend in bed thickness, grain size or sedimentary structures. However, thick sand beds are relatively rare, and the thin beds predominately exist in areas further up depositional dip, in the east and southeast Black Hills.

The limestones in this unit consist primarily of mudstones to wackestones; the wackestones contain bivalve fragments. Packstones containing phosphatic pebbles, bivalve fragments, and shark teeth lie on top of these units in the Deer Creek location and another unmeasured area (Edwards property). The thickness of the mudstones and wackestones ranges from 2 centimeters to 0.3 meters; the packstones range in thickness of 3 centimeters to 5 centimeters.

Interpretation:

The Mudstone and Limestone Facies were deposited in a marine shelf setting. The absence of other facies such as channel facies, estuarine facies, coals, or paleosol features eliminates a floodplain-type environment of deposition. The marine fossils, along with dark color of the shales and thin sandstone beds indicate a marine shelf type environment, and this facies indicates the transgression of the Early Sundance Sea. The presence of carbonates, phosphatic pebbles, bivalve fragments, and shark teeth indicates that this is a condensed section following a marine flooding event, as described by Van Wagoner et al. (1990). The limestones likely formed when siliciclastic input was cut off, and the shell beds were reworked by storms. Given the general lack of fauna in the shale unit below, these shells likely did not get reworked from underlying units. Thus, the characteristics of the wackestones and packstones observed suggest they represent a condensed section formed during the maximum marine flooding event.

Facies 4: Bioturbated Facies

The Bioturbated Facies is found in the Stockade Beaver Creek and Hulett Members of the lower Sundance Formation. This facies consists of coarsening-upwards sequences of clay, silt and sand (Figure 11, Appendix 5). The lower part generally consists of flaser-and wavy bedded shales and sands that coarsen upward into sandstone beds. Sandstone beds are generally well-sorted, well-rounded very-fine to fine sandstone, and the composition of the sand ranges from 80-95% quartz, 0-10% feldspar and 0-5% lithic fragments. The color of the sand beds varies from yellowish gray, light red and grayish orange, among other colors (Appendix 4). Structures found in the sand beds include hummocky cross-stratification, parallel lamination, bi-directional ripple marks, cross-lamination, and bioturbation; in some outcrops bioturbation is extensive. Vertically, the facies generally trend from flaser and wavy bedding, to parallel lamination, to cross-beds, to ripple marks, and finally to

bioturbation. The thickness of the sand beds increase up-section, from millimeter thickness, to several centimeter thickness, to approximately 0.5 meter thickness.

The bioturbation in this facies was identified by Rautman (1976) as *Skolithos*, *Monocraterion* or *Tigillites*, and *Diplocraterion*. Body fossils were not found during this study. The thickness of this facies ranges from approximately 5 to 20 meters. The underlying Mudstone and Limestone Facies grades vertically into this facies and the Bioturbated Facies grades vertically into Low-Angle Cross-Bedded Facies. It is continuous along strike. Due to the lack of laterally extensive outcrops over extensive distances, it is difficult to determine which facies it may have either an up-dip or down-dip association. This facies is present at all outcrop locations.

Interpretation:

These coarsening-upwards facies are interpreted as a product of a shallowing shelf-to-lower-shoreface depositional environment. The lower shoreface is an environment where fair weather waves begin to shoal and affect the bottom, but basinal or shelf processes also occur (Reinson, 1984). Flaser and wavy structures seen in the coarsening-upwards sequences, as well as hummocky cross-stratification suggest deposition in a shelf environment below fair-weather wave base. The sandstone structures, including parallel lamination and bioturbation, also suggest an environment spanning the lower shoreface to the offshore transition zone of the shelf. The presence of *Skolithos*, *Diplocraterion* and other trace fossils is indicative of relatively high levels of wave energy, and abrupt changes in sedimentation rates and physical reworking of the sediments is frequent (Pemberton and Frey, 1984). This supports the interpretation that wave energy increases through time in this facies, indicating either a temporal increase of wave intensity or shoaling associated with shoreline progradation.

Facies 5: Low-Angle Cross-bedded Sandstone Facies

This facies is present at all studied outcrop locations, and is part of the Hulett Sandstone Member of the Lower Sundance. This facies is similar to the Bioturbated Facies in that it generally consists of coarsening-upwards units of clay, silt and sand (Figure 11, Appendix 5). However, the structures, thickness, and color of sandstones of this facies are different. Vertically, the structures trend from wavy and flaser bedding, to bioturbated sands, to cross-beds, to parallel planar lamination, and oscillation ripples located on top of sand beds that are separated by shale partings. The sandstone beds are calcareous, generally well-sorted, well-rounded fine-grained sands composed of approximately 90-95% quartz, 3-7% feldspars and 2-3% lithic fragments. Color varies from yellowish gray, very pale orange, moderate orange pink and moderate reddish orange (Appendix 4). Structures found in sandstone beds include parallel lamination and bedding, oscillation ripple lamination, and low-angle cross-bedding that is on the order of 0.2-0.5 meters thick. Bioturbation is less common in this facies, and parallel bedding, lamination, and low-angle cross-bedding predominate. Shale partings are present at some locations, and sand beds below these shale partings commonly contain symmetrical ripple-marks. In the upper portion of this facies, cross-beds are higher angle, on the order of 0.1-0.2 meters thick. Body fossils were not found during this study. However, vertical trace fossils were identified as *Monocraterion* (Rautman, 1976). The underlying Bioturbated Facies grades vertically into the Low-angle Cross-bedded Facies, and it grades vertically into Parallel Planar-Bedded Sandstone Facies. It is continuous along strike. Associated facies up-dip and down-dip were difficult to determine, due to the lack of laterally extensive exposures.

Interpretation

This facies represents a middle shoreface environment. Bioturbation observed in this facies is less diverse than what was observed in the underlying bioturbated facies (Reinson, 1984). Structures generally found in middle shoreface environments include low-angle wedge-shaped sets of planar

laminae, ripple laminae, and cross-laminae. Fine- to medium grained, clean sand, containing minor amounts of silt and clay typify the middle shoreface facies (Reinson, 1984). Planar laminae, ripple laminae and cross-laminae are common in this facies. These attributes, along with decreasing bioturbation up-section, are consistent with middle shoreface deposits as described by Reinson (1984). The bioturbation that is present, *Monocraterion,* is a type of *Skolithos* trace fossil, and indicates an environment of relatively high wave energy, which is consistent with a middle shoreface environment (Frey and Pemberton, 1984).

Facies 6: Parallel Planar-Bedded Sandstone Facies

The parallel planar-bedded sandstone is a local cliff-forming unit in the northwestern Black Hills facies, at the Devil's Tower and Deer Creek locations. It is part of the Hulett Sandstone Member. This facies generally consists of fine-grained, well-sorted and rounded sandstone that is composed of approximately 90-95% quartz sand, 5% lithic fragments, and >1% feldspars (Figure 12, Appendix 5). Color ranges from very pale orange, yellowish orange, and grayish orange (Appendix 4). Structures present include bi-directional cross-beds, bed sets 0.2 to 0.5 meters thick, parallel lamination and bedding, and oscillation ripples. Bi-directional cross-beds decrease vertically and planar lamination and bedding become more common. Up-section, oscillation ripple marks and shale partings become rarer. Fossils were not observed. Thickness of this unit ranges from 10-20 meters. The contact between the underlying low-angle cross-bedded facies and the parallel planar-bedded sandstone is progressive and gradual. The unit overlying this facies is generally covered, however, where present, this unit grades into the Redbed Facies. Associated facies up and down-dip were difficult to identify, due to the lack of laterally extensive outcrop exposure.

Interpretation

The Parallel Planar-Bedded Sandstone Facies represents an upper shoreface to foreshore environment. In an upper shoreface environment, shore-normal wave action and wave -driven alongshore currents produce a complex sequence of sedimentary structures and textures (Reinson, 1984). Sedimentary structures are dominated by trough cross-bedding, low-angle planar cross-bed sets, and plane beds (Reinson 1984). The structures observed in this facies (bi-directional cross-beds, parallel lamination and bedding, as well as oscillation ripple marks, are consistent with an upper shoreface to foreshore environment. Although there is not a significant increase in grain size in this facies as expected by the processes described above, this is most likely a function of the sediment source and not indicative of the environment of deposition. All sandstone observed in the study area ranged from very fine to medium grained. The presence of bi-directional cross-beds and oscillation ripple marks in this facies may indicate that shore-parallel currents may be a strong force in this basin. The vertical gradation from middle shoreface, upper shoreface and finally to foreshore is consistent with a shallowing upward event.

Facies 7: Incised Sandstone Facies

This facies type is part of the Hulett Sandstone Member and is present only at the Star Butte location. It consists of fine-grained, well-sorted and rounded sand, and contains approximately 96% quartz, approximately 1% feldspar, and 3% lithic fragments (Figure 13, Appendix 5). Color is very pale orange (Appendix 4). Structures include parallel lamination, high-angle cross-beds, cross-sets that are on the order of 20-50 centimeters thick. Some ripple cross-lamination is evident as well. Bed thickness decreases up-section. Incision into the underlying facies, Low-Angle Cross-bedded Sandstone Facies, is clearly evident in outcrop (Figure 13). No basal lag layer is present, however, Rautman (1976) reported that very poorly preserved bivalve fragments are present. The thickness of

this facies is approximately 3 meters. The lack of laterally continuous outcrops in the area makes it difficult to identify facies lying along strike and depositional dip.

Interpretation

It appears that deposition of the Incised Sandstone Facies is associated with erosion and deposition by tidal channels. Channel-fill sequences resulting from tidal-inlet migration consist of deep channel facies comprised of bi-directional large-scale planar and/or medium scale trough cross-beds, shallow channel facies (bi-directional small to medium-scale trough cross-beds and/or plane-beds), and a fining-upward textural trend and a thinning-upward of cross-bed set thickness, overlying an erosional base, often marked by a lag deposit (Reinson, 1984).The structures and textures seen in this outcrop include parallel lamination, high-angle cross-beds, and ripple cross-lamination, which is consistent with a tidal inlet interpretation. Incision into underlying Low-Angle Cross-bedded Sandstone Facies, as seen in outcrop, is also consistent with this interpretation. In this case, the Incised Sandstone Facies lacks evidence of lateral migration within the channel deposits, which suggests that longshore drift was not a very strong force in the early Sundance Sea (Rautman 1976).

Facies 8: Redbed Facies

This facies is present and well-exposed at the Alabaugh Canyon and Wildcat Peak locations. This facies is known as the Lak Member of the Lower Sundance Formation. It consists mostly of silt and minor amounts of very fine-grained sand and clay (Figure 14, Appendix 5). Composition of the sand is approximately 95% quartz, but is difficult to determine due to the dark color. Grains are subangular to rounded and commonly frosted. Color ranges from light olive gray, in the clay units, to pale reddish brown (Appendix 4). No structures are present, and there were not any fossils found in this unit. The thickness, where exposed, is approximately 15 meters. The contact of this unit with underlying units is generally conformable and gradational. The upper contact of this unit with

overlying units is generally difficult to determine because of the fine-grained nature, however, where it is exposed the contact is generally conformable and gradational. Thickness of this unit has an inverse relationship with the underlying Hulett Member, it's thicker where the Hulett is thinner and vice versa, and changes thickness over relatively short distances in the Black Hills (Johnson, 1992).

Interpretation

The depositional environment of this facies is problematic and is tentatively interpreted to represent a sabkha mudflat environment. The bright red color of the silts and very fine sands indicate an oxygenated environment, and a complete lack of fossils and structures make identifying the depositional environment difficult. The lack of channel deposits indicates that a fluvial environment is unlikely, and a complete lack of fossils, especially marine fossils, eliminates a marine environment. A loess-type deposit is unlikely, due to the deposition of the unit upwind of the sand in the Entrada erg (Johnson, 1992). Johnson (1992) discusses this debate in detail and suggests a sabkha-like environment for the Lak Member, based on the gypsum found in the unit, (Rautman, 1978), the grain size, lack of sedimentary structures, and absence of body and trace fossils. Sabkhas are subaerially exposed most of the time, and form largely by wind deflation (Reading, 1996). The fine-grained nature of the facies supports deposition by wind deflation. The fact that there are no significant evaporites preserved in this unit may imply that the aridity needed to produce such deposits was not present, or that such deposits were not preserved, such as in a dry mudflat facies (Reading, 1996). The absence of body and trace fossils is also consistent with a sabkha-like setting, as sabkhas are generally inhospitable to most organisms (Johnson, 1992, Reading, 1996). The stratigraphic position of this unit above nearshore marine (Parallel Planar-Bedded Sandstone and Incised Sandstone Facies) and deep marine (Bioturbated Facies and Low-angle Cross-bedded Facies) facies is consistent with the long-term regressive trend.

Facies 9: Belemnite Facies

This unit is part of the Redwater Member of the Upper Sundance Formation. This facies consists of clay, silt and very fine- to fine-grained sandstone (Figure 15, Appendix 5). Color ranges from light brown, grayish green, dark greenish gray, light olive gray, dusky yellow, and yellowish gray (Appendix 4). Most of this unit was covered with grass and had to be excavated with a mattock. Abundant belemnites were found both in place and littering the surface of the outcrops. Imlay (1947) and Robinson et al. (1964) describe glauconitic sandstone in the lower part of the Member, and thin beds of oolitic coquinoid limestone in the upper portion of the Member. The thickness of this unit ranges from 16-25 meters. The contact with underlying units in generally obscured and covered, but where exposed, is sharp. The upper contact with overlying units is generally gradational and conformable. The three-dimensional shape of the unit was difficult to determine due to the fine-grained nature of the rocks and general poor exposure.

Interpretation

This facies is part of the Upper Sundance Formation, and represents a marine inundation of the area. The presence of glauconitic sands, oolitic coquinoid limestones and abundant belemnites indicate a marine origin, despite the lack of primary sedimentary structures (Imlay, 1957, Imlay, 1980). The belemnites present indicate that open-marine conditions existed in the study area during this time, and the nearshore/shoreline units have not been recognized due to erosion during the formation of the J-5 unconformity (Johnson, 1992) (Figure 2).

2. Lithostratigraphy and Stratigraphic Architecture

The Sundance Formation has been the subject of many previous investigations, all of which relied on lithostratigraphic correlation of the units and Members (Brenner and Peterson, 1994; Doyle, 1984; Imlay, 1947, 1957, 1980; Johnson, 1992; Peterson, 1954, 1957; Pipiringos and O'Sullivan,

1978; Rautman, 1976, 1978; Robinson et al., 1964; Wright, 1973). This study divides the Sundance into different lithostratigraphic units and the stacking patterns of these units are described here.

The six main lithostratigraphic architectural components of the Sundance are:

1. The High-Angle Cross-Bedded Sandstones of the Canyon Springs Member
2. The Flat-Bedded Sandstones of the Canyon Springs Member
3. The Mudstones and Limestones of the Stockade Beaver Creek Member
4. The Bioturbated and Low-Angle Cross-Bedded Facies of the Hulett Sandstone
5. The Parallel Planar-Bedded Sandstone Facies of the Hulett Sandstone
6. The Redbed Facies of the Lak Member.
7. The Belemnite Facies of the Redwater Creek Member of the Upper Sundance

The basal High-Angle Cross-bedded Sandstone Facies of the Canyon Springs Sandstone is present only in the southern and southwestern part of the Black Hills (Figure 16). The Flat-Bedded Sandstone of the Canyon Springs Sandstone is in sharp contact and cuts into the High-Angle Cross-bedded Sandstone. The Flat-Bedded Sandstone of the Canyon Springs is only present where the underlying High-Angle Cross-bedded Sandstone Facies is present (Figure 17). Overlying this are the Mudstone and Limestone Facies of the Stockade Beaver Creek Member (Figure 18). The Mudstone and Limestone Facies are pervasive throughout the study area, and are in direct contact with the underlying Spearfish Formation where the Canyon Springs Sandstone Member is missing, in the northern and eastern Black Hills (Figure 18). The Stockade Beaver Creek Member of the Lower Sundance Formation grades into the Hulett Sandstone Member of the Lower Sundance, which consists predominantly of Bioturbated Facies, Low-Angle Cross-Bedded Facies, and Parallel Planar-Bedded Sandstone (Figure 19). Some sandstones of the Hulett Sandstone Member show evidence of deposition in distal marine environments such as the Bioturbated Facies and Low-Angle Cross-Bedded Facies, while other sandstones show evidence of deposition in proximal marine

environments, such as the Parallel Planar-Bedded Sandstone Facies. The Bioturbated and Low-Angle Cross-Bedded Sandstones of the Hulett Sandstone Member are present at all outcrops observed. However, the Parallel Planar-Bedded Sandstone Facies of the Hulett are thick and prominent in the northwest region of the Black Hills (Figure 19).

The regional facies distribution is significant in terms of the gradation of the Stockade Beaver Creek into the Hulett Sandstone. In up-dip areas, the Stockade Beaver Creek coarsens upward into distal marine sand of the Hulett Formation as described above. In the down-dip area, specifically the Deer Creek and Devil's Tower locations, the distal marine facies of the Hulett Sandstone exhibit a vertical facies succession of distal marine facies grading upward into proximal marine facies. The proximal marine facies are not as thick in up-dip areas (Figure 19). Along strike, these facies associations are generally continuous, and the proximal marine facies can be traced laterally for several miles.

In the northwestern Black Hills, the proximal marine facies thicken considerably, and are a local cliff-former. The rimrock exposure of this unit generally does not occur in other areas of the Black Hills. The units above the Hulett are generally poorly exposed. They consist of the Redbed Facies of the Lak Member of the Lower Sundance Formation, and the Belemnite Facies of the Redwater Creek Member of the Upper Sundance Formation (Figure 19, 20). In the southern and southeast Black Hills, exposure of the units overlying the Hulett Sandstone is especially poor, and the units were likely eroded from many locations (Figure 19).

Rautman (1976, 1978) gives the most detailed interpretation of the Sundance Formation, and because of this will be directly compared to this study's interpretation. He interprets the Sundance facies geometry as a barrier-island environment (1976, 1978) primarily based on the presence of laterally thick, continuous proximal marine sandstones in basin-ward locations. It is important to note that proximal marine sandstone facies are present at all outcrops, but thicken considerably in basin-

ward locations. However, the stacking patterns presented in this study show this basin geometry is likely due to the progradation of the shoreline and aggradation of proximal marine sandstones in basin-ward locations through time (Figure 21 a, b). The units above these proximal sandstones are missing (presumed eroded) or poorly exposed in up-dip areas. However, they are present in the subsurface and are interpreted in well log cross sections to consist of coastal plain/sabkha facies (Figure 21a, 22 a, b). Rautman's (1976, 1978) interpretation is based primarily on lithostratigraphic correlation of outcrops, rather than chronostratigraphic correlation of outcrops and well logs (Figure 21 b, 22 b, 23 b).

3. Sequence Stratigraphy

Outcrops were compared to well logs in order to identify facies present in the subsurface and interpret chronostratigraphic relationships among the well logs. This was done by comparing measured section outcrops to wells located closest to them (Figure 24). Gamma-ray logs were used to determine shale vs. sand content, and higher gamma-ray values were assumed to represent shalier facies, while lower gamma-ray values were assumed to represent cleaner, sandier facies. Grain-size patterns in outcrop, such as coarsening-upward or fining upward were interpreted to be analogous in gamma-ray signatures (Figure 24). Stacking patterns in outcrop were generally comparable to stacking patterns in well logs, thus facies present in outcrop were interpreted in well log cross-sections accordingly.

Facies interpreted in well logs were generalized to encompass facies identified in outcrop and to account for inherent differences when comparing lower-resolution well log data to higher-resolution outcrop data. Bioturbated and Low-angle Cross-bedded Facies were interpreted as Distal Marine Sandstone facies in well logs, and Parallel Planar-Bedded Sandstone Facies were interpreted as Proximal Sandstone facies in well logs (Figure 24). Redbed Facies were interpreted as Coastal

Plain/Mudflat facies in well logs, and Belemnite Facies were interpreted in both outcrop and well log (Figure 21, 22, 23).

The first step in establishing chronostratigraphic relationships among the well logs used in this study is identification and correlation of a suitable datum. The maximum flooding surface that is present in the Redwater Shale Member of the Upper Sundance Formation was used as a datum for the well log cross sections (Figures 21 a, b; 22 a, b; and 23 a, b). It was chosen as the datum because maximum flooding surfaces are usually well preserved, laterally extensive, and nearly horizontal surfaces. These qualities make them robust datums for stratigraphic correlation. Maximum flooding surfaces are associated with the time that relative sea level changes from rising to falling and thus are used to approximate isochronous surfaces. Setting the datum of the well log cross sections as the maximum flooding surface provided a time line and helped to establish the correct intervals of well logs to compare to outcrop lithofacies. Facies identified in well logs are based on the lithostratigraphy of outcrops, the geometry of facies associations, and the vertical trends of gamma ray emissions of the logs. Marine flooding surfaces were then identified and correlated between well logs in order to identify parasequences, parasequence sets, interpret systems tracts and sequences, and develop a higher-resolution chronostratigraphy for the Sundance Formation.

The chronostratigraphic correlation presented in this study allows systems tracts to be identified in the Lower Sundance Formation. The High-Angle Cross-bedded Sandstone Facies of the Canyon Springs Sandstone Member of the Lower Sundance Formation is interpreted to represent the lowstand systems tract and early transgressive systems tract. The lowstand systems tract is bound by the subaerial unconformity and its marine correlative conformity at the base, and by the maximum transgressive surface at the top (Catuneanu, 2006). The sharp and unconformable contact of the lower Canyon Springs sandstone with the underlying unit, the Triassic-age Spearfish Formation indicates that this contact is a subaerial unconformity. The High-Angle Cross-bedded Sandstone Facies are overlain by the Flat-Bedded Sandstone Facies of the Canyon Springs Sandstone Member which have

evidence of reworking by marine waters. The lack of transitional facies between these two units, such as lower and upper shoreface facies, indicates that the base of the Flat-Bedded Sandstone Facies is an unconformity likely created by landward migration of a higher-energy shoreline across an eolian environment. This unconformity is interpreted to represent a ravinement or transgressive surface (Figure 21 a, b). The vertical succession of a subaerial unconformity below terrestrial facies, underlying a transgressive surface and sand sheets is consistent with the stacking pattern of the lowstand systems tract, and is not consistent with stacking patterns anticipated in transgressive and highstand systems tracts (Appendix 6) (Figure 21 a, b) (Catuneanu, 2006).

The transgressive systems tract is represented by the upper Canyon Springs Sandstone Member and the lower Stockade Beaver Creek Member (Appendix 6, Figure 21 a, b). The Flat-Bedded Sandstone Facies of the Canyon Springs Sandstone is coarser grained than the underlying sediments, and locally the underlying units are eroded into by this unit. This, along with abraded shell fragments suggest a landward migration of a high energy shoreline environment across an eolian environment created the transgressive sheet sands (Catuneanu, 2006). The marine fossil-bearing mudstones and limestones of the Stockade Beaver Creek Member overlying them represent deposition in open marine water. The transgressive systems tract is bound by the maximum regressive surface at its base and by the maximum flooding surface or condensed section at the top, and forms when rates of sea level rise outpace sedimentation rates at the shoreline (Catuneanu, 2006). The transgressive systems tract develops during intervals when creation of accommodation is at its highest rate, and can be recognized by either retrogradational stacking patterns which result in overall fining-upwards packages in marine successions, or by abrupt transitions between landward facies to seaward facies (Appendix 6). The abrupt transition from eolian sands to marine shales in the Lower Sundance Formation, separated by transgressive sheet sands, are evidence for the beginning of the transgressive systems tract. The condensed section is present in outcrop, and is located in the Mudstone and Limestone Facies. In general, it consists of limestones, specifically mudstones to wackestones, with

wackestones containing bivalve fragments. The packstones contain phosphatic pebbles, bivalve fragments, and shark teeth, and represents the condensed section at the top of the transgressive systems tract (Figures 21, 22 and 23) (Catuneanu, 2006). The stacking pattern of a transgressive surface, underlain by reworked sheet sands, marine mudstones and limestones, and a condensed section are consistent with a transgressive systems tract succession (Appendix 6). In the down-dip cross section, the transgressive systems tract is represented only by marine shales, because the transgressive sheet sands are not preserved in down-dip areas (Figures 23 a, b).

The highstand systems tract (HST) is represented by the Stockade Beaver Shale, Hulett Sandstone, and Lak Members. These Members consist of the Mudstone and Limestone Facies, lower, middle (distal marine sands), and upper shoreface/foreshore facies (proximal marine sands), and the sabkha/coastal plain facies (Figure 21, b, Appendix 6). This systems tract is dominated by a succession of offlapping parasequences (Figure 21 a, b, Figure 7) and is the dominant systems tract in the Lower Sundance. The highstand systems tract is bound by the maximum flooding surface at its base, and by a composite surface at the top, which includes the subaerial unconformity, the basal surface of forced regression, and the oldest portion of the regressive surface of marine erosion (Catuneanu, 2006) .The HST identified in the Sundance Formation is bound below by the maximum flooding surface in the Mudstone and Limestone Facies of the Stockade Beaver Creek Member at its base, and the subaerial deposits of the Lak Member at its top (Figure 21a, b, 22b, 23b). Many workers hypothesize that an unconformity lies above the Redbed Facies, separating the Lower and Upper Sundance (summarized in Johnson, 1992). This unconformity represents a sequence boundary, indicating subaerial exposure and sea level fall. The stacking pattern of a maximum flooding surface, coarsening-upward, progradational parasequences above, and subaerial deposits at the top is consistent with the highstand systems tract (Appendix 6).

The parasequences of the highstand systems tract show a dominance of Mudstone and Limestone Facies coarsening up into marine sandstone facies. In the up-dip areas (S-SE end of cross section, Figures 21 a, b) these proximal sand facies transition into the sabkha or coastal plain facies of the Lak Member. The Mudstone and Limestone Facies are down-dip of the distal marine facies, which are down-dip of the proximal marine facies. The proximal marine facies are down-dip of the coastal plain/sabkha facies. The highstand systems tract generally includes most depositional systems, ranging from fluvial, coastal, shallow marine, and deep marine. However, the bulk of deposits consist of fluvial, coastal and shoreface deposits, and are located close to the basin margin (Catuneanu, 2006). These facies are identified in cross section A-A' (Figures 21 a, b), and provide additional evidence for this interpretation of the highstand systems tract (Appendix 6).

The cyclic nature of deposition in the HST is demonstrated in the stratigraphy by the presence of parasequences and shallowing-upward events (Figure 7). In the Stockade Beaver Creek location, the vertical succession of distal marine, lower, middle, and upper shoreface facies suggest a shallowing upward interval. This interval, overlain by a flooding surface, represents a nearshore parasequence. The interpreted parasequence in the Stockade Beaver Creek location also contains smaller scale shallowing-upward intervals (white arrows, Figure 7 A) consisting of distal marine shales and sands grading up-section into hummocky sand beds. These smaller-scale shallowing-upward intervals suggest possible 5^{th}-order cyclic deposition within the larger-scale parasequence. In the Sundance Type-Section location (Figure 7) three parasequences are represented by shallowing-upward intervals, overlain by distal marine facies indicating an abrupt increase in water depth, interpreted as a flooding surface. These parasequences (black arrows, Figure 7) and higher-order cyclic depositional packages (white arrows, Figure 7 A) within the parasequences are interpreted to represent cyclic deposition in a shallow marine environment. The recurring nature of these packages suggests high-frequency (4^{th} and 5^{th} order) influence on deposition during this interval.

Depositional trends and stacking patterns of the HST are dominated by a combination of aggradation and progradation (Catuneanu, 2006). The early highstand systems tract is associated with relatively higher rates of sea level rise, which results in stacking patterns with strong aggradational trends. Through time, the late highstand systems tract is defined by stronger progradational stacking patterns through time (Catuneanu, 2006). In wells and 49-045-09191, 49-045-07939, and 49-045-22584 (center of Figure 21 a), the aggradational stacking pattern of parasequences is evident, and the aggradation of proximal marine facies approximates the position of the paleoshoreline during this time period. The stacking pattern shifts to progradational as the paleoshoreline moves basinward. The highstand systems tract forms during the late stage of sea level rise, when rates of rise progressively decline below rates of sediment supply, and generate a normal regression of the shoreline (Catuneanu, 2006). The stratigraphy illustrated in the cross section (Figure 21 a, b) displays a long-term regressive trend that is punctuated by multiple higher-frequency cycles, as evidenced by the presence of parasequences. The presence of parasequences are also evident in the stratigraphy of the area (Figure 7). These multiple frequencies suggest an interaction of depositional controlling factors, such as sea level, sediment supply, or tectonic activity.

The variation of facies in the highstand systems tract is evident when comparing the up-dip areas and down-dip areas (Figure 22 a, b; 23 a, b). In the up-dip areas, the marine Mudstone and Limestone Facies, distal marine sand facies, and proximal marine sand facies are relatively minor facies, compared to the coastal plain/sabkha facies, which generally represent the HST (Figure 23 a). Conversely, in the down-dip areas, the dominant facies are the Mudstone and Limestone Facies, distal marine sands, and proximal marine sands; the coastal plain/sabkha facies are not present (Figure 22 a). The absence of terrestrial facies is consistent with the interpretation of this profile being located in a more distal shelf location (Catuneanu, 2006).

The stratigraphy presented in cross section A-A' shows a normal regression of the shoreline represented by the Mudstone and Limestone Facies, distal and proximal marine sandstone facies, and coastal plain/sabkha facies, as described above. A stratigraphic complex is identified from the correlated well logs (left of Figure 21 a, b, Figures 23 a, b) that is interpreted as transgressive facies of the second marine inundation of the Upper Sundance Formation. This complex is not exposed in outcrop, rather, the stratigraphy shows an overall normal regression, as described above in the stratigraphic architecture section. Since outcrop data is not available, the well log data is the highest-resolution data available for correlation and interpretation. The interpretation of these facies with well log data alone is not fail-proof (Cant 1992), however, lacking outcrop data, the interpretation is based on the signature of the gamma ray emission of the logs, and the lateral association of known facies.

The well logs in Figure 15a, and b, specifically logs 49-011-05297, 49-011-05069, 49-045-21157, and 49-045-09191 show a distinct gamma ray emission pattern above the proximal marine sand facies. The relatively lower gamma ray emission, coarsening-upward patterns that display an overall backstepping pattern indicate these facies are unlikely to be distal or proximal marine sand facies related to the earlier normal regression that occur below and further up-dip (Figure 21 a, b). The backstepping pattern suggests a transgressive event, and the pattern exhibited is not consistent with the prograding shoreline environment, or with the coastal plain/sabkha facies up-dip of the proximal marine sands. It is also not consistent with a lagoonal environment that may be present land-ward of upper-shoreface to foreshore deposits. Lagoonal deposits, which are dominated by fine-grained siliciclastics, sand-sheet overwash deposits, and coals would not produce such a regular, coarsening-upward backstepping pattern as is displayed. They would likely display an overall high gamma ray emission, irregular pattern due to the fine-grained, variable nature of the deposits (Reinson, 1984). However, fluvial infill may produce the coarsening-upward trend.

This study's interpretation of these facies is that they consist of coarsening-upward fluvio-deltaic and estuarine sediments that are part of the transgressive systems tract, related to the marine inundation associated with the deposition of the Redwater Shale Member of the Upper Sundance. These deposits were likely preserved in an incised-valley, fluvio-deltaic and estuarine sediments would likely fill an incised valley formed during sea level rise, and the valley likely formed due to river erosion during a sea level fall, or after the Early Sundance Sea retreated (Dalrymple et al., 1994).

The coarsening-upward pattern is correlated down-dip to sandy facies that are interpreted to be estuarine mouth sands (Figure 21 a, b, Figure 23 a, b). Dalrymple et al. (1992) describes that in both tide-dominated and wave-dominated estuarine settings, sand bodies are created at the mouth of the estuary. In a tide dominated setting, elongate sand bars typically develop due to increased tidal-current energy at the estuarine mouth (Dalrymple et al., 1992). In wave-dominated settings, the sand typically forms a barrier and flood-tidal deltas in the estuarine mouth (Dalrymple et al., 1992). This could account for the thick, amalgamated sand bodies down-dip of the coarsening-upwards fluviodeltaic facies. Uhlir et al. (1988) provides evidence for the influence of tidal regimes in the Upper Sundance, describing a 20 meter thick tidal inlet, backbarrier shoal, and sandy tidal-flat sequence deposited in north-central Wyoming. This indicates that tidal forces were active in the Late Sundance seaway, and suggests that tides may have had influences on estuarine facies during the marine inundation.

Wave-ravinement sand-sheet deposits top the transgressive valley fill, and indicate the reworking of sediments during the second inundation by marine waters (Catuneanu, 2006, Zaitlin, 1994). These sand facies are represented in well logs by a significantly low gamma spike, indicating coarser-grained materials are present. They are not laterally continuous and present only in down-dip areas (Figure 21 a, b, Figure 23 a, b). The sand and wave ravinement surface above it indicate the

beginning of another marine inundation, and the transgressive systems tract is bound by the maximum-flooding surface above, which is used as the datum (Figure 21 a, b; 22 a, b; 23a, b). The fine-grained nature of the Belemnite Facies of the Redwater Shale Member of the Upper Sundance Formation is reflected by the high gamma ray emissions displayed (Figure 21a, b; 22 a, b; 23 a, b). This unit is hypothesized to contain parasequences based on field data and other studies, due to the transition from fining-upward to coarsening-upward sediments (summarized in Johnson, 1992). However, the overall fine-grained nature of the unit makes it difficult to identify these parasequences in cross section and outcrop. Johnson (1992) indicates that this unit represents the most widespread marine inundation of the Jurassic.

V. DISCUSSION

1. Age of the Sundance Formation

Ages are important in stratigraphic studies to constrain depositional time scales and global sea level changes. Different studies have published various ages for the Sundance Formation, and significant differences exist in published age data. Robinson et al. (1964) estimate the age of the Stockade Beaver Creek Member, Hulett Member, and Lak Members as Callovian, and the Redwater Shale Member as Oxfordian, based on previous work by Imlay (1947, 1952, 1957), Schmitt (1953), and Peterson (1954, 1957, 1958). Robinson et al. (1964) make no mention of possible ages for the Canyon Springs, and in the published stratigraphic column, the Canyon Springs Member is placed in the Lower Callovian. Many other studies concur with these ages, including Doyle (1984) and Rautman (1976, 1978). Imlay (1980) based his age constraints on abundant faunal data and estimated that the Canyon Springs Sandstone is late Bathonian, the Stockade Beaver Creek is Late Bathonian, the Hulett Sandstone is earliest Callovian, and the Lak Member is early to possibly middle Callovian (Figure 2). The Redwater Shale Member is estimated to be early Oxfordian. Using the 2009 GSA timescale as calibration (Walker, 1999), the Lower Sundance was deposited in approximately 4

million years, and the Lower and Upper Sundance were deposited in 8-9 million years, including the J-4 unconformity (Figure 2). These ages are used in this study because of the extensive fossil evidence Imlay (1980) reported.

2. Controls on Deposition and Stratigraphic Architecture

Characterizing global climatic conditions during the Jurassic is important for understanding the stratigraphic framework and controls on Sundance deposition. During the Jurassic, high sea-floor spreading rates associated with the break-up of Pangea produced relatively high global sea level, resulting in many epeiric seaways (Ziegler et al., 2003, Kauffman and Caldwell, 1993, Rees et al., 2000). The Gulf of Mexico and the northeast-trending central Atlantic opened due to this rifting, and the North American plate migrated northward and rotated clockwise until the southern coast was roughly parallel to the 30° latitude line (Rees et al., 2000) (Figure 25). As North America moved through the subtropical belt toward the temperate climate belt during the Mesozoic the climate changed from hot and arid equatorial conditions toward more humid, temperate conditions (Brenner and Peterson, 1994, Johnson, 1992).

The Middle to Late Jurassic is characterized by greenhouse climatic conditions that lacked evidence of glaciers (Frakes, 1979; Coe et al., 2003, Rees et al., 2000, Rees et al., 2004). During intervals of icehouse conditions of Earth's history, glacioeustacy is believed to have a major role in controlling the higher-frequency cyclicity that is preserved in the stratigraphic architecture of marine and marginal marine sediments (Plint, 1992). During Icehouse intervals, variation in Earth's orbital parameters (obliquity, precession, and eccentricity) trigger changes in insolation, which leads to rapid expansion and contraction of ice sheets and high-frequency glacioeustic change. There is no evidence of tundra, glacial biomes or till within Jurassic strata; suggesting that this interval was not

subjected to icehouse conditions (Frakes, 1979; Rees et al., 2000). Therefore, glacioeustacy was not a major influence on the deposition and evolution of the of the Sundance Formation.

Jurassic climate belts have been extensively modeled. It's been proposed that five main biomes existed worldwide: seasonally dry (summerwet or subtropical), desert, warm temperate, cool temperate, and seasonally dry (winterwet) (Rees et al., 2000, Rees et al., 2004) (Figure 26). Over long time periods, continents moved through these different biomes, which maintained near-constant paleolatitude boundaries (Rees et al., 2000). Ziegler et al. (2003) show that the likely cause of the transition from evaporites to temperate coals in parts of western North America is due to this northward craton migration and not widespread climate change. This interpretation is supported by the coeval stratigraphy in Asia that shows the reverse trend of temperate coals to evaporites (Rees et al., 2000). This work is based on climate models, biogeographical studies of fossil groups, and spatial distributions of climate-sensitive rock types such as coals, peats and carbonates.

The facies of the Sundance Formation displays the overall shift from carbonates and evaporites to the dominance of siliciclastics during the Middle and Late Jurassic in the Western interior. The stratigraphy indicates that the climate changed from warm and arid, which produced predominantly evaporites, carbonates, and fine-grained siliciclastics, such as the deposits of the Gypsum Springs Formation (Johnson, 1992, Imlay, 1980, Brenner and Peterson, 1994), to more humid and temperate conditions, which produce coarser-grained siliciclastics, minor carbonates, and a general lack of evaporites, such as the deposits of the Lower and Upper Sundance Formations, and the Morrison Formation (Johnson, 1992). The poleward drift of North America through different biomes during the Jurassic is thought to be the cause for the shift from carbonates, evaporates and minor fine-grained siliciclastics to the siliciclastic-dominant stratigraphy of the Sundance Formation. Likely mechanisms for the higher-order cyclicity that is present in the stratigraphy of the Sundance Formation are explored below.

Global sea level change is probably responsible for the third-order change in relative sea level interpreted from the stratigraphy of the Sundance. A local relative sea level curve was constructed based on the temporal variation in facies and stratigraphic surfaces within the Lower Sundance and numerous descriptions of the stratigraphy of underlying and overlying units (Figure 27) (summarized in Johnson, 1992). The trend of the third-order relative sea level cycles on the local relative sea level curve is consistent with that of the global eustatic curve of the Mesozoic (Haq et al., 1988), which suggests that the regional third-order trend of relatively slow sea level change controlled the overall transgression and regressions that occurred locally, especially in the Lower Sundance Formation.

In addition to global sea level changes, local accommodation changes may have had an effect on deposition of the Sundance Formation. Regionally, the study area was located on a quiet, passive margin shelf (Johnson, 1992) where subsidence rates were very low. Pipiringos and O'Sullivan (1978) estimate the subsidence rate during the Late Jurassic in the Williston Basin in Montana (north of the study area) to be approximately 0.01 millimeters per year, and the subsidence rate in the medial part of the basin to be 0.07millimeters per year. Relative to third-order eustatic cycles, the subsidence rates of the study area were essentially constant. The local sea level curve constructed in this study compares favorably with the global eustatic curve, and given the small variation in subsidence rates of the area, it appears that the accommodation variation that is associated with relative sea level change in the area was driven by the third-order global eustatic change. Higher-frequency, asymmetrical transgressive-regressive cycles, or parasequences, are also present in the stratigraphy (Figure 7). Given that there is no evidence of glacioeustatic control on higher-frequency eustatic change, and subsidence rates are constant, there does not appear to be an accommodation-related mechanism that could have produced the parasequences.

Global and regional climate patterns also likely affected the stratigraphic architecture of the Sundance Formation. One factor affecting local precipitation rates is the Inter-Tropical Convergence

Zone (Figure 25). The ITCZ occurs where winds from the northern and southern hemisphere converge near the equator, and form a low-pressure belt in the equatorial region associated with high precipitation. The position of this precipitation belt can cause drought or flooding depending on the migration path. At the beginning of the Jurassic, the study area was located at approximately 15° and 20° N latitude and migrated northward to approximately 35° to 40° N latitude by Late Jurassic time (Figure 25) (Kocurek and Dott, 1983, Rees et al., 2000). It is estimated that the ITCZ migrated during this time to its present-day summer position, at approximately 40° N latitude (Kocurek and Dott, 1983). It's likely that through variance in the migration of the ITCZ and the associated Hadley circulation cells, more humid, wetter conditions affected the study area during the Mid- to Late Jurassic. Rees et al. (2000) note that due to the presence of a large continental land-mass at the equator, much of this land-mass was arid, and the ITCZ latitudinal excursion would have been more extreme (Figure 25) (Ziegler et al., 1987). Rees et al. (2000) indicate that Hadley cells and the Intertropical Convergence Zone (ITCZ) are the primary driving forces of the spatial distribution of key tropical sediment types during warm periods of earth's history. The latitudinal distribution of climatically-sensitive sediments, such as coal and evaporites, does not change through time, suggesting that the controls over the circulation patterns that operate today (ITCZ and Hadley Cell) were probably the same through time (Ziegler et al., 2003) (Figure 28). The latitudinal position of the sub-tropical high associated with Hadley and Ferrel Cell circulation was likely the same during the Jurassic as it is today (Ziegler et al, 2003) (Figure 28). The evidence presented above shows how increased moisture could have migrated in and out of the study area, causing cyclic variations in precipitation rates and thus changes in sediment flux. This would create cyclic sedimentary pulses in the study area, without the influence from active tectonic uplift.

The circulation patterns associated with Hadley and Ferrel cells also likely influenced the study area (Figure 28). During times of high insolation the Hadley cells enlarge while the Ferrel cells shrink, due to the increased heat at the equator. This causes the descending arm of the Hadley cell to

migrate poleward, and bring warm, dry air to northern regions (Figure 28) (Perlmutter and Matthews, 1989). During times of low insolation, the Hadley cells shrink and the Ferrel cells enlarge, bringing more moisture to lower latitudes (Perlmutter and Matthews, 1989). These climate belts, or biomes, migrated due to the expansion and contraction of Hadley and Ferrel cells (Figure 26, 28) (Perlmutter and Matthews, 1989, Frakes 1979). These changes in precipitation rates and influx of sediment, coupled with the movement of the ITCZ, likely affected the Sundance Formation depositional framework, accounting for the cyclic parasequences observed.

Cyclic variation in solar insolation, driven by changes in Earth's orbital parameters (Milankovitch cycles) also influenced global climate during the Middle and Late Jurassic. Strasser et al.. (2000) and Huang et al. (2009) give evidence that high frequency Milankovitch cyclicity was active during this time interval, implying that Milankovitch cyclicity altered the magnitude of solar insolation. Particularly, Huang et al. (2009) point out that the dominant Milankovitch forcing during the Late Jurassic is the 405-kyr eccentricity cycle observed in the deep-sea sediments of the late Jurassic Kimmeridge Clay found in Dorset, England. Strasser et al. (2000) stressed the importance of the 400-kyr cycle in forming sequence boundaries in carbonate-dominated sequences during this time period, and noted the importance of the regional subsidence pattern and long-term, tectono-eustatic trend of accommodation change in formation of beds, bedsets and sequence boundaries.

Carbonate-dominated systems produce their own sediments which makes them different from siliciclastic systems having externally derived sediment input. However, the sequence boundaries that form in 400-kyr cycles in the carbonate-dominated stratigraphy of the Strasser et al. study (2000) are interpreted to be formed by sea level changes. In this study, the long-term trend of regression punctuated by asymmetrical transgressive-regressive cycles lacks unconformities and thus is not interpreted as a product of low-amplitude sea level changes superimposed on the long-term regressive signal. I interpret these cycles as the result of a product of sediment input fluctuation, which are likely

controlled by Milankovitch-forcing, as there is evidence of its effect in other contemporaneous sediments (Strasser et al., 2000, Huang et al., 2010).

Milankovitch cycles have a large effect on the expansion and contraction of climate belts through time. Climate belts are not completely stationary, but migrate to a small degree according to variation in the magnitude of insolation received by the Earth (Perlmutter and Matthews, 1989). As described above, the North American craton migrated through different climate belts during the Jurassic, but the distribution of these belts was likely affected by shorter-term changes due to Milankovitch forcing. Change in the position and width of these climate belts and thus humidity could have provided the mechanism for the observed changes in sediment supply at shorter-term Milankovitch frequencies. Regular changes in climate directly affect weathering processes and rates, runoff, and potential sediment transport to a system (Perlmutter and Matthews, 1989). These variables, interacting with provenance and other factors such as topography, control sediment yield to a basin. Perlmutter and Matthews (1989) modeled the variations in the position and width of these climate belts as modulated by Milankovitch forcing during the Jurassic. Given that the Jurassic was a greenhouse period, and the study area was predicted to lie between 35° and 40° N latitude (Kocurek and Dott, 1983, Rees et al., 2000), the migration of temperate arid to temperate humid climate belts is hypothesized, using models based on a climatic maximum (Perlmutter and Matthews, 1989).

Based on the presence of higher-frequency, transgressive-regressive cycles present in the stratigraphy (Figure 7), the lack of sequence boundaries signifying negative accommodation, and the lack of evidence of tectonic influence in the study area, it appears that during deposition of the Sundance Formation, Milankovitch insolation variation triggered cyclic changes in sedimentation rates that shaped the stratigraphy of the area. The climate belt migration caused the expansion of the Hadley cell during times of high insolation, bringing more arid conditions to the study area. During times of low insolation, the Hadley cell shrank, and more moisture was brought to the study area,

producing a winterwet climate (Figure 26, 28). These regular cycles of change in the amount of moisture to the area caused a change in precipitation and erosion and sediment flux. With increased precipitation, increased sediment was deposited in the Sundance basin and available accommodation was filled. During times of low precipitation, the sediment flux waned while subsidence continued, causing transgressions and flooding surfaces to develop in the basin.

While there is not a simple correlation between an increase in precipitation and an increase in sediment yield (Wilson, 1973), higher erosion rates occur in seasonal climates (with a rainy season and dry season) than in non-seasonal climates (year-round moisture or aridity). These conditions are characteristic of the winterwet climate predicted for the study area during times of low insolation (Rees et al., 2000). Increased precipitation during the winter months produces higher erosion rates and thus an increase in sediment yield to the Sundance Basin. During times of high insolation and expansion of the Hadley cell, precipitation was probably low, as sediment yield is lower in non-seasonal climates (Wilson, 1973).

Lengbein and Schumm (1958) note that peak sediment yield occurs at approximately 12 inches (300 mm) of mean annual precipitation. This rate of precipitation would correspond to a semi-arid climate. In areas that have higher average precipitation rates, vegetation cover increases and protects the ground from erosional processes. In drier areas, the plant cover is insufficient to reduce erosion, but lower rates of rainfall preclude sediment erosion (Lengbein and Schumm, 1958). The strata of the Sundance lacks evidence of plant fossils, woody debris, and root structures, which indicates that vegetative cover was minimal, and the cyclic variation in precipitation was sufficient enough to cause significant changes in sediment supply to the basin. During times of low insolation and winter-wet climatic conditions, precipitation was likely not high enough to increase vegetative cover, given the lack of woody and vegetative fossils and root structures.

3. Model of Deposition

The following depositional model is proposed for the Sundance Formation in the study area. In the Lower Sundance Formation, the High-Angle Cross-bedded Sandstone Facies was deposited in an eolian environment as dunes, and transgression by the Sundance Sea re-worked these eolian deposits to form the Flat-Bedded Sandstone Facies. Given the limited lateral extent of these facies, these units probably were only preserved in paleovalleys in the Spearfish Formation.

The Mudstone and Limestone Facies of the Stockade Beaver Creek Member were deposited after an interval of sea level rise, and after the marginal marine facies of the Flat-Bedded Sandstones of the upper Canyon Springs Member were deposited. Deposition of the Stockade Beaver Creek is part of a coarsening upward succession which includes the Bioturbated Facies, Low-angle Cross-bedded Facies, the Parallel Planar-Bedded Sandstone, and the Incised Sandstone Facies of the Hulett Sandstone, during an interval in which there was a combination of a decrease in the rate of rise in relative sea level, accompanied by an increase in sediment supply, leading to infill of accommodation more rapidly than it was created (Figure 29). The Redbed Facies of the Lak Member was deposited in a subaerial, sabkha-type environment, and the Belemnite Facies, which overlies the Redbed Facies, was deposited during the transgression of the Late Sundance Sea, and is associated with a 3rd order flooding event, shown by an inflection point on the 3rd order relative sea level curve (Figure 27).

The chronostratigraphic framework of the Sundance Formation presented in this study indicates that a combination of fluctuations in sediment supply as well as eustacy controlled deposition of the lower Sundance. The evidence presented in the stratigraphy of the Sundance, along with the controls discussed above imply that the lower Sundance Formation was deposited on a passive margin shelf with low subsidence rates (Pipiringos and O'Sullivan, 1978). During times of climatic minimums, precipitation and sediment flux was at its maximum for the area, and available accommodation in the basin was filled. During climatic maximums, precipitation was minimal due to

the expansion of the Hadley cell, which brought arid air to the study area. Sediment flux to the basin was essentially shut off during these time periods. The Milankovitch-driven variation in climate, from an arid climate to a winterwet climate was essential in producing the stratigraphy of the Sundance.

The Lower Sundance Formation spans approximately 4 million years, as previously discussed. Using these age constraints, the timing of the transgression and regression of the Lower Sundance is approximately 4 million years. The timing of this transgressive/regressive event suggests that it is probably a third-order relative sea level cycle (Vail et al., 1991).

The higher frequency cycles of the Lower Sundance suggest that third-order sea level change is not the only control on stratal architecture in the Lower Sundance (Figure 7). The periodicity of these cycles averages between approximately 437,500 - 500,000 years (eight cycles over the approximate period of 3.5-4 million years), so Milankovitch forcing is plausible. Given the incompleteness of the stratigraphic record, more cycles likely were deposited but not preserved. If this is the case, the timing of cyclicity would be closer to Milankovitch eccentricity periodicity of 405 kyr. Sediment pulses driven by active tectonic uplift is unlikely, due to the quiet passive margin tectonic setting (Johnson, 1992, Lawton, 1994). However, slight perturbations of climate may cause sediment pulses, and thus the higher-frequency cycles superimposed on the longer-term regression. Data presented in this study show that during greenhouse intervals, higher-frequency fourth or fifth order fluctuations occur and are evident in the stratigraphy of the time.

4. Interpretation of Facies

Because of the lack of outcrop associated with the fluvio-deltaic and estuarine facies, the best approximation of what they consist is based on the architecture and stacking patterns seen in well logs (Figure 21 a, 23). The stratigraphy shown indicates sandier facies down-dip, and coarsening-upward facies up-dip (Figure 21 a, green and brown facies). If these facies were falling-stage deposits associated with higher-frequency fourth and fifth order accommodation variations or sea level

fluctuations, the stratigraphy would contain evidence of forced regressions associated with higher-frequency sea level variations (Posamentier and Vail, 1988). Similarly, if the deposits were lowstand deposits associated with higher-frequency fourth and fifth order negative accommodation events, the stratigraphy would reflect the same. However, if the cyclicity was caused by sediment input variations rather than accommodation variations, unconformities and forced regressive deposits would not be present. The stratigraphy displayed in the cross sections lacks evidence on negative accommodation events (incision and abrupt vertical transitions from marine to terrestrial facies) and is consistent with sediment supply fluctuation as the primary driver for creating the high frequency cyclicity of the stratigraphy (Figure 21 a). Therefore, these facies are interpreted to consist of coarsening upwards, fluviodeltaic deposits aggrading, then retrograding through time in response to fluctuations in sediment supply.

Zaitlin et al. (1994) predict a change in fluvial style in response to rising sea level. They theorize that fluvial systems within incised valleys generate an overall fining-upward succession during intervals of rising relative sea level. The overall fining-upward pattern of the fluvio-deltaic sediments observed in the study area (Figures 21 a, b; Figures 23 a, b) is consistent with the trend described by Zaitlin et al. (1994). The higher-order coarsening-upward trends superimposed on the overall fining-upward succession are interpreted as sediment fill of the valley over shorter time scales.

VI. CONCLUSIONS

1. The use of both outcrop and well log data in the chronostratigraphic correlation of the Sundance Formation allowed for identification of plausible forcing mechanisms on deposition in a greenhouse world.

2. Despite the lack of glacio-eustatic forcing on deposition, higher-frequency cyclicity was produced and evident in the stratigraphy of the Sundance Formation.

3. The stratigraphy of the Lower and Upper Sundance shows a shift in the dominance of carbonates, evaporites, and fine-grained siliciclastics of the underlying Formations, to siliciclastics and minor carbonates. This reflects the migration of the study area through arid, dry climatic conditions to more humid, seasonal, wetter conditions.

4. The stratigraphy of the Sundance Formation shows the presence of high-frequency sediment pulses, likely caused by Milankovitch-induced climatic forcing, superimposed on a long-term regressive trend in the Lower Sundance, and transgressive trend in the Upper Sundance.

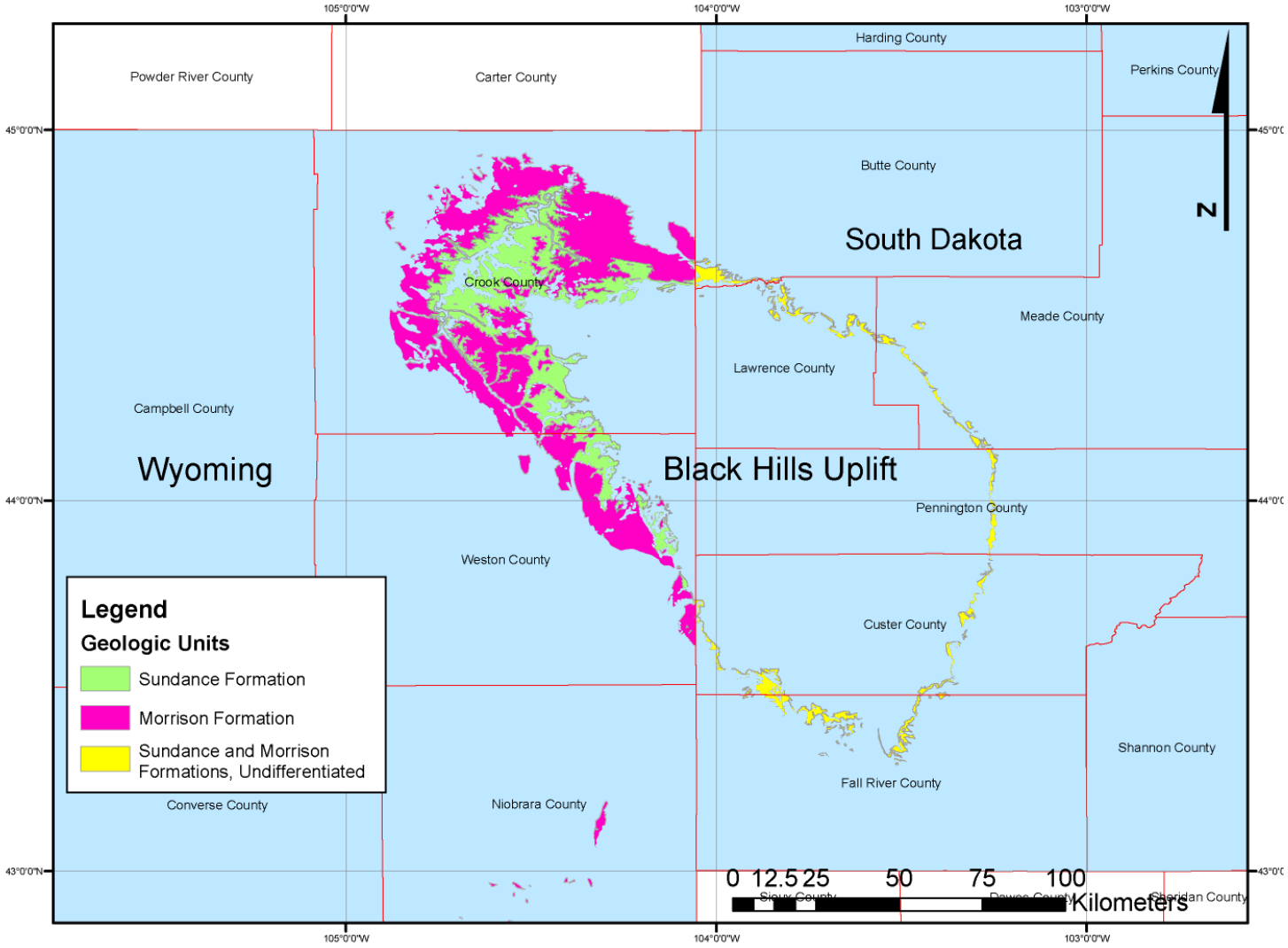

Figure 1. Outcrops of the Sundance and Morrison Formations in the Black Hills area, Wyoming and South Dakota.

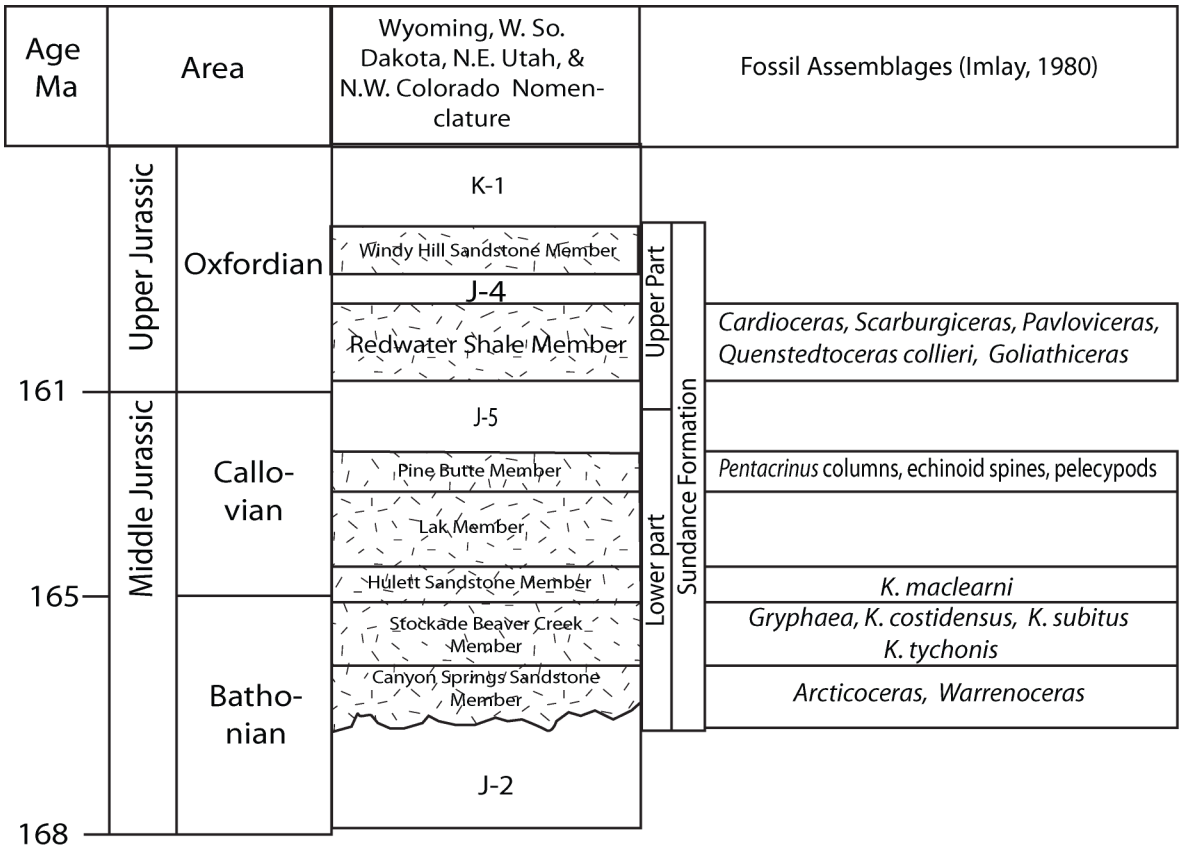

Figure 2. Generalized Stratigraphy of Jurassic Rocks in the Black Hills area. J-2, J-4, J-5, and K-1 represent unconformites discussed in the text. Modified from Johnson, 1992, and Brenner and Peterson, 1994. Fossil Data from Imlay, 1980.

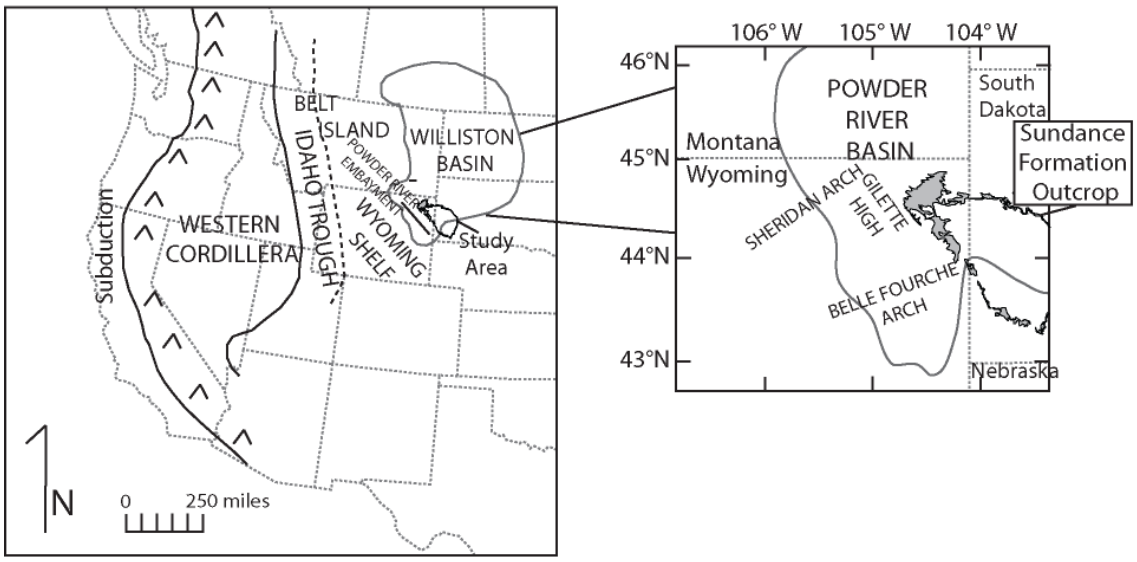

Figure 3. Relations between tectonic regime and the Sundance area of deposition, and tectonic elements in the Black Hills region. Modified from Johnson, 1992.

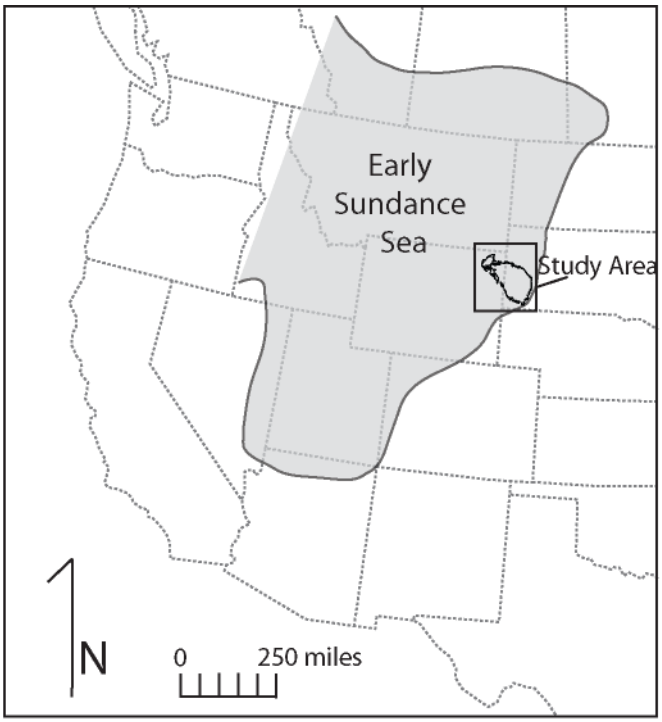

Figure 4. Extent of the early Sundance Sea, and current outcrops of the Sundance Formation in the Black Hills area, Wyoming and South Dakota. Modified from Johnson, 1992, and Brenner, 1983.

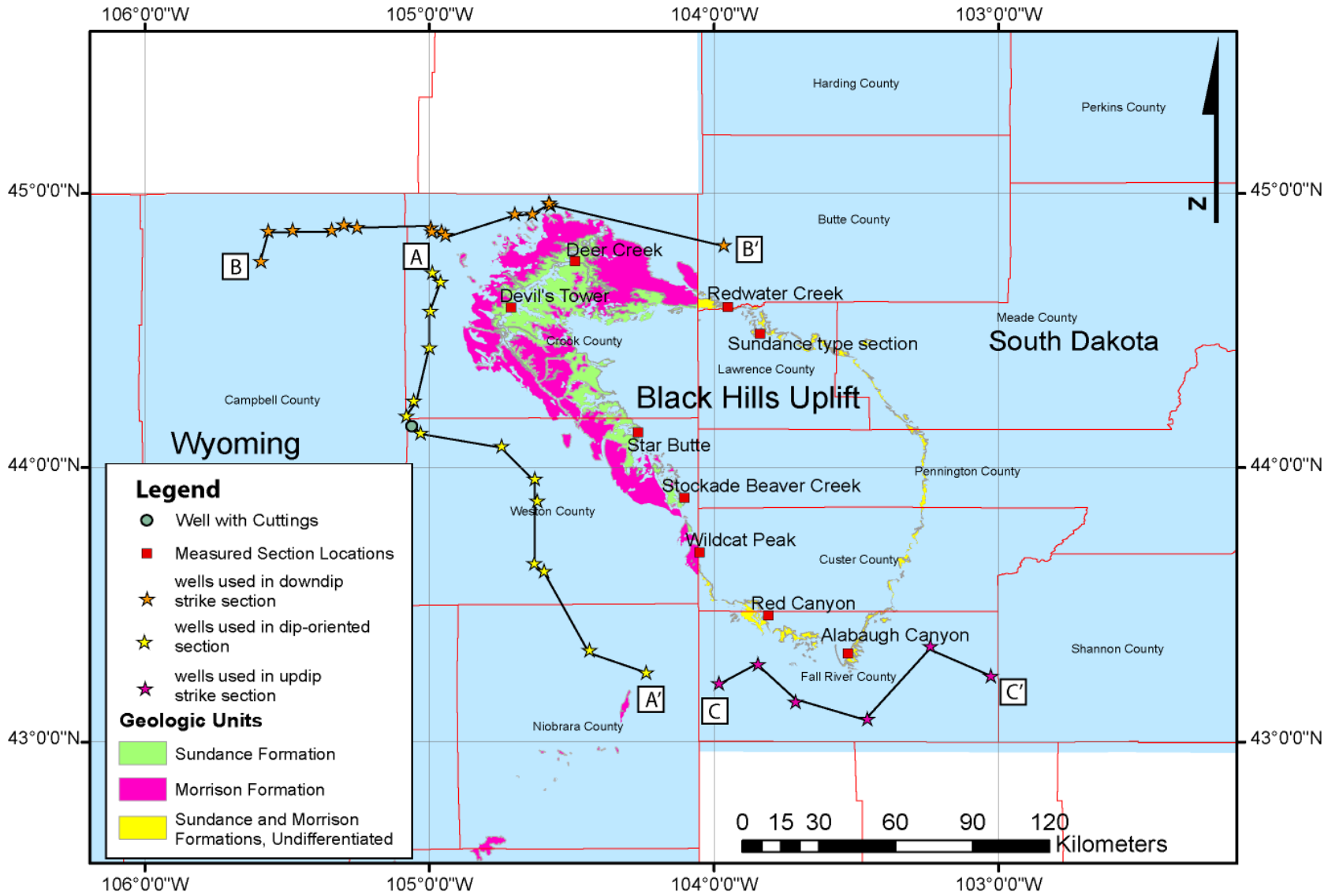

Figure 5. Sundance and Morrison Formation Outcrops, Measured Section Locations, Cuttings Location, and Cross Section Locations, Black Hills, South Dakota and Wyoming.

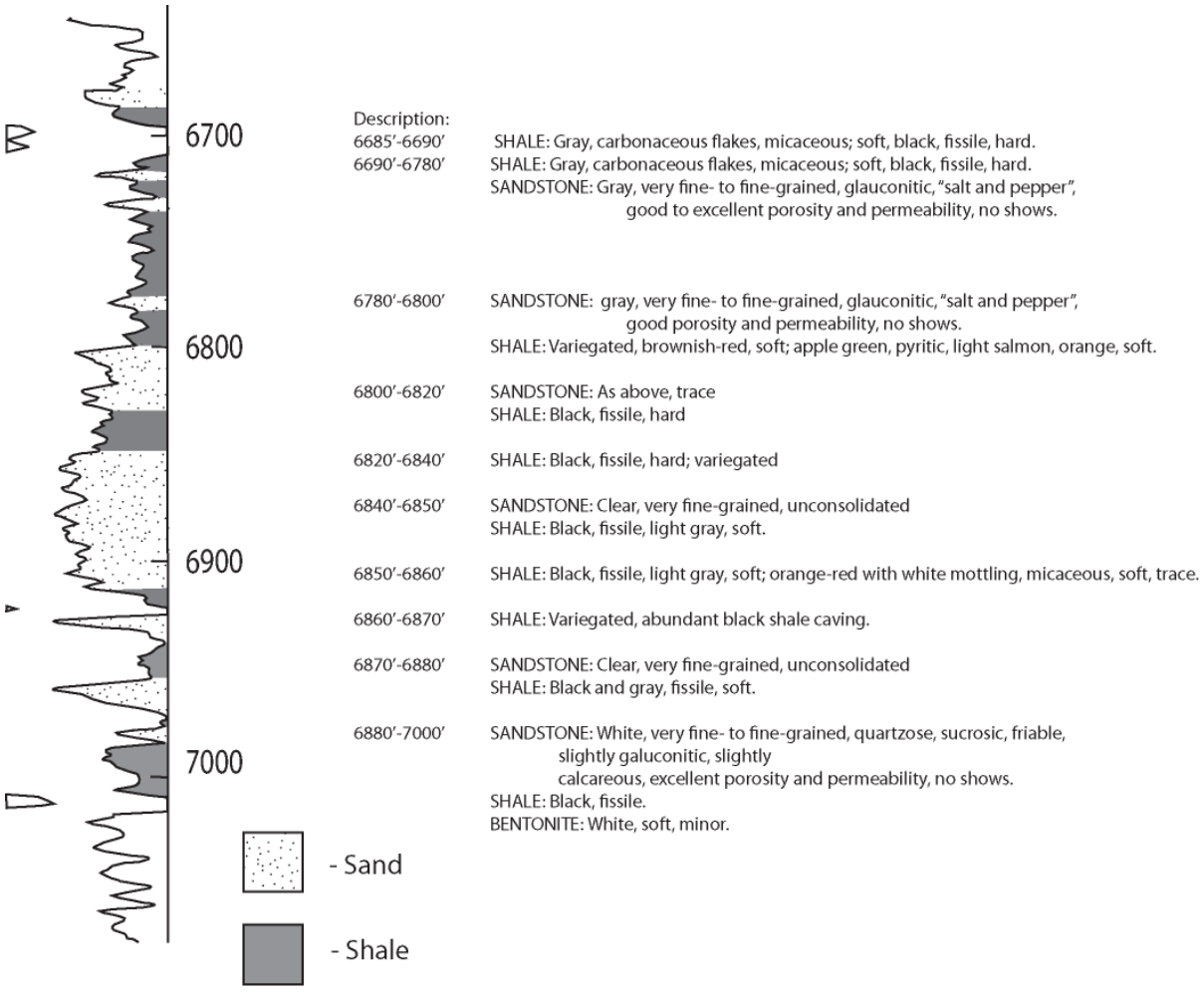

Figure 6. Description of Core from Krauss Patented 1 well, located in Crook County, Wyoming. Lithologies illustrated on Gamma Ray are interpretted from the description of the core and the signature of the log.

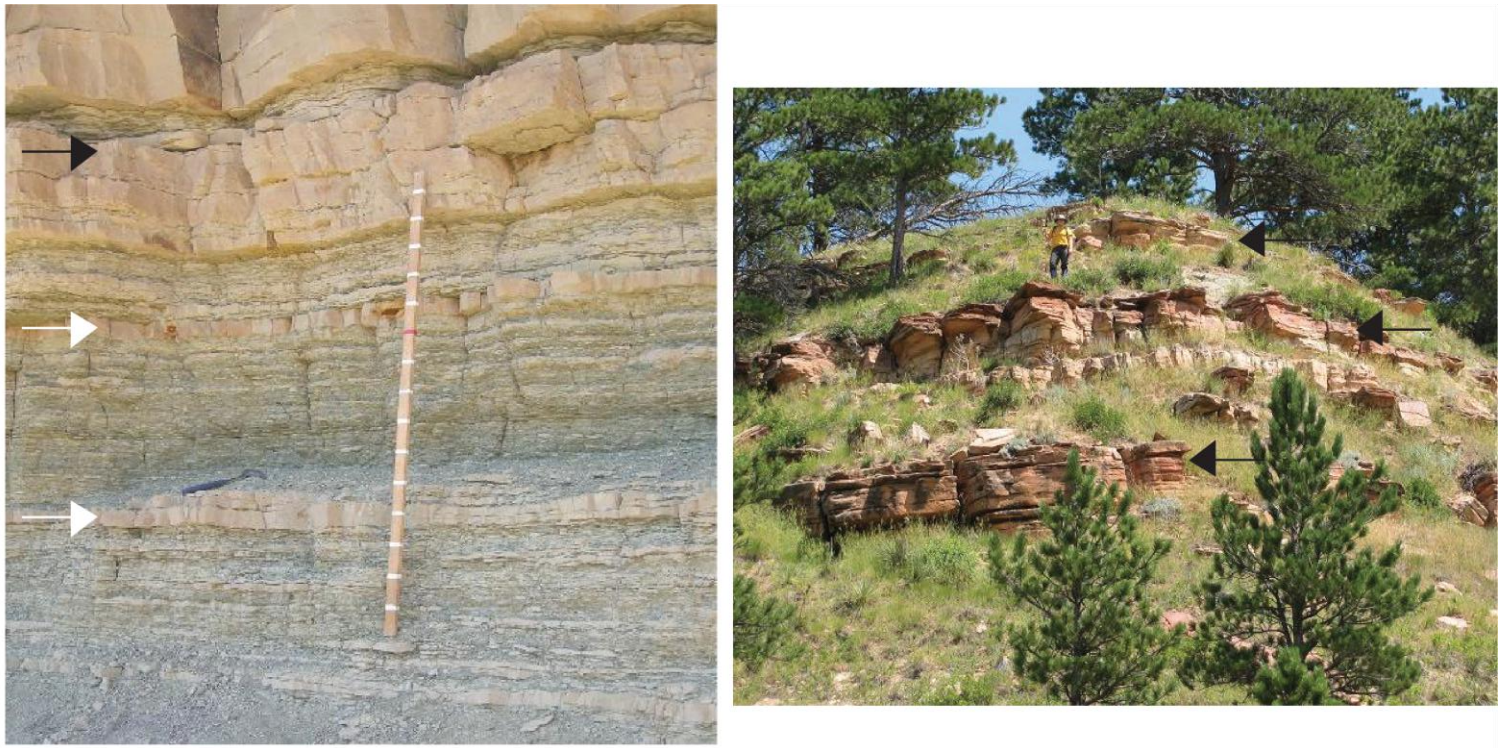

Figure 7. Example of parasequences at A) the Stockade Beaver Creek location and B) the Sundance Type-Section. Black arrows indicate flooding surfaces and parasequence boundaries. A) Outcrop at Stockade Beaver Creek location displays high-order depositional events (white arrows, described in text). Jacob's Staff for scale (meters) B) Field Assistant for scale.

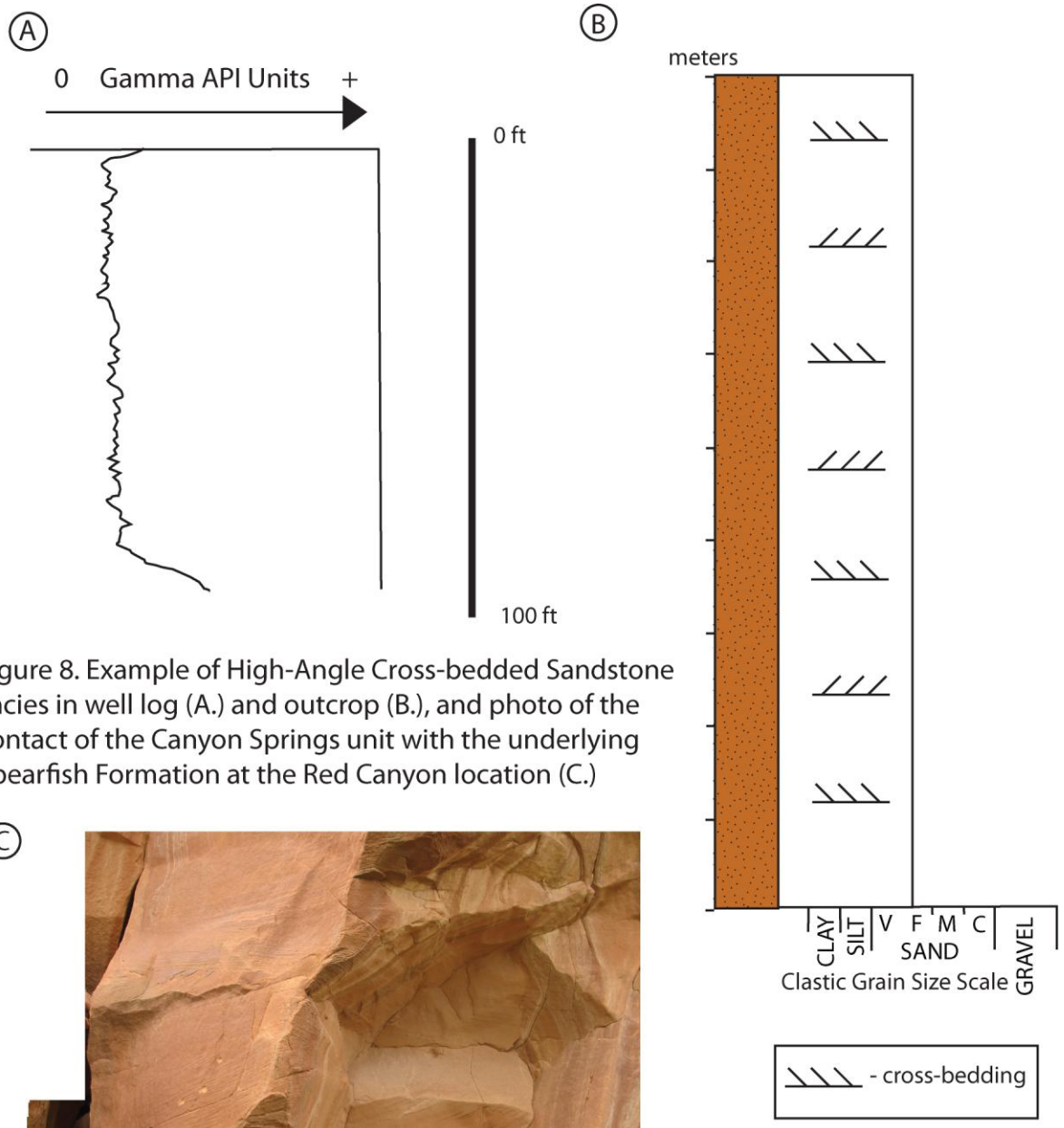

Figure 8. Example of High-Angle Cross-bedded Sandstone Facies in well log (A.) and outcrop (B.), and photo of the contact of the Canyon Springs unit with the underlying Spearfish Formation at the Red Canyon location (C.)

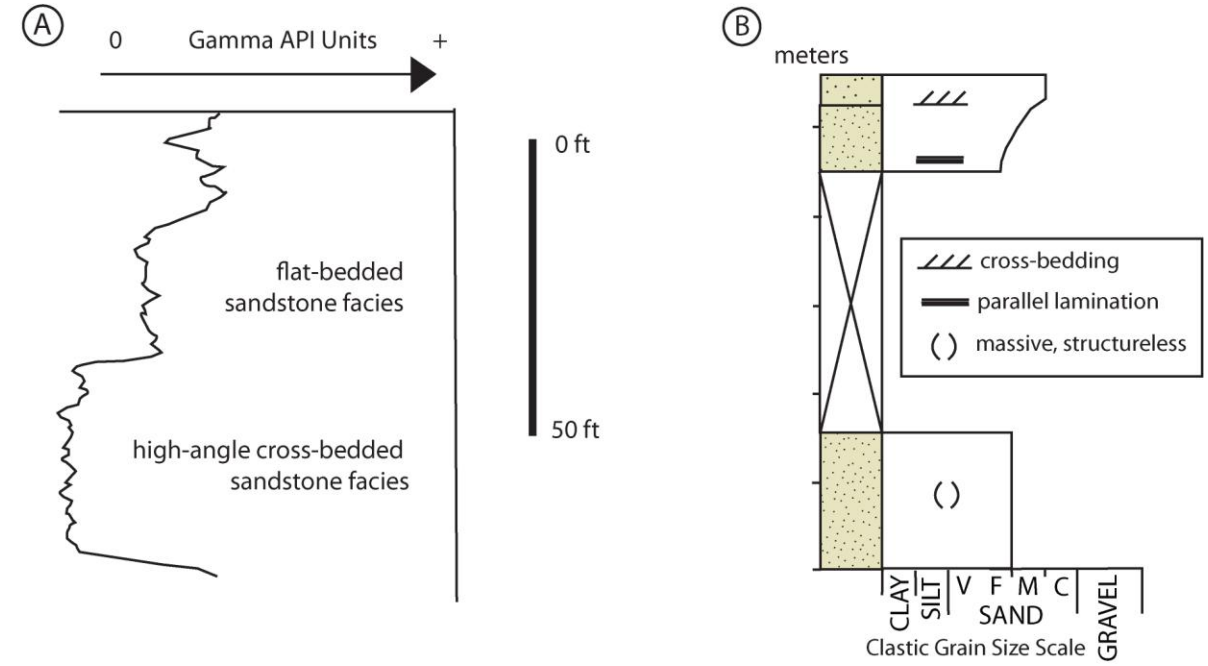

Figure 9. Example of Flat-Bedded Sandstone Facies in well log (A.) and outcrop (B.), and photo of the High-Angle Cross-Bedded Sandstone Facies and Flat-Bedded Sandstone facies at the Red Canyon location (C.)

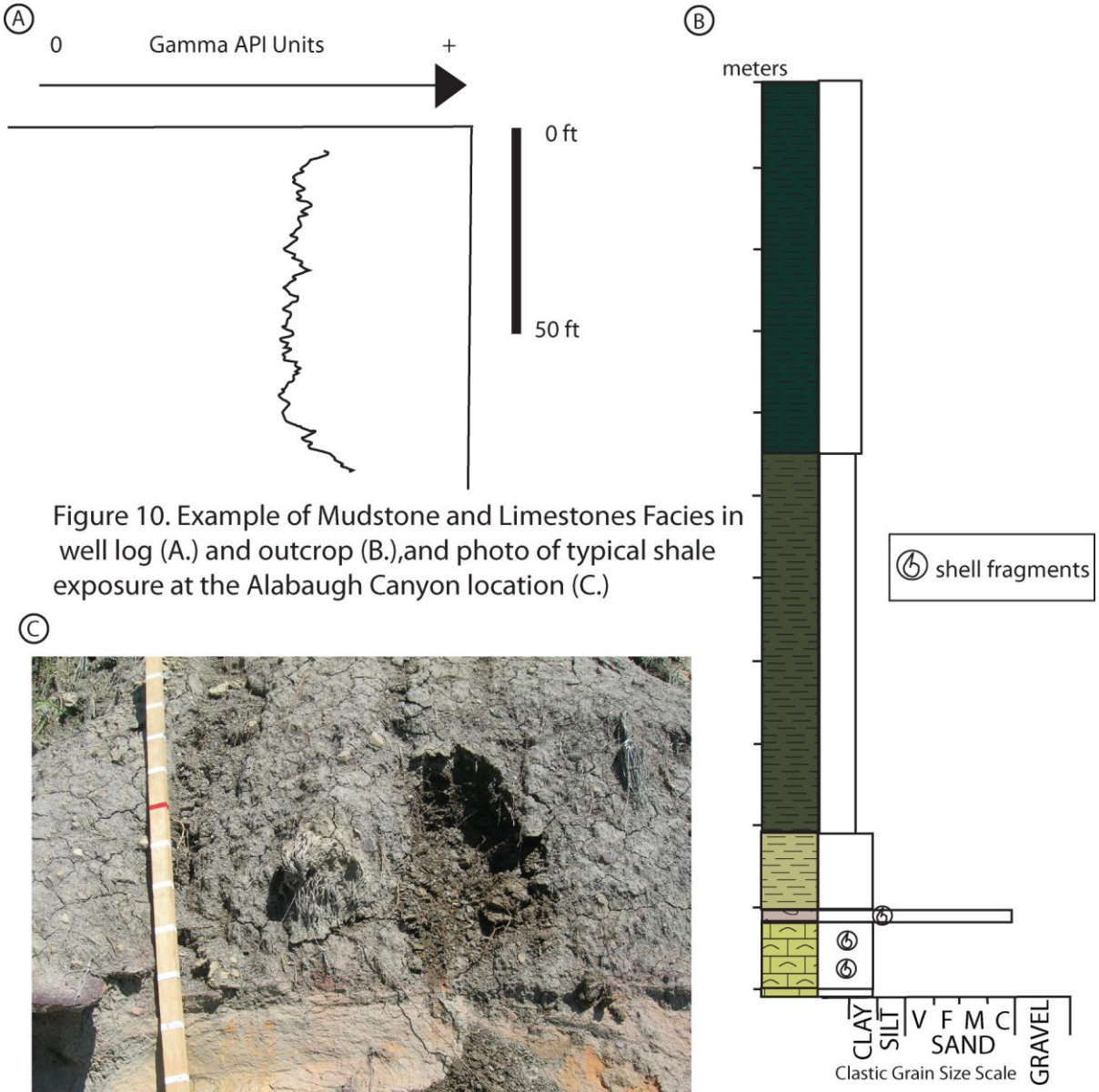

Figure 10. Example of Mudstone and Limestones Facies in well log (A.) and outcrop (B.),and photo of typical shale exposure at the Alabaugh Canyon location (C.)

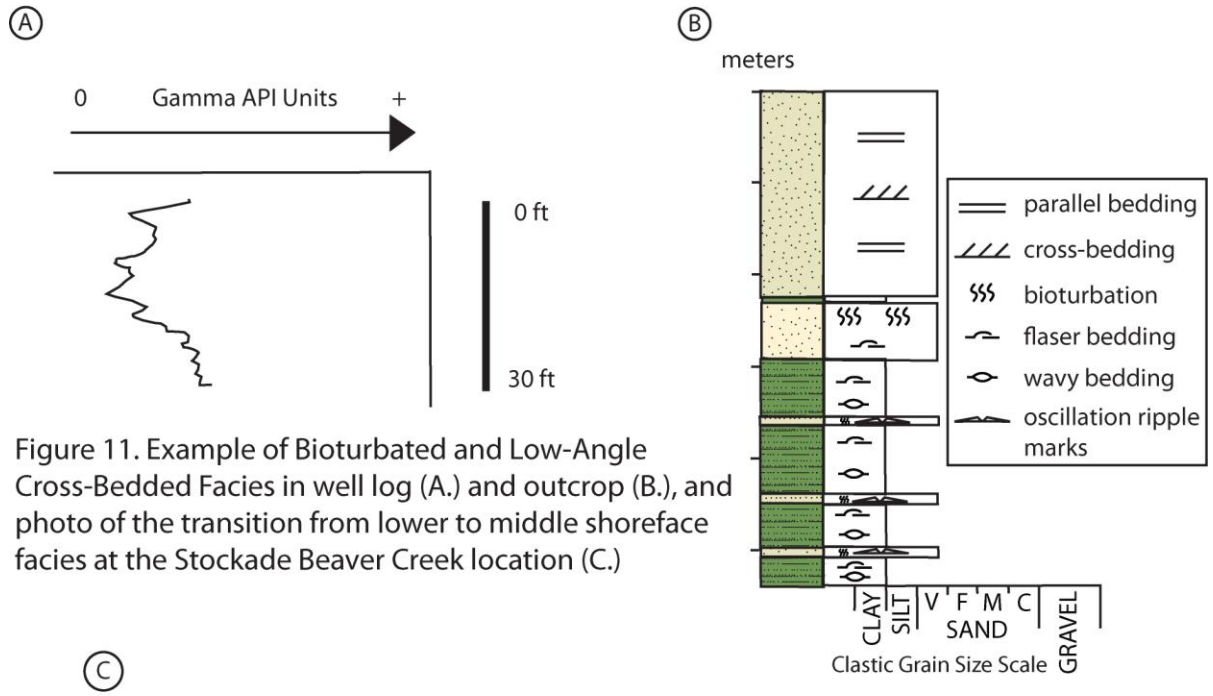

Figure 11. Example of Bioturbated and Low-Angle Cross-Bedded Facies in well log (A.) and outcrop (B.), and photo of the transition from lower to middle shoreface facies at the Stockade Beaver Creek location (C.)

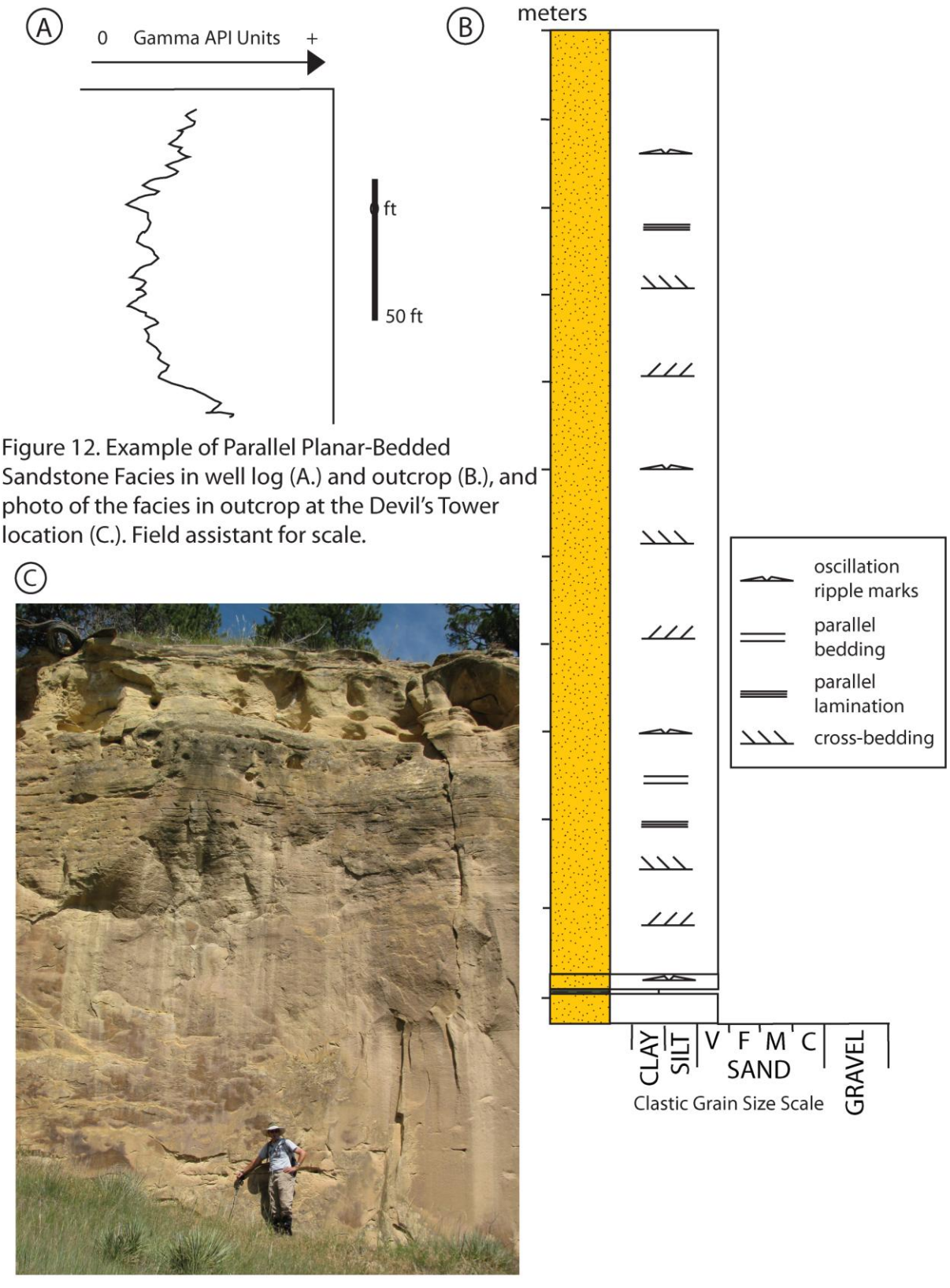

Figure 12. Example of Parallel Planar-Bedded Sandstone Facies in well log (A.) and outcrop (B.), and photo of the facies in outcrop at the Devil's Tower location (C.). Field assistant for scale.

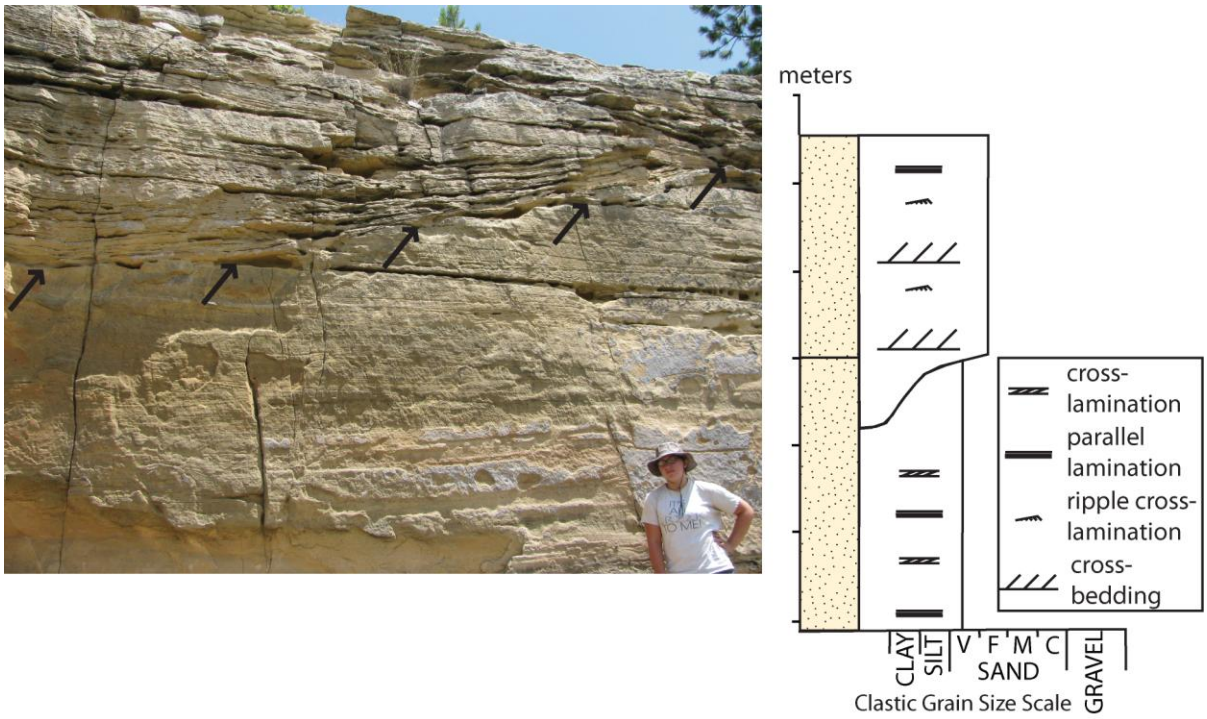

Figure 13. Photo and example of Incised Sandstone Facies in outcrop at the Star Butte location. Field assistant for scale. Channel incision indicated by arrows in photograph.

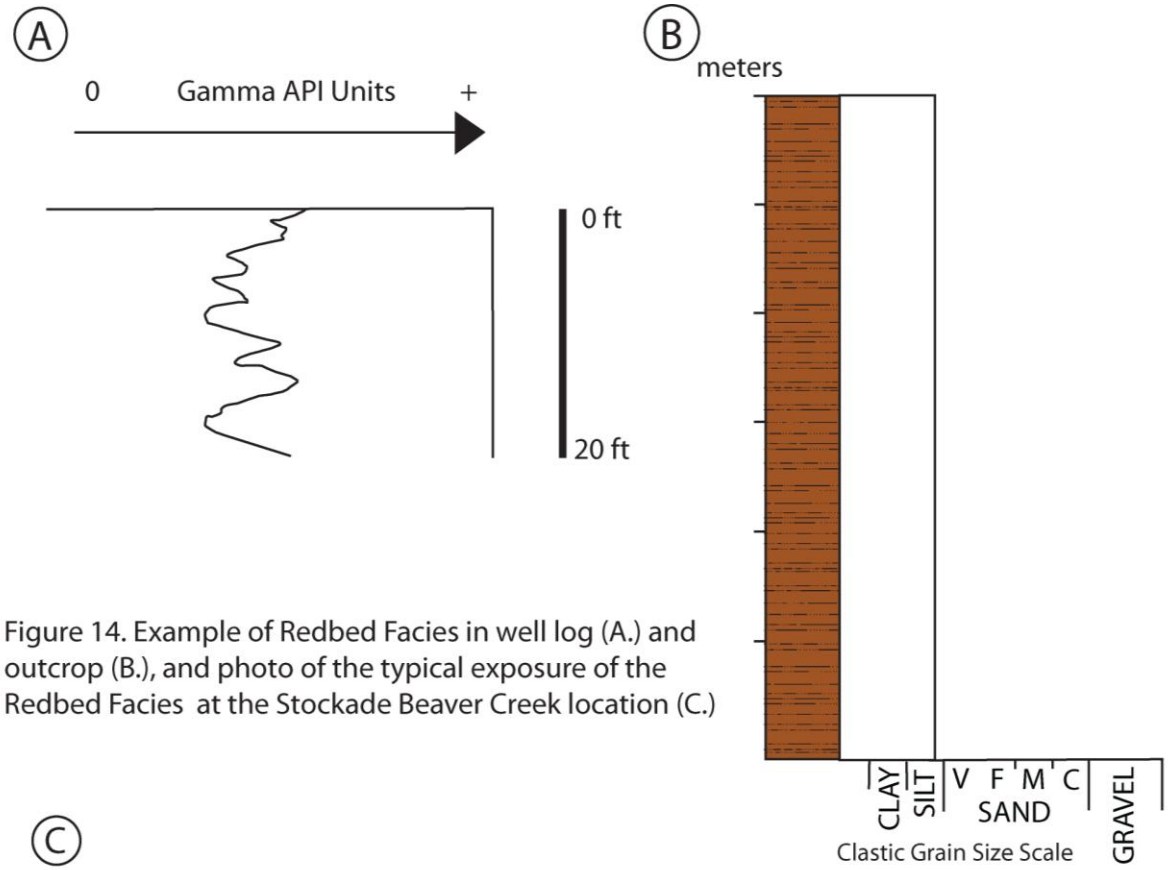

Figure 14. Example of Redbed Facies in well log (A.) and outcrop (B.), and photo of the typical exposure of the Redbed Facies at the Stockade Beaver Creek location (C.)

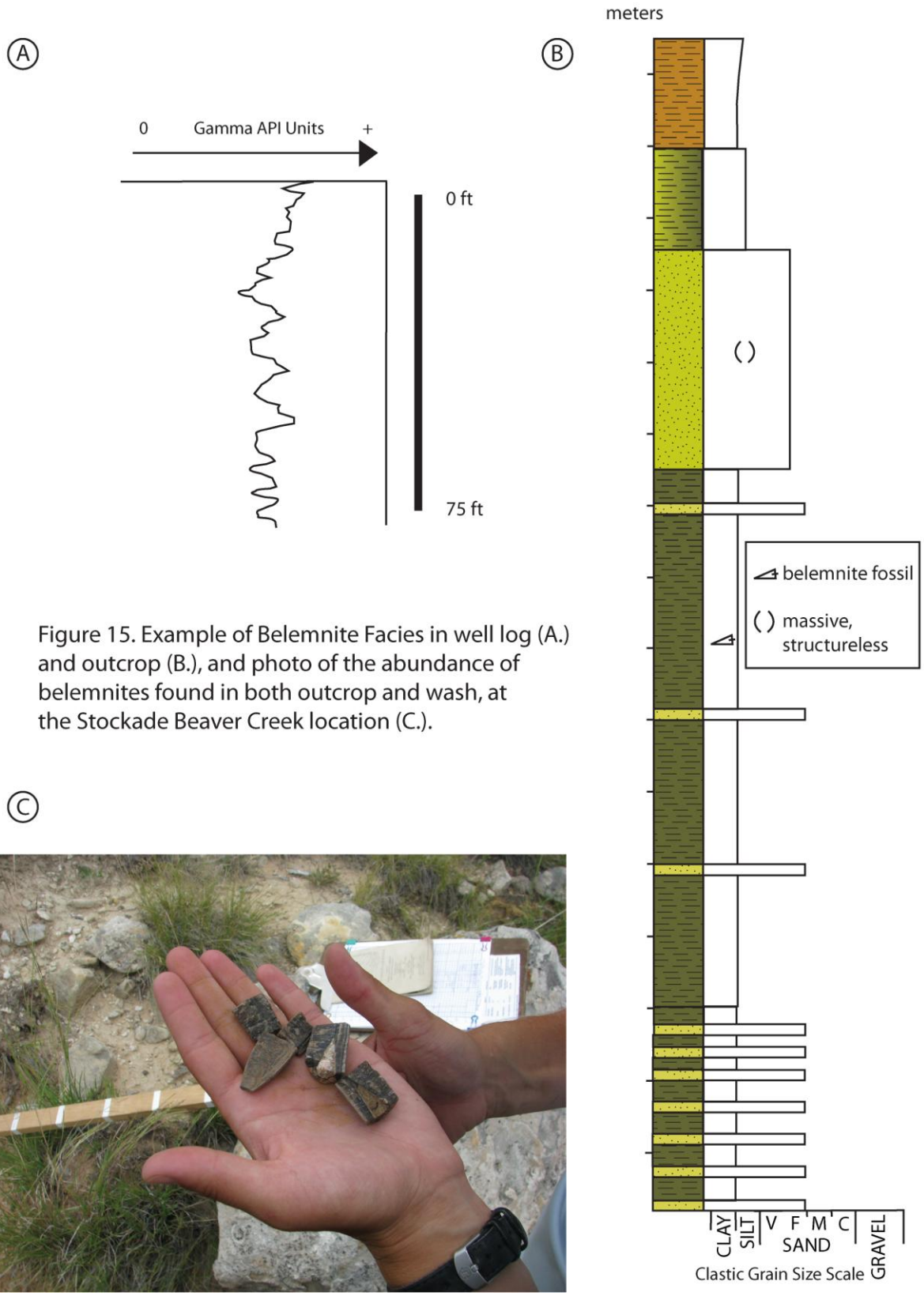

Figure 15. Example of Belemnite Facies in well log (A.) and outcrop (B.), and photo of the abundance of belemnites found in both outcrop and wash, at the Stockade Beaver Creek location (C.).

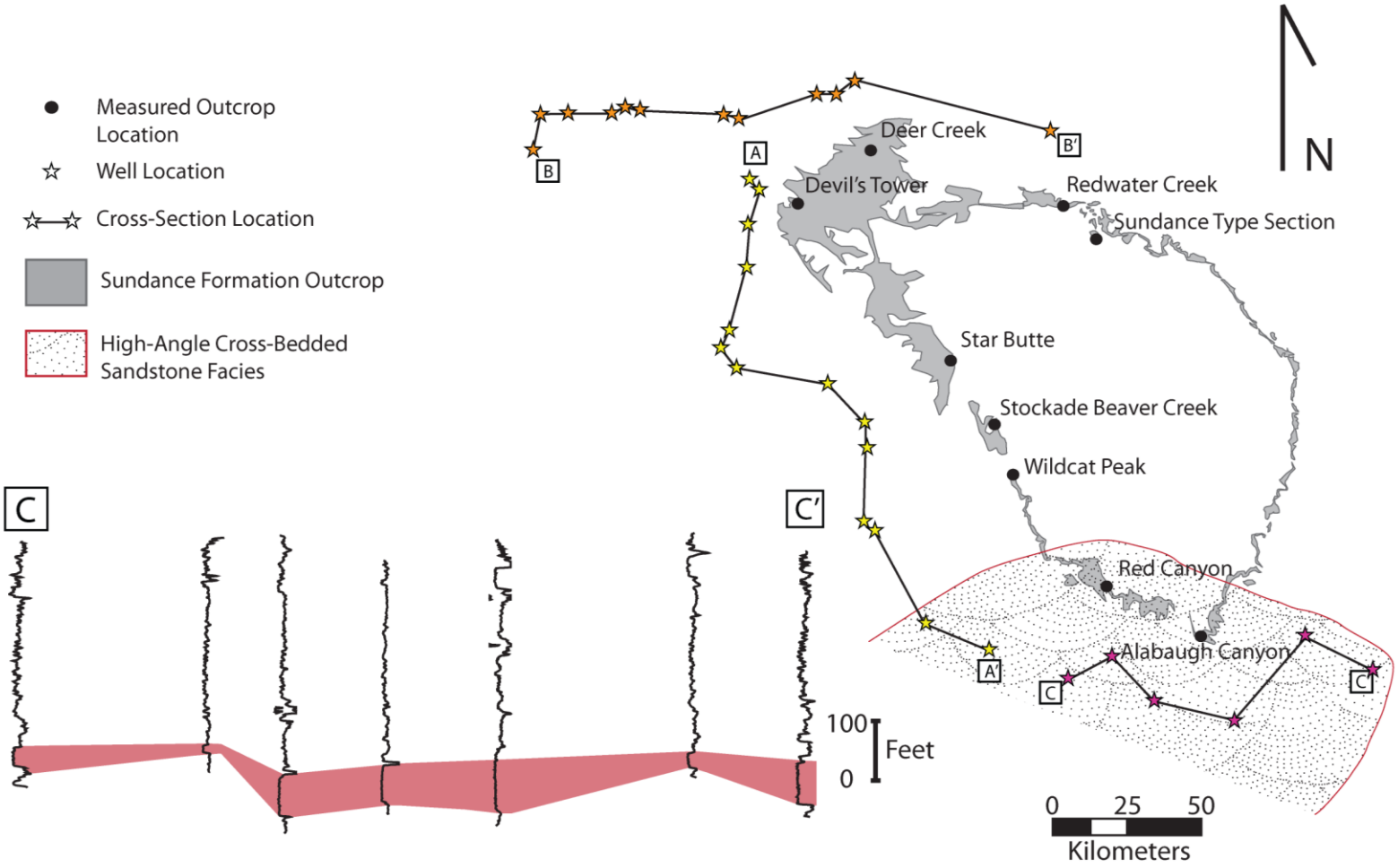

Figure 16. Regional Distribution of High-Angle Cross-bedded Sandstone Facies in the Study Area, with Cross-Section C-C′ for comparison.

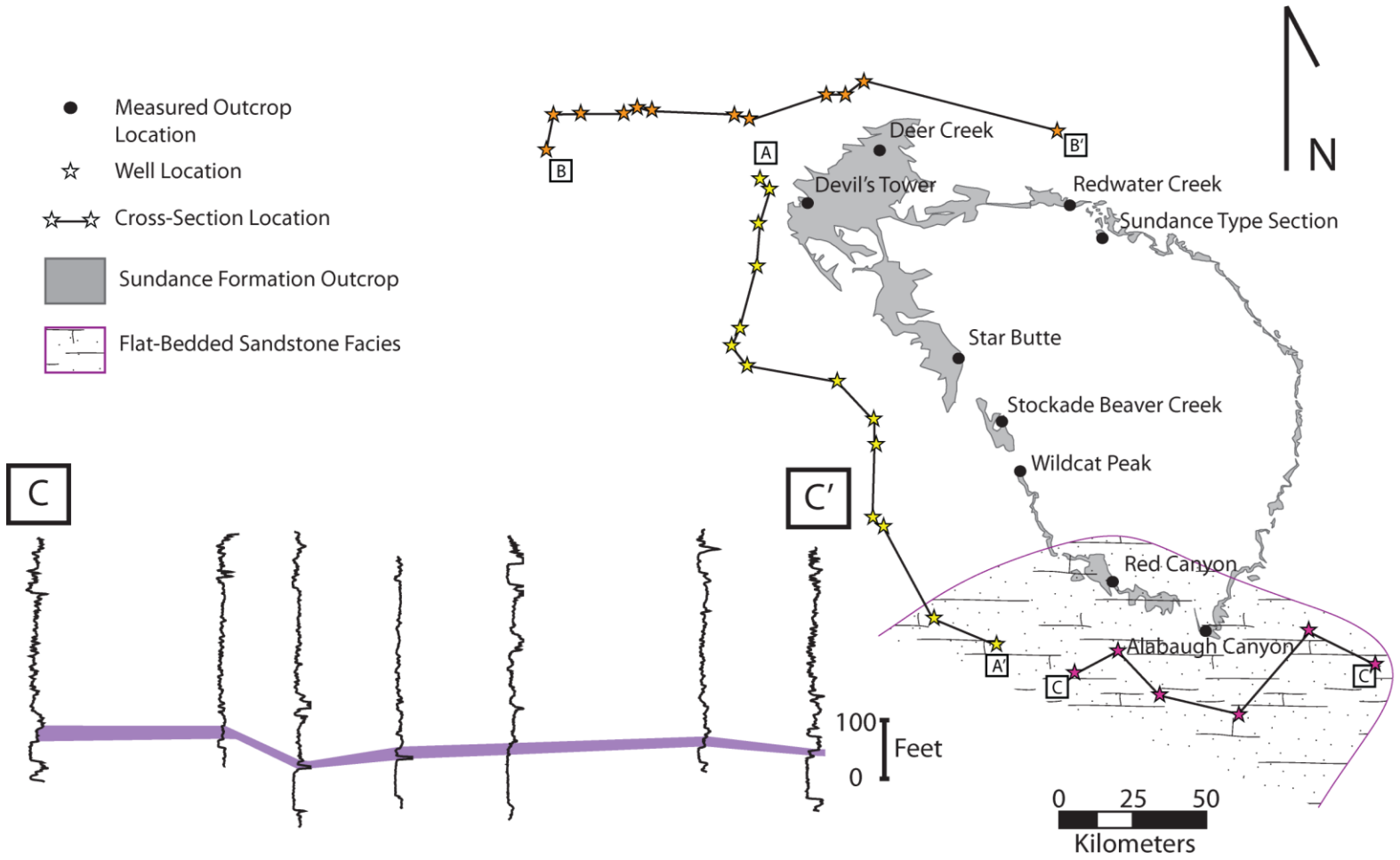

Figure 17. Regional Distribution of Flat-Bedded Sandstone Facies in the Study Area, with Cross-Section C-C' for comparison

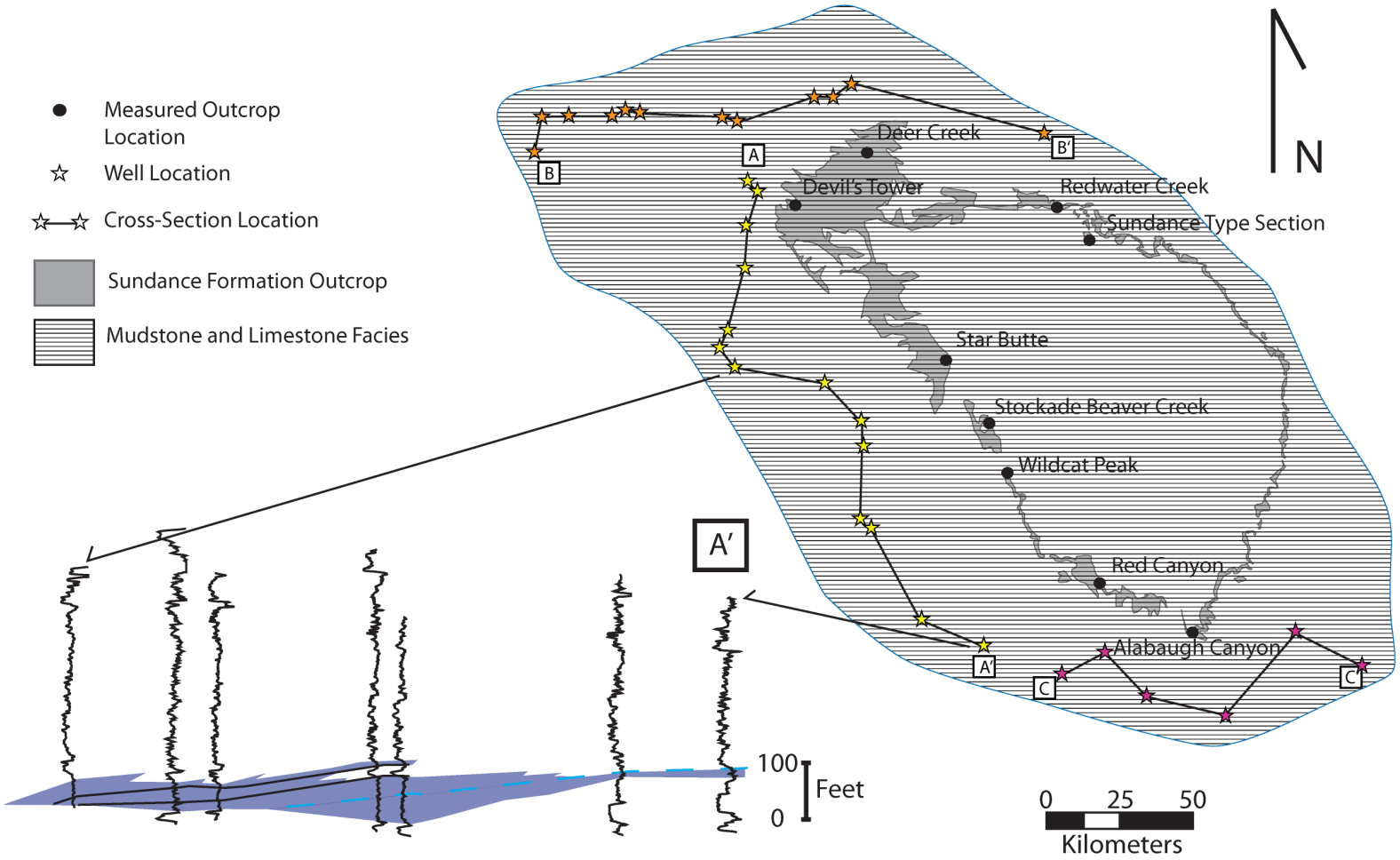

Figure 18. Regional Distribution of Mudstone and Limestone Facies in the Study Area, with a portion of Cross-Section A-A' for comparison.

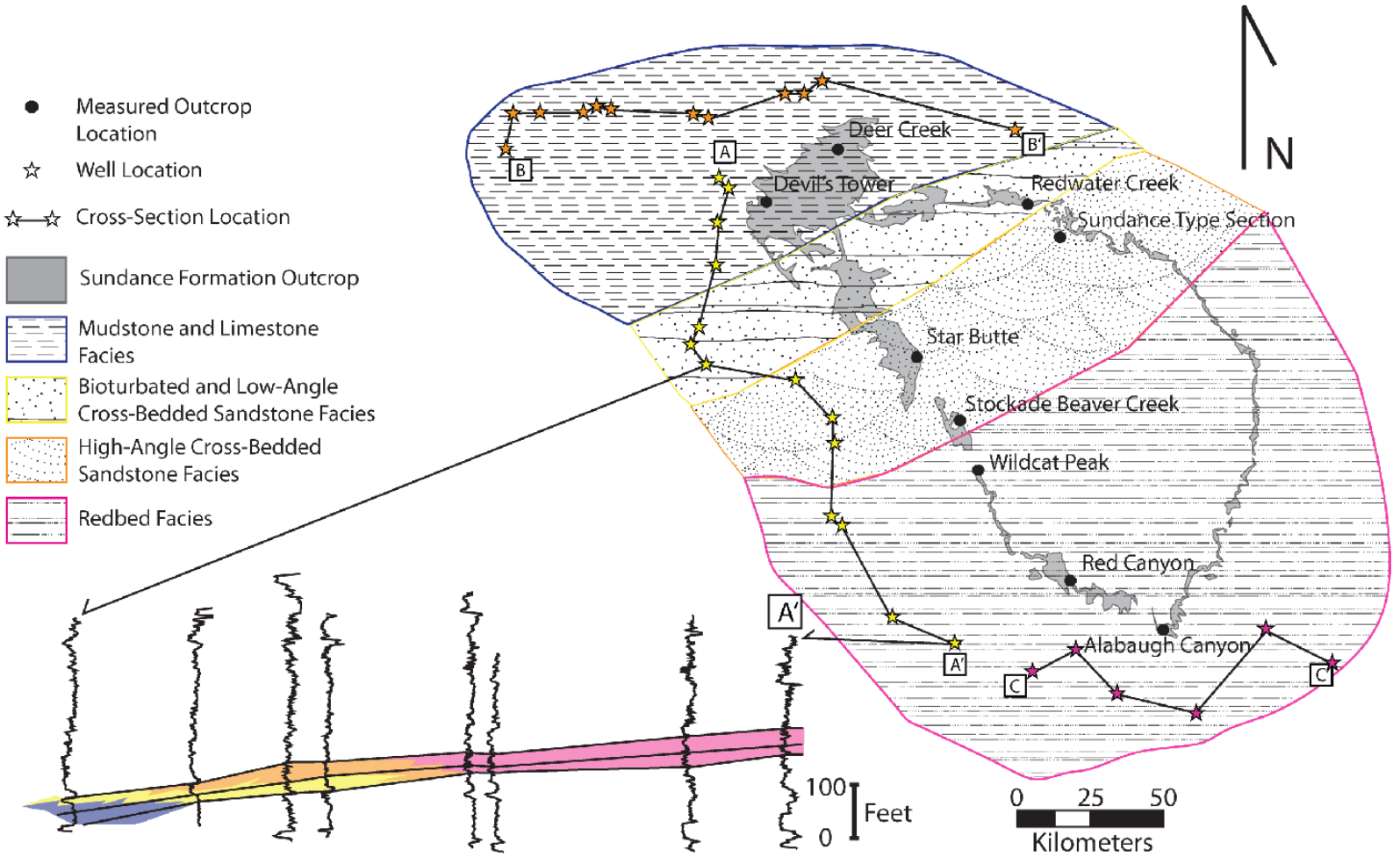

Figure 19. Regional Distribution of High-Angle Cross-bedded Sandstone and Flat-Bedded Sandstone Facies in the Study Area, With a portion of Well-Log Cross Section A-A' for Comparison

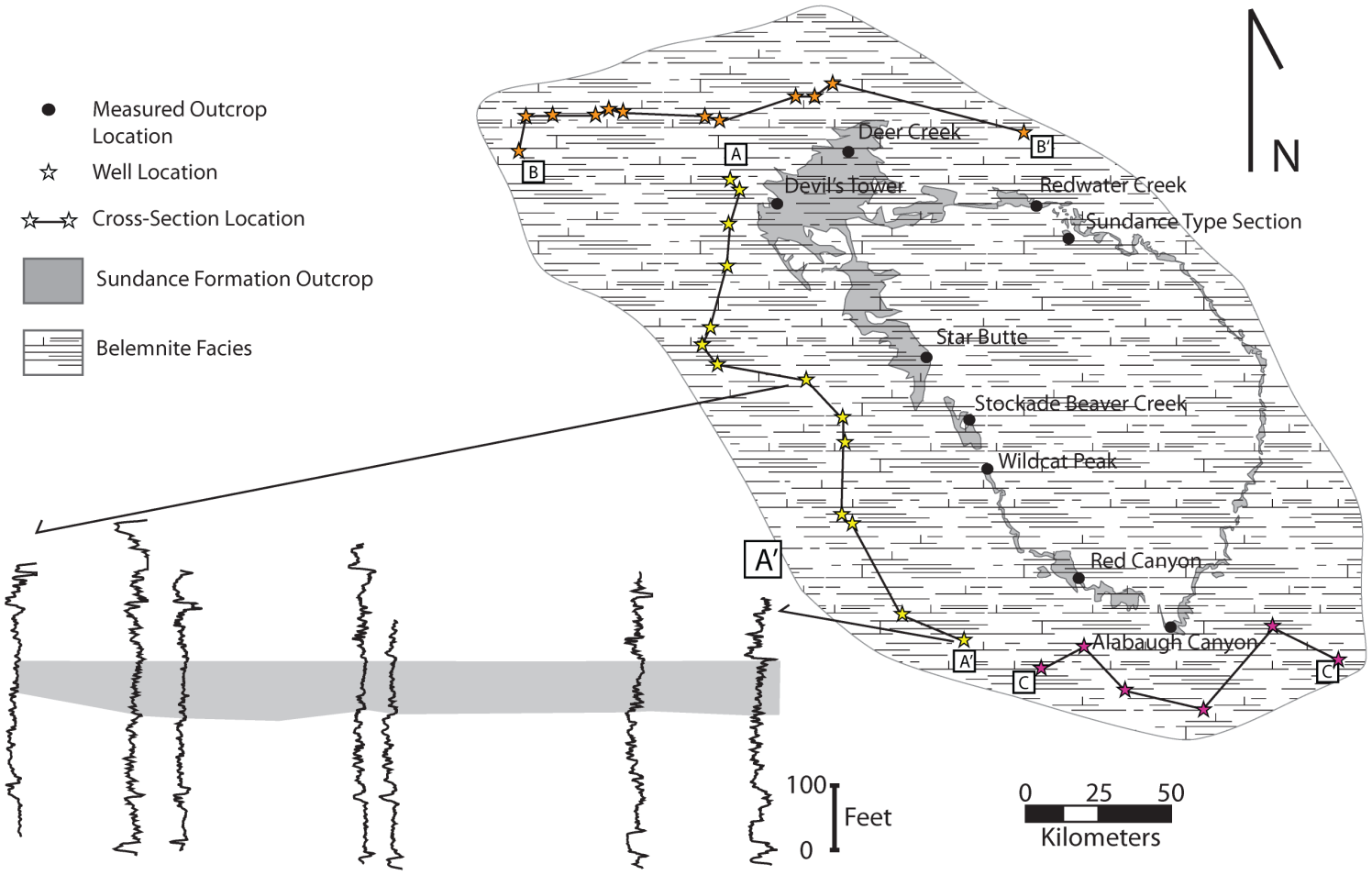

Figure 20. Regional Distribution of the Belemnite Facies in the Black Hills Area, with a portion of Cross-Section A-A' for comparison. The Facies is interpreted to exist in all localities from well data, despite being covered or eroded from some outcrop locations.

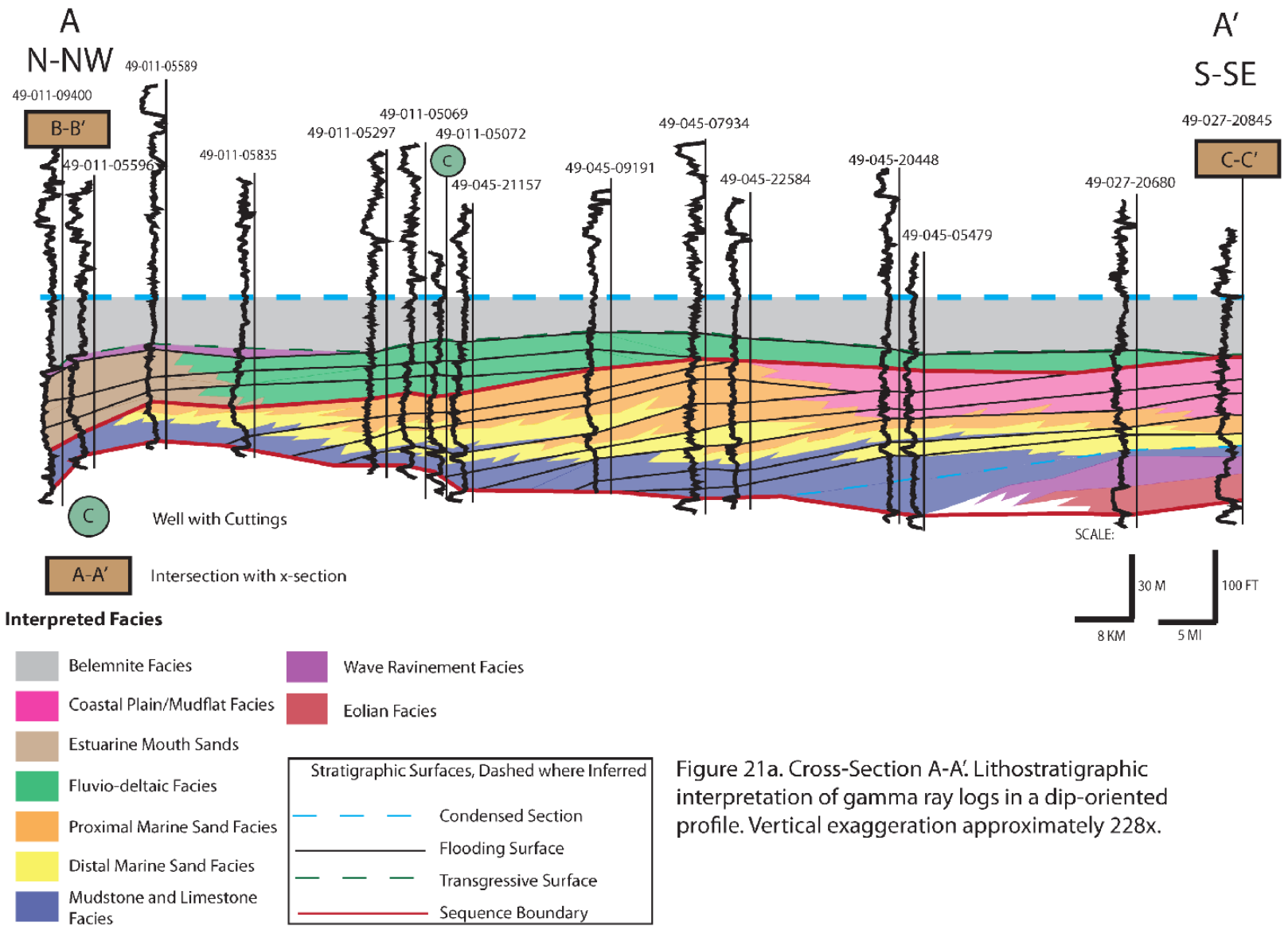

Figure 21a. Cross-Section A-A′. Lithostratigraphic interpretation of gamma ray logs in a dip-oriented profile. Vertical exaggeration approximately 228x.

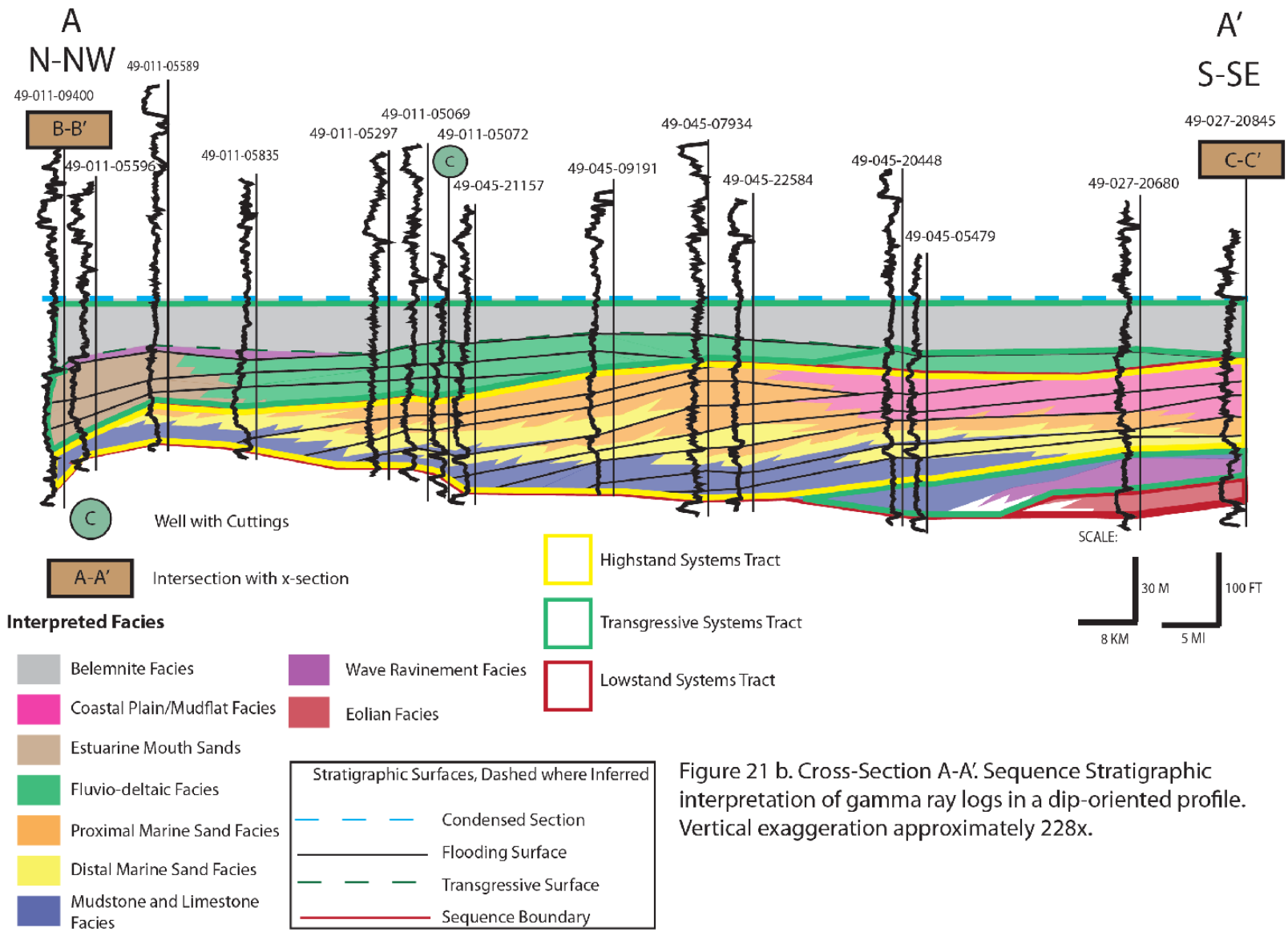

Figure 21 b. Cross-Section A-A′. Sequence Stratigraphic interpretation of gamma ray logs in a dip-oriented profile. Vertical exaggeration approximately 228x.

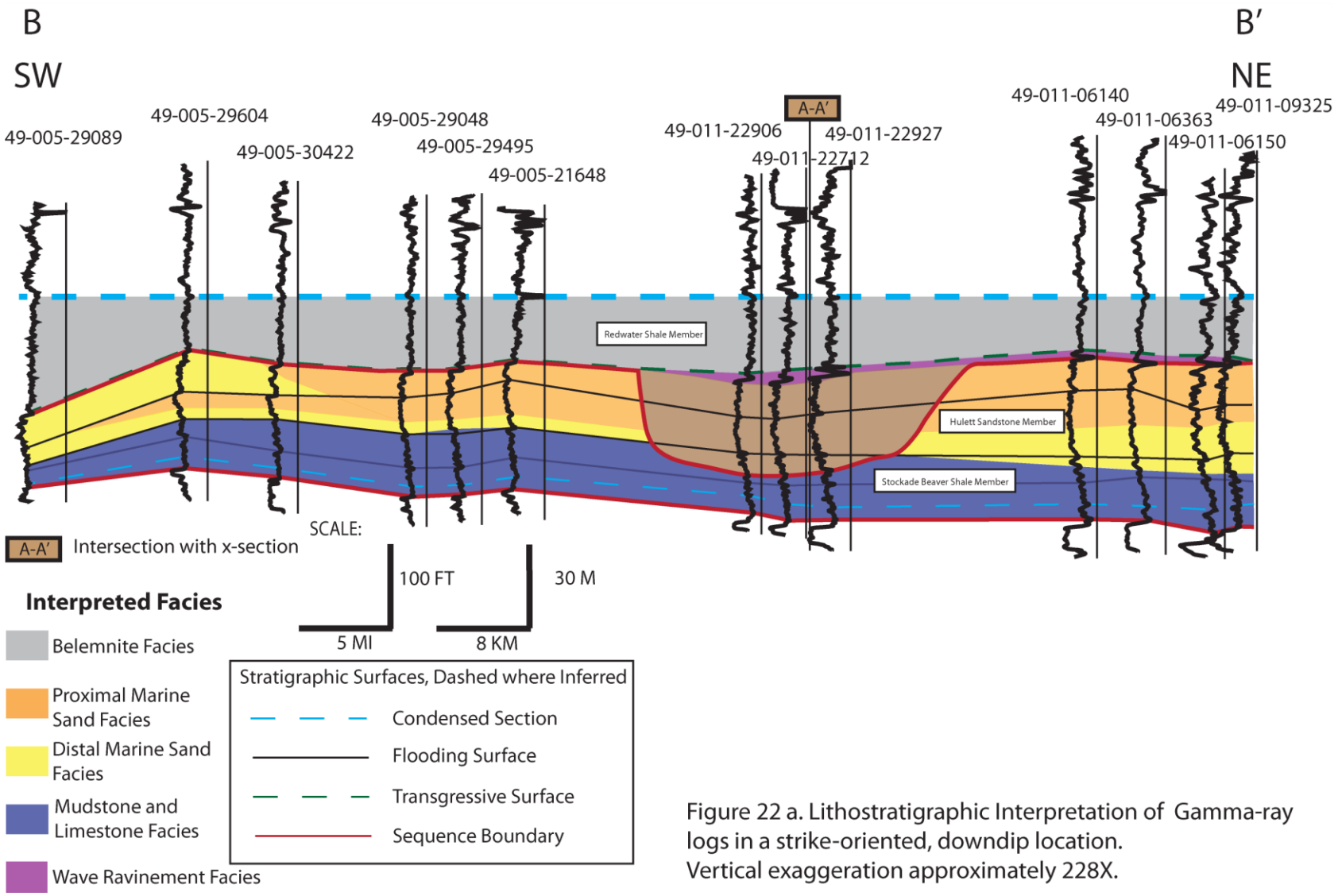

Figure 22 a. Lithostratigraphic Interpretation of Gamma-ray logs in a strike-oriented, downdip location. Vertical exaggeration approximately 228X.

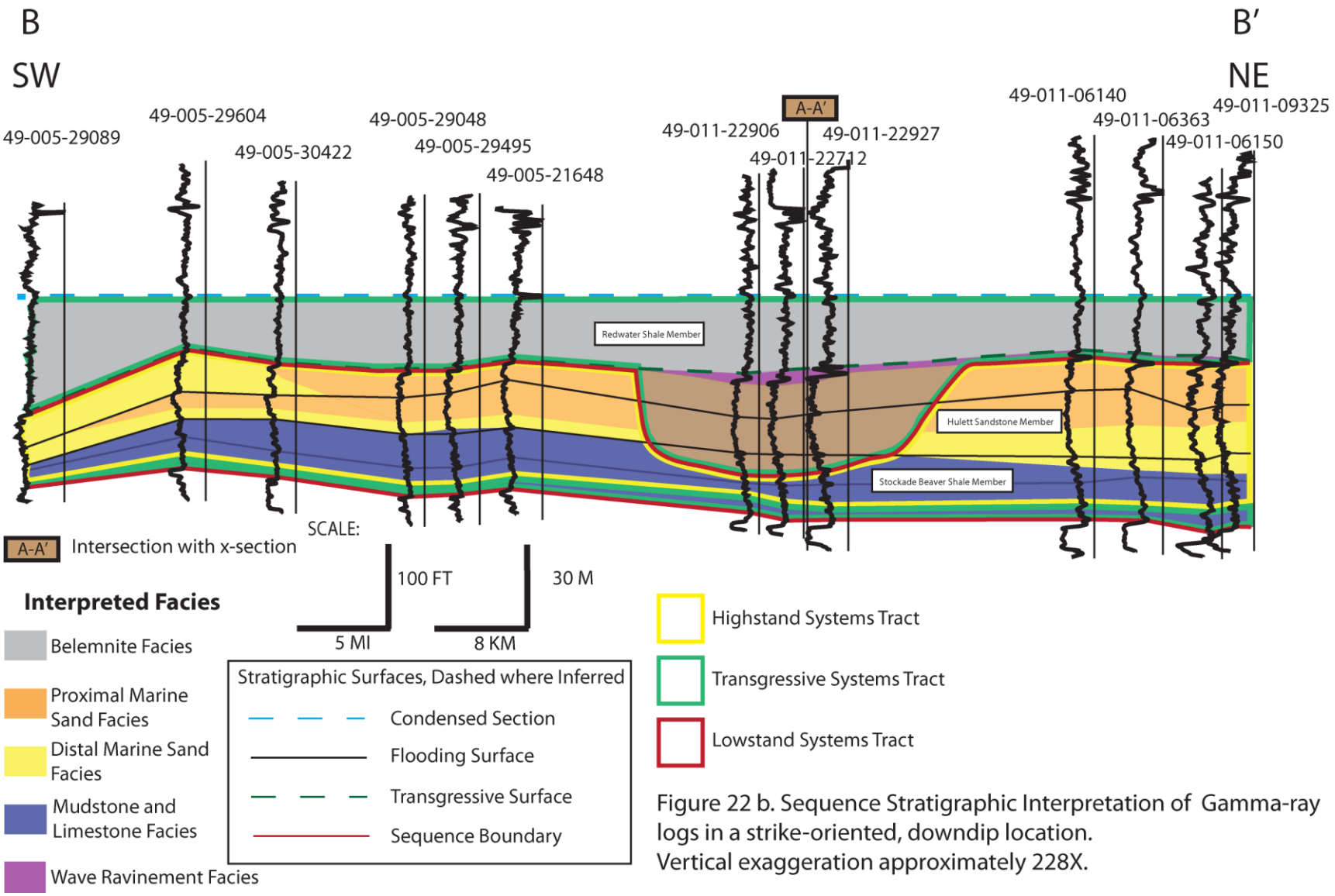

Figure 22 b. Sequence Stratigraphic Interpretation of Gamma-ray logs in a strike-oriented, downdip location.
Vertical exaggeration approximately 228X.

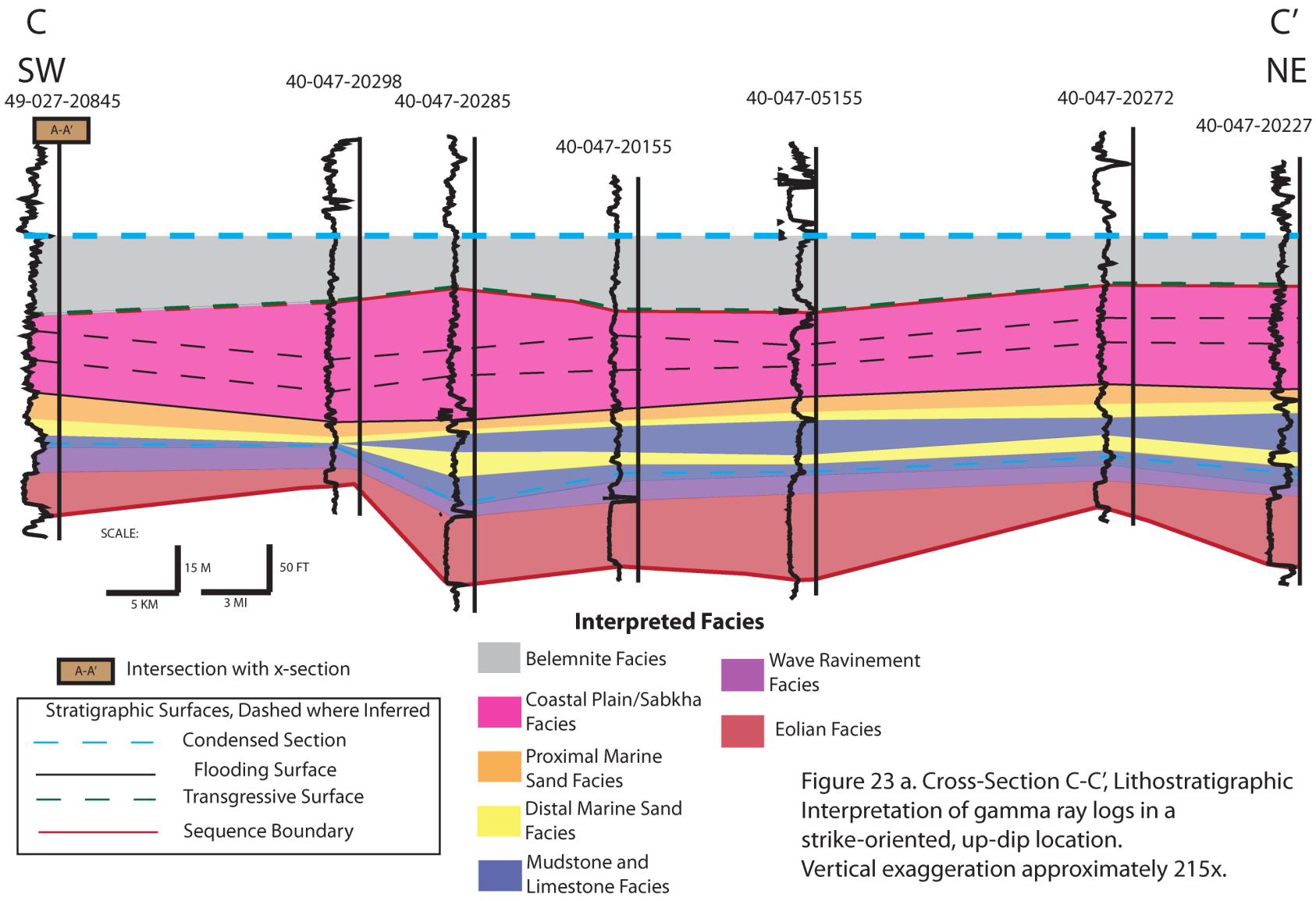

Figure 23 a. Cross-Section C-C′, Lithostratigraphic Interpretation of gamma ray logs in a strike-oriented, up-dip location.
Vertical exaggeration approximately 215x.

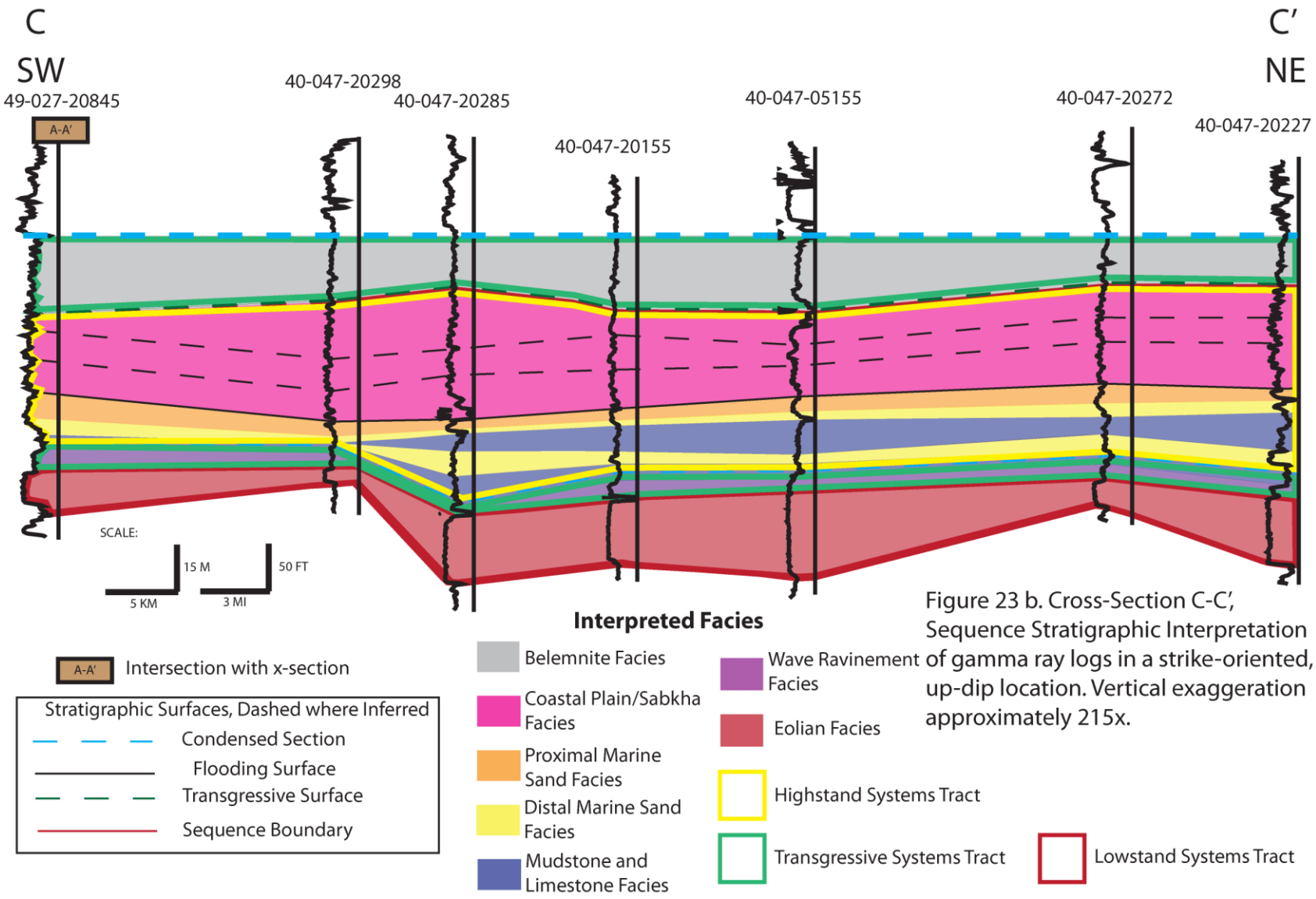

Figure 23 b. Cross-Section C-C′, Sequence Stratigraphic Interpretation of gamma ray logs in a strike-oriented, up-dip location. Vertical exaggeration approximately 215x.

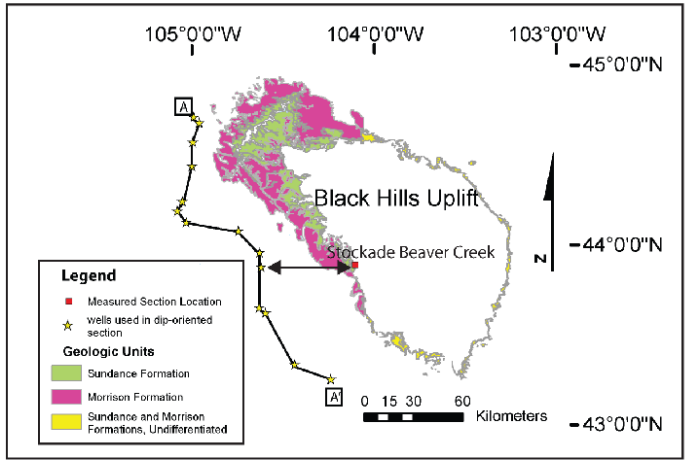

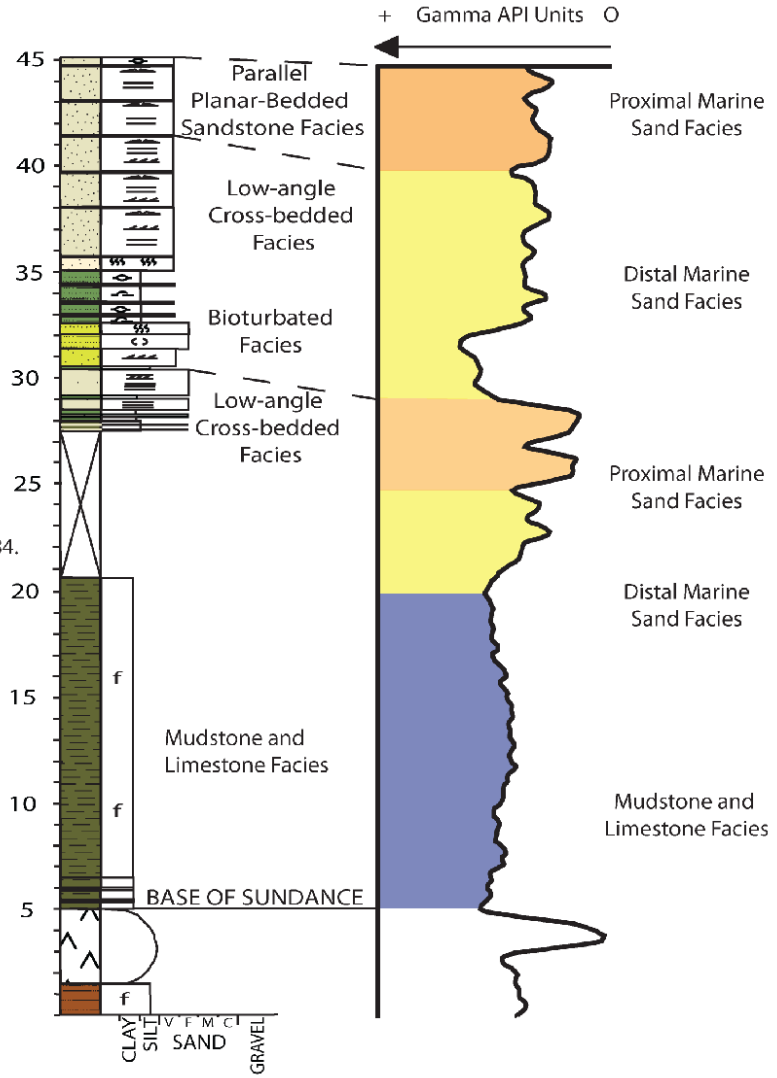

Figure 24. Example of interpretation of facies from Stockade Beaver Creek Measured Section to well La Bon Temps Roule 1, API Number 49-045-22584. Vertical grain-size trends were interpreted to coincide with gamma ray trends. Facies identified in outcrop described in text. Base map shows location of outcrop and well. Outcrop located at Latitude 43.889583, Longitude -104.103611, and well located at Latitude 43.88021, Longitude -104.62120.

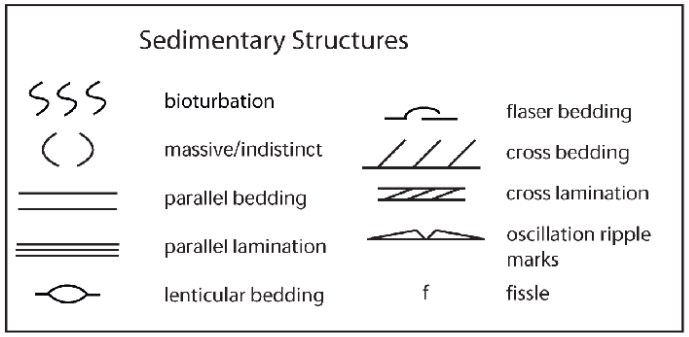

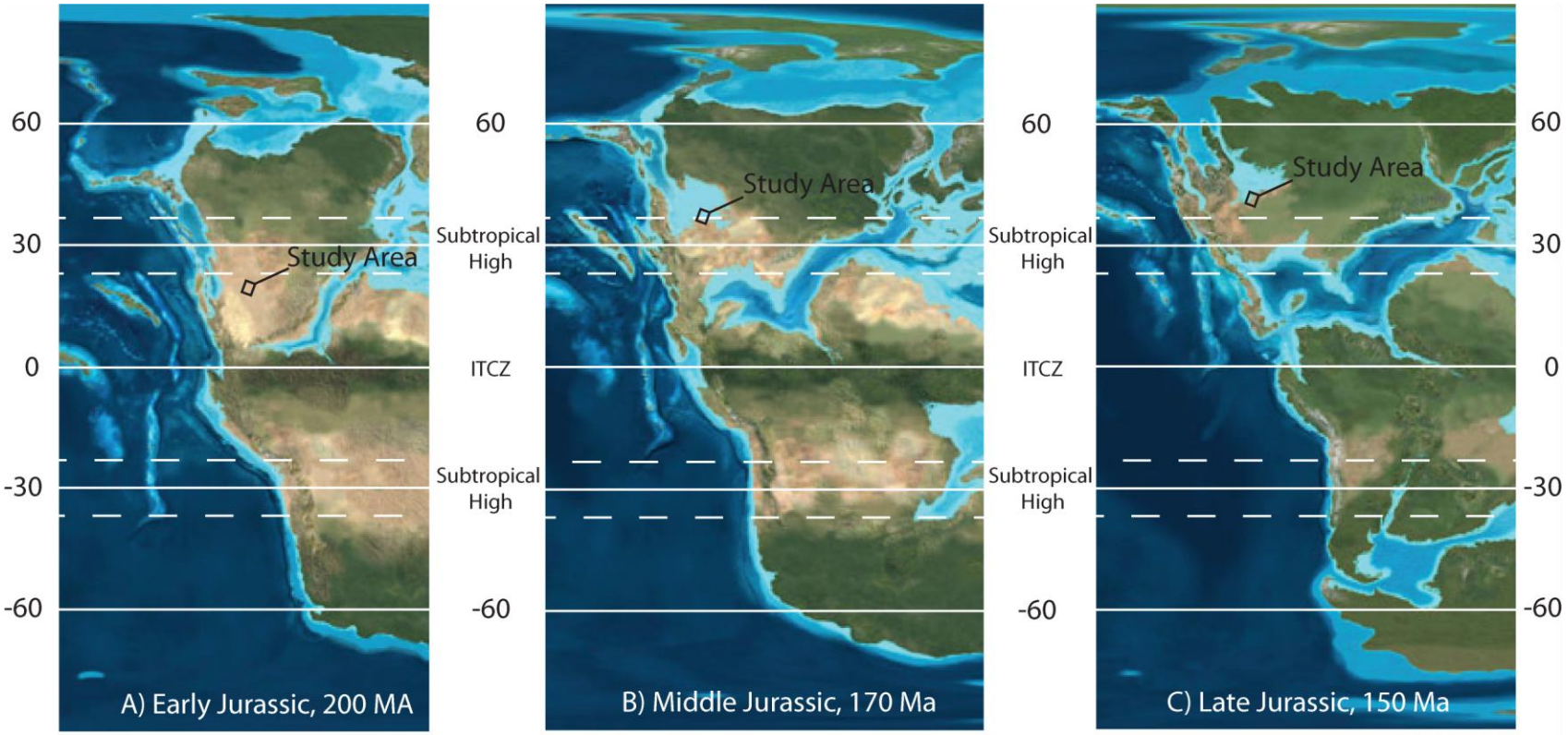

Figure 25. Paleogeography of the Western Hemisphere during the Jurassic Period. Study area is highlighted. Subtropical high and ITCZ latitudes indicated. The deposition of the Sundance Formation occured during late-Middle Jurassic to early-Late Jurassic time. All maps modified from Blakey, http://jan.ucc.nau.edu/~rcb7/.

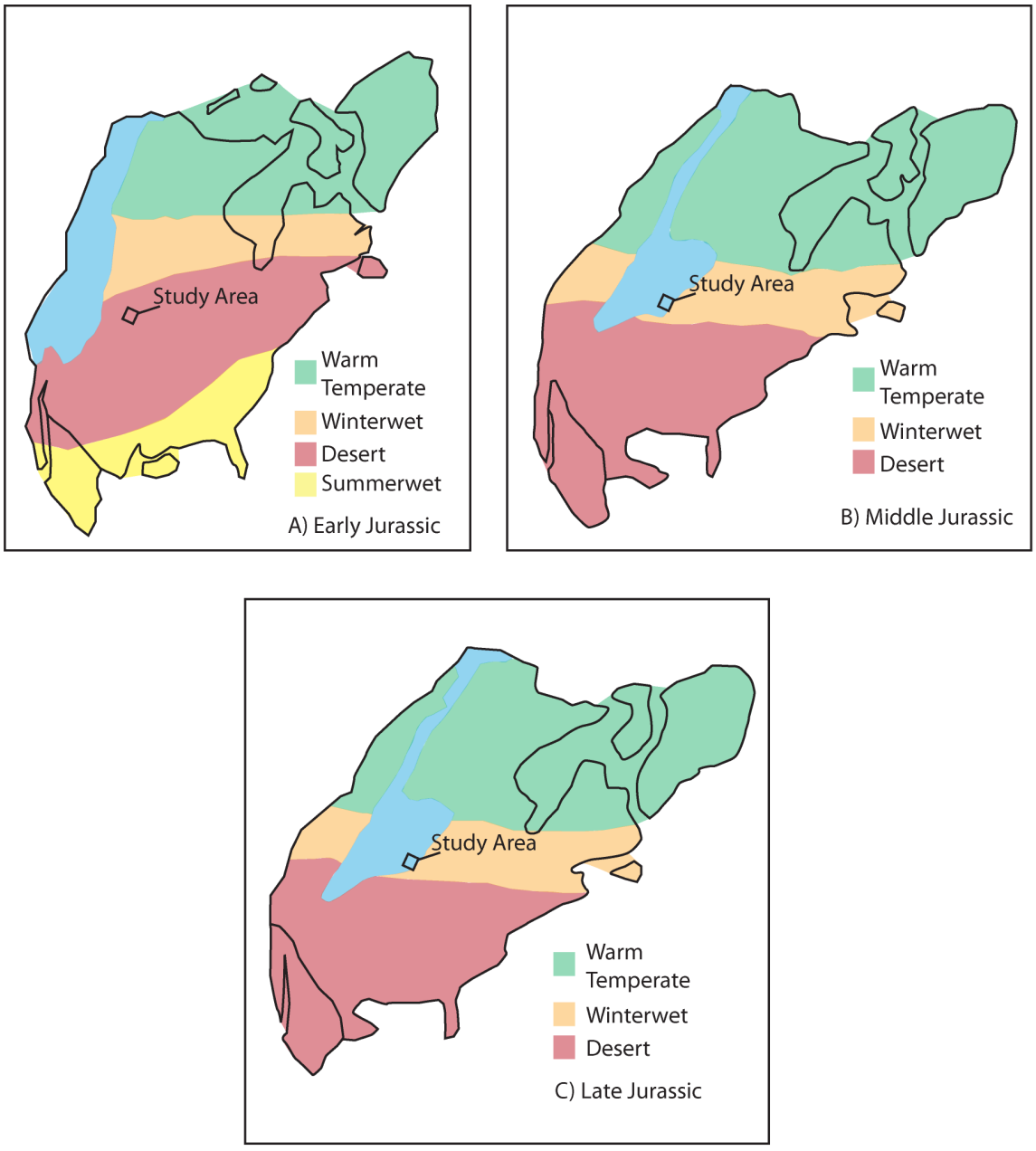

Figure 26. Predicted Biomes of North America through the Jurassic period. The climate of the study area transitioned from a desert biome to a winterwet biome due to migration of the continent through climate belts. Predicted biomes are based on climate modelling, flora and lithologic data. Modified from Rees et al, 2000.

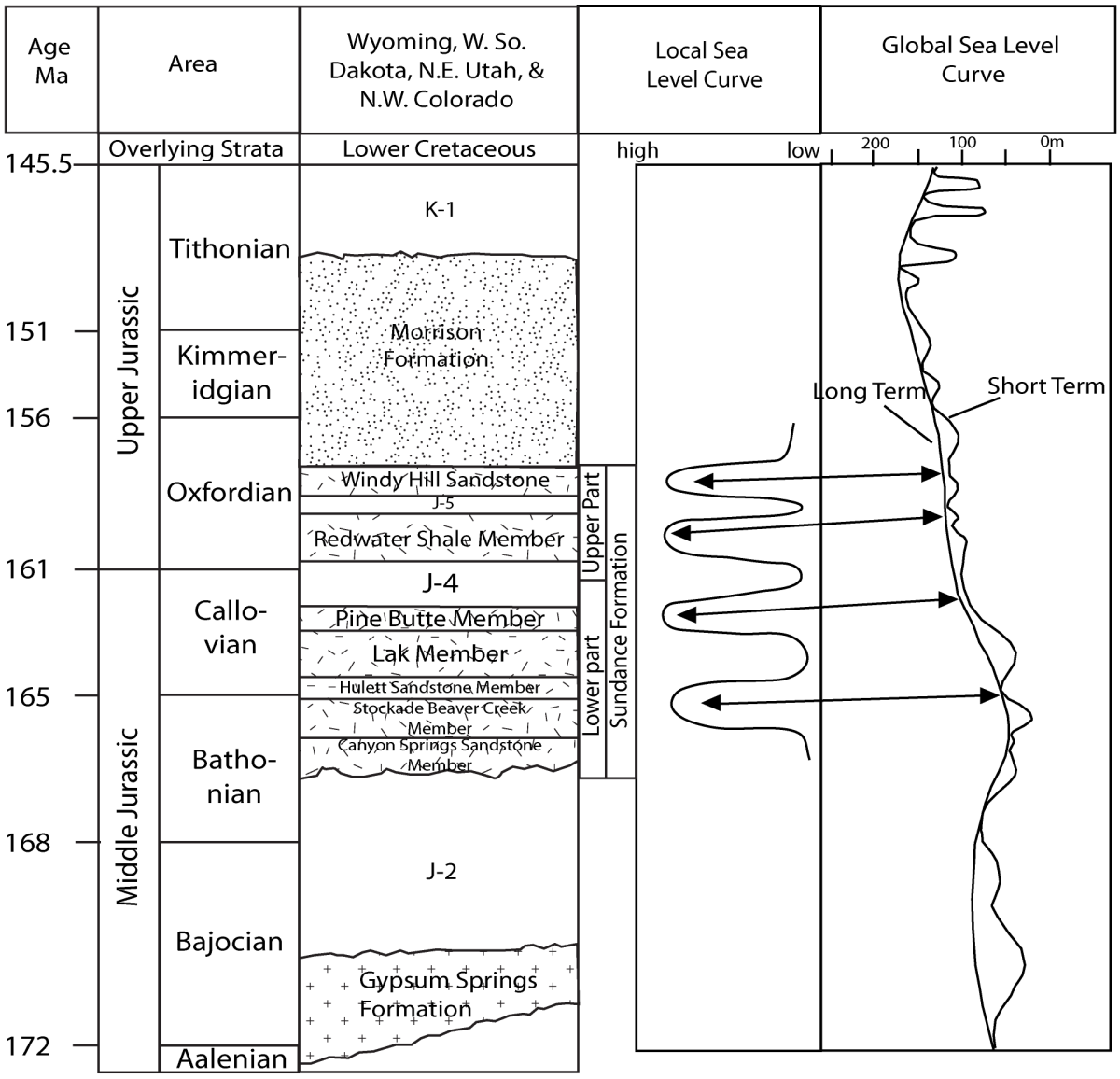

Figure 27. Generalized Stratigraphy of Jurassic Rocks in the Black Hills area. J-2, J-4, J-5, and K-1 represent unconformites discussed in the text. Modified from Johnson, 1992, and Brenner and Peterson, 1994. Sea Level Curve from Haq et al, 1988.

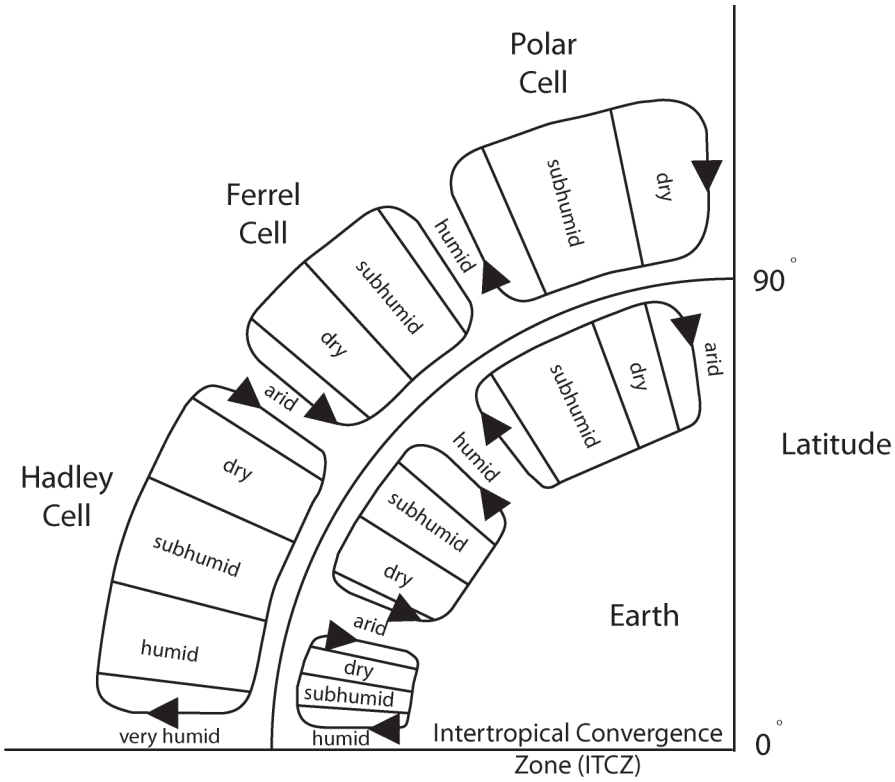

Figure 28. Simplified view of Hadley, Ferrel and Polar Cells, showing estimated latitudinal distribution of precipitation and humidity. Modified from Matthews and Perlmutter, 1994.

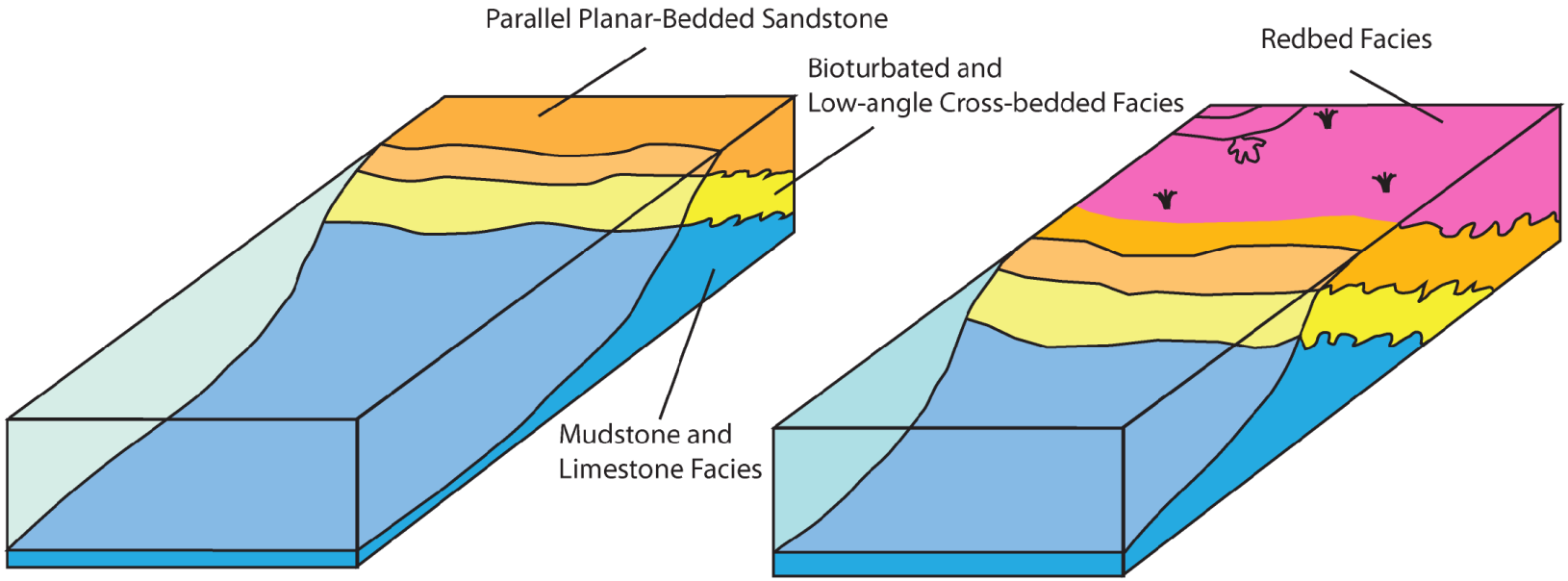

Figure 29. Example of depositional systems during Early Sundance deposition. Facies types are labeled and described in the results portion of the text.

Appendix 1. Table of Measured Outcrop Sections

Measured Section	Latitude	Longitude	Altitude
Sundance Type-Section	44.488550	-103.8393830	6652 ft
Redwater Creek	44.585950	-103.9511330	6480 ft
Alabaugh Canyon	43.323417	-103.5298170	5470 ft
Wildcat Peak	43.690683	-104.0509330	4893 ft
Stockade Beaver Creek	43.889583	-104.1036110	NULL
Devil's Tower	44.584056	-104.7147780	4943 ft
Deer Creek	44.752817	-104.4891170	4004 ft
Red Canyon	43.461806	-103.8079440	NULL
Starr Butte	44.128556	-104.2668060	NULL

Appendix 2. Measured Outcrop Sections

Measured Section outcrops include the Sundance Type Section location, Redwater Creek location, Alabaugh Canyon, Wildcat Peak location, Stockade Beaver Creek location, Devil's Tower location, Deer Creek location, Red Canyon location, and Star Butte location. For location information, see previous table included in appendix 1.

Appendix 3. Table of Wells Used in Study

Well Name	County	State	Well Number	Latitude	Longitude
Advantage Res 4-15 Federal	Fall River	South Dakota	4004720244	43.100133	-103.992405
Barnes 1 Nixon	Pennington	South Dakota	4010320018	44.155644	-102.01971
Beer 1 Burns Govt	Butte	South Dakota	4001905075	44.896313	-103.125048
Beer 1 Morell Livestock	Meade	South Dakota	4009305087	44.790176	-102.873851
Beer 1 Norsworthey Reger Govt	Butte	South Dakota	4001905074	44.80149	-103.203225
Beer 1 Sterling Govt	Butte	South Dakota	4001905073	44.689025	-103.10696
Benedum 1 Kaiser Ranch	Custer	South Dakota	4003320003	43.725291	-102.901695
Bond Govt 1	Crook	Wyoming	4901105531	44.292598	-104.883387
Bullock Carlisle 1	Niobrara	Wyoming	4902720985	42.96972	-104.71194
Burrows B B-041274 16	Crook	Wyoming	4901105297	44.244254	-105.05417
Cedar Ridge-Federal 23-7	Crook	Wyoming	4901122926	44.85081	-104.94416
Chan W-68210 1	Campbell	Wyoming	4900529604	44.86401	-105.56681
Citation 21-30 Porter Federal	Fall River	South Dakota	4004720212	43.244282	-103.92939
Conroy 1 Helsel	Fall River	South Dakota	4004705059	43.233376	-103.702838
Conroy 1 Ideen Federal	Fall River	South Dakota	4004705067	43.2622	-103.874366
Conroy 1 Trotter Lane Fed	Fall River	South Dakota	4004705092	43.429517	-103.882491
Consldtd Royalty 1 Wulf Ideen	Fall River	South Dakota	4004705084	43.360229	-103.858005
Consolidated Royalty 1 State	Fall River	South Dakota	4004705090	43.425719	-103.952837
Core Hole Patented 1	Crook	Wyoming	4901109325	44.95938	-104.57539
Crook 1	Crook	Wyoming	4901105835	44.43842	-104.99981
Depco 24-25 Kane	Fall River	South Dakota	4004720155	43.14639	-103.713127
Downing 3	Niobrara	Wyoming	4902705118	42.97096	-104.69901
Fed Kerr W-055355B 1	Niobrara	Wyoming	4902706161	43.246836	-104.241092
Federal C-034630-B 2	Weston	Wyoming	4904505479	43.62383	-104.59753
Federal RJ 1-21	Niobrara	Wyoming	4902720680	43.3366	-104.43792
Federal W-038708 1	Crook	Wyoming	4901106150	44.96669	-104.58043
Flag Redfern 1-29 Federal	Fall River	South Dakota	4004720227	43.242392	-103.026948
Fowler 12-7	Crook	Wyoming	4901105596	44.680353	-104.960011
French Federal 33-1	Crook	Wyoming	4901122927	44.86236	-104.95841
Galion 1	Campbell	Wyoming	4900529089	44.75365	-105.59271
Gary 1 State	Fall River	South Dakota	4004705030	43.145963	-103.466598
Gary 7-4 Gary Federal	Fall River	South Dakota	4004720021	43.287779	-103.69828
Gibson 1	Crook	Wyoming	4901109400	44.71269	-104.991122
Greenwing W-92328 24-1	Campbell	Wyoming	4900529048	44.86789	-105.34269
Grynberg 1	Weston	Wyoming	4904521157	44.12818	-105.031955
Ham Krause Patented 1	Crook	Wyoming	4901105077	44.190558	-105.063368

Well Name	County	State	Well Number	Latitude	Longitude
Jessen W-30711A 1-5	Weston	Wyoming	4904521248	44.07727	-105.04749
Krauss Patented 1	Crook	Wyoming	4901105072	44.189708	-105.069606
La Bon Temps Roule 1	Weston	Wyoming	4904522584	43.88021	-104.6212
Lightning Creek Unit 1	Niobrara	Wyoming	4902705122	42.97128	-104.73238
M L Stone 1 Clark	Pennington	South Dakota	4010320017	44.148328	-102.025066
Madden Patented 1	Crook	Wyoming	4901106363	44.92648	-104.63816
Maggie W-054670 23-19	Campbell	Wyoming	4900521648	44.87893	-105.25433
Materi Patented 1	Weston	Wyoming	4904509191	44.07863	-104.74652
Maurer Patented 1	Crook	Wyoming	4901106140	44.92589	-104.69925
Mobil F-11-14-P Sipila	Butte	South Dakota	4001905014	44.74819	-103.117129
NCOC 1-7 State	Fall River	South Dakota	4004720064	43.109663	-103.452957
Newcastle Unit 72-A	Weston	Wyoming	4904520448	43.65242	-104.632154
O Rohlff 17	Niobrara	Wyoming	4902720313	43.04758	-104.69641
Olmstead W-39061 1R	Campbell	Wyoming	4900530422	44.8677	-105.48026
Panam 1 Govt Dorough	Fall River	South Dakota	4004705011	43.042241	-104.049895
Pfister 13-19	Niobrara	Wyoming	4902720845	43.253657	-104.239407
Roosevelt 16-14 B&H Ranch	Fall River	South Dakota	4004720272	43.348901	-103.238724
Roosevelt 5-11 Heppner	Fall River	South Dakota	4004720305	43.197158	-103.737987
Roosevelt 7-11 Miller State	Fall River	South Dakota	4004720285	43.283783	-103.845545
RPG Federal 13-2	Crook	Wyoming	4901122712	44.86303	-104.99175
RPG Federal 44-3	Crook	Wyoming	4901122906	44.87615	-104.99544
Sawgras 33-32 107601 2	Campbell	Wyoming	4900529495	44.8862	-105.30051
SHELL 23-23 JOHNSON	Butte	South Dakota	4001905018	44.812384	-103.966165
Sinclair 1 State 4000	Fall River	South Dakota	4004705155	43.084454	-103.462058
SOJOURNER 1 WIDOSS	Butte	South Dakota	4001920006	44.999136	-103.871249
Sophia Woods 1	Crook	Wyoming	4901105589	44.572896	-104.996133
Startech 031001-1 Federal	Fall River	South Dakota	4004720298	43.215949	-103.98351
State 62-20723 1	Crook	Wyoming	4901105069	44.189805	-105.080581
Sun 1 Lance Nelson	Fall River	South Dakota	4004705089	43.42795	-103.997224
Sun 1 Wallway Govt	Fall River	South Dakota	4004705068	43.284462	-103.938437
Total 14-9 Eckard	Fall River	South Dakota	4004720209	43.103309	-103.658891
Unit 272	Weston	Wyoming	4904507934	43.95904	-104.630105
Vista 1 Adamski	Meade	South Dakota	4009320028	44.476537	-103.476539
W-123	Weston	Wyoming	4904507509	43.93778	-104.72598
Westech 4-16 Moreau River	Butte	South Dakota	4001920068	45.093752	-103.160559
Ziegler 1	Niobrara	Wyoming	4902705935	43.352296	-104.126736

Appendix 4. GSA Color Codes

Color Name	**GSA Rock-color Chart Number**
Grayish Green	10GY 5/2
Dark reddish brown	10R 3/4
Grayish red	10R 4/2
Moderate reddish brown	10R 4/6
Pale reddish brown	10R 5/4
Moderate reddish orange	10R 6/6
Moderate orange pink	10R 7/4
Moderate yellowish brown	10YR 5/4
Dark yellowish orange	10YR 6/6
Grayish orange	10YR 7/4
Very pale orange	10YR 8/2
Pale yellowish orange	10YR 8/6
Light greenish gray	5G 8/1
Dark greenish gray	5GY 4/1
Greenish gray	5GY 6/1
Grayish yellow green	5GY 7/2
Grayish red	5R 4/2
Pale red	5R 6/2
Light Red	5R 6/6
Grayish pink	5R 8/2
Olive gray	5Y 4/1
light olive gray	5Y 5/2
light olive gray	5Y 6/1
Dusky yellow	5Y 6/4
Yellowish gray	5Y 7/2
Yellowish gray	5Y 8/1
Grayish yellow	5Y 8/4
Brownish gray	5YR 4/1
Moderate brown	5YR 4/4
Pale brown	5YR 5/2
Light brown	5YR 5/6
Light brownish gray	5YR 6/1
Light brown	5YR 6/4
Grayish orange pink	5YR 7/2
Pinkish gray	5YR 8/1

Moderate orange pink	5YR 8/4
Light gray	N7

Appendix 5. Table of Facies Descriptions

Facies Type	Name	Composition	Color	Fossils	Grain Size	Structures	Sorting	Notes
Facies 1 (Part of Canyon Springs Sandstone Member)	High-Angle Crossbedded Sandstone Facies.	sand	ranges from grayish pink, very pale orange to moderate reddish orange	none	fine	bi-directional high-angle cross-beds	very-well sorted	Observations by Ahlbrandt and Fox (1997) include inversely graded sandstone laminae, a fraction of an inch thick, overlying tabular, tapering-upwards w edges that exhibit loose packing and typically a two-fold grain-size segregation, and megaripples composed of larger grained (4-30 mm) particles
Facies 2 (Part of Canyon Springs Sandstone Member)	Flat-Bedded Sandstone Facies	sand, ooids locally	grayish pink to light gray	bioturbation, rare external molds of bivalves and oysters, abraded bivalves	fine- to medium-grained	parallel thick laminations w ith w avy to flat bedding planes, ripple marks, cross-beds	w ell-sorted	Algal structures present at some locations. Locally, this unit cuts into and erodes into the underlying unit (Facies 1).
Facies 3 (Part of Stockade Beaver Creek Member)	Mudstone and Limestone Facies	predominately silt and clay, rare interbeds of sandstone and limestone	light olive gray to olive gray	bivalves, oysters, ammonites and crinoids	sand is very fine to fine-grained	shales are fissile	sands are w ell-sorted	The limestones in this unit generally consist of mudstones to w ackestones; the w ackestones contain bivalve fragments
Facies 4 (Part of Stockade Beaver Creek and Hulett Members)	Bioturbated Facies	clay, silt and sand	sand beds varies from yellow ish gray, light red, and gravish orange	bioturbation identified as *Skolithos*, *Monocraterion* or *Tigillites*, and *Diplocraterion*	Sand is very fine to fine-grained	flaser-and w avy bedded shales, hummocky cross-stratification, parallel lamination, bi-directional ripple marks, cross-lamination, and bioturbation in sands	w ell-sorted	Vertically, the facies generally trend from flaser and w avy bedding, to parallel lamination, to cross-beds, to ripple marks, and finally to bioturbation.
Facies 5 (Part of Stockade Beaver Creek and Hulett Members)	Low-angle Cross-bedded Facies	clay, silt and sand	yellow ish gray, very pale orange, moderate orange pink and moderate reddish orange	trace fossils, probably *Monocraterion*	fine-grained	parallel lamination and bedding, oscillation ripple lamination, and low-angle cross-bedding, bioturbation, shale partings locally, bi-directional ripple-marked sand beds	w ell-sorted	Vertically, the structures trend generally from w avy and flaser bedding, to bioturbated sands, to crossbeds, to planar parallel lamination, and oscillation ripple marks on top of sand beds separated by shale partings

Facies Type	Name	Composition	Color	Fossils	Grain Size	Structures	Sorting	Notes
Facies 6 (Part of Hulett Member)	Parallel Planar-Bedded Sandstone	sand	very pale orange, yellowish orange, and grayish orange	none	fine-grained	bi-directional cross-beds, cross-sets on the order of 0.2 to 0.5 meters, parallel lamination and bedding, and oscillation ripple marks	well-sorted	Vertically, bi-directional cross-beds became rarer and planar lamination and bedding became more common. Up-section in this facies, the oscillation ripple marks and shale partings become rare
Facies 7 (Part of Hulett Member	Incised Sandstone Facies	sand	very pale orange	very poorly preserved bivalve fragments	fine-grained	parallel lamination, high-angle cross-beds, cross-sets on the order of 20-50 cm thick. Some ripple cross-lamination is evident as well. Bed thickness decreases up-section.	well-sorted	Incision into the underlying facies, low-angle cross-bedded sandstone facies, is clearly evident in outcrop.
Facies 8 (Part of Lak Member)	Redbed Facies	silt, minor amounts of sand and clay	light olive gray in clay units, pale reddish brown in silt and sand	none	very fine-grained	none observed	poorly-sorted	grains are commonly frosted
Facies 9 (Part of Redwater Creek Member)	Belemnite Facies	clay, silt and sand	light brown, grayish green, dark greenish gray, light olive gray, dusky yellow, and yellowish gray.	abundant belemnites	sand is very-fine to fine-grained	none observable, destroyed during excavation if present	poorly-sorted	

Appendix 6. Table Summarizing Diagnostic Characteristics of Systems Tracts

Systems Tracts	Stacking Patterns	Bounding Surfaces	Example Stacking Pattern
Lowstand Systems Tract	Stacking patterns dominated by low-rate aggradation and progradation, facies generally include entire suite of depositional systems, from fluvial to coastal, shallow-marine to deep-marine.	Subaerial unconformity and marine correlative conformity at base, maximum regressive surface at top	can include coastal plain sandstones and mudstones in updip areas, in downdip areas it may consist of shelf mudstones underlying shallow marine sandstones, consisting of the lowstand wedge.
Transgressive Systems Tract	Diagnostic retrogradational stacking patterns, overall fining-upward profiles in both marine and non-marine successions, facies generally include entire suite of depositional systems, from fluvial to coastal, shallow-marine to deep-marine.	Maximum regressive surface at the base, and the maximum flooding surface at the top	shelf mudstones coarsening-upward into shallow marine sandstones, underlying shelf mudstones. Overall fining-upward.
Highstand Systems Tract	In a shallow-marine portion of a basin, stacking patterns show coarsening-upward, prograding trend related to the basinward shoreline shift.	Maximum flooding surface at base in both marine and non-marine settings. Bound on top in non-marine strata by the subaerial unconformity, and in marine strata by the maximum regressive surface.	Shelf mudstones, coarsening upward into shallow marine sandstones, underlying coastal plain sandstones and mudstone

VII. REFERENCES

Ahlbrandt, T.S., and Fox, J.E., 1997, Middle Jurassic Incised Valley Fill (Eolian/Estuarine) and Nearshore Marine Petroleum Reservoirs, Powder River Basin: The Mountain Geologist v. 34, p. 97-115.

Brenner, R.L., 1983, Late Jurassic Tectonic Setting and Paleogeography of Western interior, North American, *in* Reynolds, M.W., and Dolly, E.D., eds., Mesozoic Paleogeography of West-Central United States, Society of Economic Paleontologists and Mineralogists, Rocky Mountain Section, p. 119-132.

Brenner, R. L., and Peterson, J.A., 1994, Jurassic Sedimentary History of the Northern Portion of the Western interior Seaway, USA, *in* Caputo, M.V., Peterson, J.A., and Franczyk, K.J., eds., Mesozoic Systems of the Rocky Mountain Region, 217-232, Denver: The Rocky Mountain Section SEPM.

Cant, D.J., 1992, Subsurface Facies Analysis, *in* Walker, R.G., and James, N.P., eds., Facies Models: Response to Sea level Change, 27-45, St Johns, Newfoundland: Geological Association of Canada, p. 27-45.

Catuneanu, O., 2006, Principles of Sequence Stratigraphy, Oxford, United Kingdom, Elsevier, 375 p.

Dalrymple, R.W., Zaitlin, B.A., and Boyd, R., 1992, Estuarine Facies Models: Conceptual Basis and Stratigraphic Implications: Journal of Sedimentary Petrology, v. 62, p. 1130-1146.

Dalrymple, , R.W., Boyd, R., and Zaitlin, B.A., 1994, History of Research, Types and Internal Organization of Incised-Valley Systems: Introduction to the Volume: *in* Dalrymple, , R.W., and Zaitlin, B.A., eds., Incised Valley Systems: Origin and Sedimentary Sequences, 3-10, Tulsa, Oklahoma: Society for Sedimentary Geology, p. 3-10.

Doyle, A.B., 1984, Stratigraphy and Depositional Environments of the Jurassic Gypsum Springs and Sundance Formations, Sheep Mountain Anticline Area, Big Horn County, Wyoming, unpublished Master's thesis, University of Wisconsin – Milwaukee, 96 p.

Frakes, L.A., 1979, Climates Throughout Geologic Time, New York, New York, Elsevier Scientific Publishing Company, 310 p.

Frey, R.W., and Pemberton, S.G., 1984, Trace Fossil Facies Models, in Walker, R.G., ed., Facies Models: Geological Association of Canada, Geoscience Canada Reprint Series 1, p. 189-207

Hay, W.W., and Leslie, M.A., 1990, Could Possible Changes in Global Groundwater Reservoir Cause Eustatic Sea level Fluctuations? In Revelle, R., ed., Sea level Change: National Research Council, Studies in Geophysics, Washington, D.C., National Academy Press, p. 141-158.

Haq, B.U., Hardenbol, J., and Vail., P.R., 1988, Mesozoic and Cenozoic Chronostratigraphy and Cycles of Sea Level Change, *in* Wilgus, C.K., et al.., eds, Sea level Changes: an Integrated Approach: Society of Economic Paleontologists and Mineralogists, Special Paper 42., p. 71-108.

Huang, C., Hesselbo, S.P., and Hinnov, L., 2010, Astrochronology of the late Jurassic Kimmeridge Clay (Dorset, England) and implications for Earth system processes: Earth and Planetary Science Letters, v. 289, p.242-255.

Hunter, R.E., 1977, Basic Types of Stratification in Small Eolian Dunes: Sedimentology, v. 24, p. 361-387.

Imlay, R.W., 1947, Marine Jurassic of the Black Hills area, South Dakota: American Association of Petroleum Geologists Bulletin, v. 31, p. 227-273.

Imlay, R.W., 1952, Marine origin of the Preuss Sandstone, Idaho, Wyoming, and Utah: American Association of Petroleum Geologists Bulletin, v. 36, p. 1735-1753.

Imlay, R.W., 1957, Paleoecology of Jurassic Seas in the Western interior of the United States, *in* Ladd, H.S., eds., Treatise on Marine Ecology and Paleoecology, v. 2, Paleoecology, Geological Society of America Memoir 67, p. 469-504.

Imlay, R.W., 1980, Jurassic Paleobiogeography of the Conterminous United States in Its Continental Setting: U.S. Geological Survey Professional Paper, 1062.

Jacobs, D.K., Sahagian, D.L., 1995, Milankovitch Fluctuations in Sea level and Recent Trends in Sea level Change: Ice May Not Always Be the Answer, in Haq, B.U., ed., Sequence Stratigraphy and Depositional Response to Eustatic, Tectonic, and Climate Forcing: Dordrecht, The Netherlands, Kluwer Academic Publishers, p. 329-359.

Johnson, E.A., 1992, Depositional History of Jurassic Rocks in the Area of the Powder River Basin, Northeastern Wyoming and Southeastern Montana: U.S. Geological Survey Bulletin, 1917-J.

Kauffman, E.G., and Caldwell, W.G.E., 1993, The Western interior Basin in Space and Time, *in* Caldwell, W.G.E., and Kauffman, E.G., eds., Evolution of the Western interior Basin: Geological Association of Canada, Special Paper 39, p. 1-30.

Kocurek, G., and Dott, R.H., 1983, Jurassic Paleogeography and Paleoclimate of the Central and Southern Rocky Mountain Region, *in* Reynolds, M.W., and Dolly, E.D., eds., Mesozoic paleogeography of the west-central United States*:* Society of Economic Paleontologists and Mineralogists, Rocky Mountain Section, p. 101-116.

Langbein, W.B., and Schumm, S.A., 1958, Yield of Sediment in Relation to Mean Annual Precipitation: American Geophysical Union Transaction, v.39, p. 1076-1084.

Lawton, T.F., 1994, Tectonic Setting of Mesozoic Sedimentary Basins, Rocky Mountain Region, United States, *in* Caputo, M.V., Peterson, J.A., and Franczyk, K.J., eds., Mesozoic Systems of the Rocky Mountain Region, 1-25, Denver: The Rocky Mountain Section SEPM, p. 1-26.

Matthews, M.D., and Perlmutter, M.A., 1994, Global Cyclostratigraphy: an application to the Eocene Green River Basin: Special Publication of the International Association of Sedimentologists: v. 19, p. 459-481.

Miall, A.D., 1992, Alluvial Deposits, *in* Walker, R.G., and James, N.P., eds., Facies Models: Response to Sea level Change, 119-142, St Johns, Newfoundland: Geological Association of Canada, p. 119-142.

Perlmutter, M.A., and Matthews, M.D., 1989, Global Cyclostratigraphy: A Model, *in* Cross, T.A., ed., Quantitative Dynamic Stratigraphy, 233-260, Englewood Cliffs: Prentice Hall, p. 233-260.

Pemberton, S.G., and Frey, R.W., 1984, Quantitative Methods in Ichnology: Spatial Distribution Among Populations: Lethaia, v. 17., p. 33-49.

Peterson, J.A., 1954, Marine Upper Jurassic, Eastern Wyoming: American Association of Petroleum Geologists Bulletin, v. 38, p. 463-507.

Peterson, J.A., 1957, Marine Jurassic of Northern Rocky Mountains and Williston Basin: American Association of Petroleum Geologists Bulletin, v. 41, p. 399-440.

Peterson, J.A., 1958, Paleotectonic Control of Marine Jurassic Sedimentation in the Powder River Basin, *in* Wyoming Geologic Association Guidebook 13th Annual Field Conference, Powder River Basin, 1958, p. 56-63.

Pipiringos, G.N., and O'Sullivan, R.B., 1978, Principal Unconformities in the Triassic and Jurassic rocks, Western interior United States – a preliminary survey: U.S. Geological Survey Professional Paper 1035-A: A1-A29.

Plint, A.G., Eyles, N., Eyles, C.H., and Walker, R.G., 1992, Controls of Sea level Change, *in* Walker, R.G., and James, N.P., eds., Facies Models: Response to Sea level Change, 15-25, St Johns, Newfoundland: Geological Association of Canada, p. 15-25.

Posamentier, H.W., Jervey, M.T., and Vail, P.R., 1998, Eustatic Controls on Clastic Deposition I – Conceptual Framework, *in* Wilgus, C.K., et al.., eds, Sea level Changes: an Integrated Approach: Society of Economic Paleontologists and Mineralogists, Special Paper 42., p. 109-124.

Posamentier, H.W., and Vail, P.R., 1989, Eustatic Controls on Clastic Deposition II – Sequence and System Tract Models, , *in* Wilgus, C.K., et al.., eds, Sea level Changes: an Integrated Approach: Society of Economic Paleontologists and Mineralogists, Special Paper 42., p. 125-154.

Rautman, C.A., 1976, Depositional Environments of the "Lower Sundance" Formation (Upper Jurassic) of the Eastern Wyoming Region: unpublished Ph.D. dissertation, University of Wisconsin – Madison.

Rautman, C. A., 1978, Sedimentology of Late Jurassic Barrier-Island Complex – Lower Sundance Formation of the Black Hills: American Association of Petroleum Geologists Bulletin, v. 62, p. 2275-2289.

Reading, H.G., 1996, Sedimentary Environments: Processes, Facies and Stratigraphy: Oxford, Blackwell Science Ltd.

Rees, P.M., Ziegler, A.M., and Valdes, P.J., 2000, Jurassic Phytogeography and Climates: New Data and Model Comparisons, in Huber, B.T., Macleod, K.G., and Wing, S.L., eds., Warm Climates in Earth's History, p. 297-318, Cambridge, Cambridge University Press.

Rees, P.M., Noto, C.R., Parrish, J.M., Parrish, J.T., 2004, Late Jurassic Climates, Vegetation, and Dinosaur Distributions: The Journal of Geology, v. 112, p. 643-653.

Reinson, G.E., 1984, Barrier-Island and Associated Strand-Plain Systems, *in* Walker, R.G., ed., Facies Models, Second Edition, 119-140, St Johns, Newfoundland: Geological Association of Canada, p. 119-140.

Robinson, C.S., Mapel, W. J., and Bergendahl, M.H. , 1964, Stratigraphy and Structure of the Northern and Western Flanks of the Black Hills Uplift, Wyoming, Montana, and South Dakota: U.S. Geological Survey Professional Paper 404: 1-134.

Schmitt, G.T., 1953, Regional Stratigraphic Analysis of Middle and Upper Marine Jurassic in Northern Rocky Mountains- Great Plains: American Association of Petroleum Geologists Bulletin, v. 37, p. 355-393.

Sloss, L.L., 1962, Stratigraphic Models in Exploration: American Association of Petroleum Geologists Bulletin, v. 46, p. 1050-1057.

Strasser, A., Hillgärtner, H., Hug, W., Pittet, B., 2000, Third-order depositional sequences reflecting Milankovitch cyclicity: Terra Nova, v. 12, p. 303-311.

Uhlir, D.M., Akers, A., and Vondra, C.F., 1988, Tidal Inlet Sequence, Sundance Formation (Upper Jurassic), north-central Wyoming: Sedimentology v. 35, p. 739-752.

Vail, P.R., Audemard, F., Bowman, S.A., Eisner, P.N., and Perez-Cruz, C., 1991, The Stratigraphic Signatures of Tectonics, Eustasy, and Sedimentology – An Overview: in Einsele, G., Ricken., W., and Seilacher, A., eds., Cycles and Events in Stratigraphy, 617-659, Berlin: Springer-Verlag, p. 617-659.

Vail, P.R., Mitchum, R.M., and Thompson, S., III, 1977, Seismic Stratigraphy and Global Changes of Sea Level, Part 3: Relative Changes in Sea level from Coastal Onlap, in Payton, C.E., ed., Seismic Stratigraphy – Applications to Hydrocarbon Exploration: American Association of Petroleum Geologists Memoir 26, p. 63-81.

Van Wagoner, J.C., Mitchum, R.M., Campion, K.M., and Rahmanian, V.D., 1990, Siliciclastic Sequence Stratigraphy in Well logs, Cores, and Outcrops: Concepts for High-Resolution Correlation of Time and Facies: American Association of Petroleum Geologists Methods in Exploration Series, 7, Tulsa.

Walker, J.D., and Geissman, J.W., compilers, 2009, Geologic Time Scale: Geological Society of America, doi: 10.1130/2009.CTS004R2C. ©2009 The Geological Society of America.

Walker, R.G., 1992, Facies, Facies Models, and Modern Stratigraphic Concepts, in Walker, R.G., and James, N.P., eds., Facies Models: Response to Sea level Change, 1-14, St Johns, Newfoundland: Geological Association of Canada, p. 1-14.

Wilson, L., 1973, Variations in Mean Annual Sediment Yield as a Function of Mean Annual Precipitation: American Journal of Science, v. 273, p. 335-349.

Wright, R.P., 1973, Marine Jurassic of Wyoming and South Dakota – its Paleoenvironments and Paleobiogeography: University of Michigan Museum of Paleontology, Papers on Paleontology (2): 1-49.

Zaitlin, B.A., Dalrymple, R.W., and Boyd, R., 1994, The Stratigraphic Organization of Incised-Valley Systems Associated with Relative Sea level Change: *in* Dalrymple, , R.W., and Zaitlin, B.A., eds., Incised Valley Systems: Origin and Sedimentary Sequences, 46-60, Tulsa, Oklahoma: Society for Sedimentary Geology, p. 46-60.

Ziegler, A.M., Raymond, A.L., Gierlowski, T.C., Horrell., M.A., Rowley, D.B., and Lottes, A.L., 1987, Coal, Climate and Terrestrial Productivity: The Present and the Early Cretaceous Compared, *in* Scott, A.C., ed., Coal and Coal-Bearing Strata: Recent Advances, Geological Society Special Publication No. 32, 25-49, London: Geological Society, p. 25-49.

Ziegler, A.M., Eshel, G., Rees, P.M., Rothfus, T.A., Rowley, D.B., and Sunderlin, D., 2003, Tracing the tropics across land and sea: Permian to Present: Lethaia, v. 36, p. 227-254.